DETERMINATION OF DESIGN PARAMETERS AND INVESTIGATION ON OPERATION PERFORMANCE FOR AN INTEGRATED GAS CLEANING SYSTEM TO REMOVE TARS FROM BIOMASS GASIFICATION PRODUCER GAS

A thesis submitted in partial fulfilment of the requirements

for the

degree of

Doctor of Philosophy in Chemical and Process Engineering

in the University of Canterbury

by Gershom Mwandila

October 8, 2010

ABSTRACT

Determinations of design parameters and investigation on operation performance of a tar removal system for gas cleaning of biomass producer gas have been undertaken. The presence of the tars in the producer gas has been the major hindrance for the commercialisation of the biomass gasification technology for power generation, hydrogen production, Fischer Tropsch (FT) synthesis, chemical synthesis and synthetic natural gas (SNG) synthesis. The characteristic of the tars to condense at reduced temperatures cause problems in the downstream processing as the tars can block and foul the downstream process equipment such as gas engines reactor channels, fuel cells, etc. Considerable efforts have been directed at the removal of tars from the producer gas where the tars can be either chemically converted into lighter molecular weight molecules or physically transferred from gas phase to liquid or solid phase. In the former, the tars have been removed in a scrubber by transferring them from the producer gas to a scrubbing liquid and then removed from the liquid to air in a stripper and finally recycled them into air to a gasifier to recover their energy.

A tar removal test system involving a scrubber and stripper has been designed based on the predicted tar solubility in canola methyl ester (CME) as the scrubbing liquid and its measured properties (CME is a type of methyl ester biodiesel). The tar solubility has been predicted to decrease with increasing temperatures and thus its value increases at lower temperatures. In designing the test system, the design parameters are needed including equilibrium coefficients of the gas-liquid system, molar transfer coefficient and the optimum liquid to gas flow rate ratio. The equilibrium coefficients have been predicted based on thermodynamic theories where the required data are determined from CME composition and known properties of each component of the CME as well as the properties of the model tar (naphthalene). The molar transfer coefficients are then experimentally determined and the correlations as a function of liquid and gas flow rates are proposed which are consistent with literature.

The optimum liquid to gas flow rate ratios have been found to be 21.4±0.1 for the scrubber and 5.7±0.1 for the stripper. Using these optimum ratios, the tar removal efficiencies in the scrubber and the stripper are 77 and 74%, respectively. The

analysis of the system performance has been achieved after an innovative method of determining tar concentrations in both the liquid and gas phase had been developed based on the concept of the density of liquid mixtures. However, these tar removal efficiencies are low due to the fact that the targeted tar concentration in the scrubber's off-gas was large. As a result the system has been redesigned based on the determined design parameters and its operation performance retested. In the redesigned system, the tar removal efficiency in the scrubber and stripper is 99%. The redesigned system would be integrated with the UC gasifier for downstream gas cleaning. Since 1% of tars are not removed, a makeup tar free CME of 0.0375 litres per hour for the 100kW UC gasifier has been introduced in the recycle stream between the scrubber and stripper to avoid tar accumulation in the system.

ACKNOWLEDGEMENTS

I would like to express my heartfelt gratitude, appreciation and thanks to my supervisor Professor Shusheng Pang for all the support, guidance, time, advice and encouragement during the course of this work. Sir, I am forever indebted to you for instilling in me your writing skills, presentation of research work and understanding of the subject. I have gained valuable experience by working with you, which will no doubt advance my academic career. I also wish to thank my co-supervisors Dr. Chris Williamson and Mr. Ian Gilmour, thank you Chris for helping me to rekindle my knowledge in thermodynamics. Ian, thank you for the well thought technical conversations. Finally, I would like to thank Douglas Bull for helping me with the drawing, Chris Penniall for helping to assemble my laboratory and Dr. Woei-Lean Saw for helping me to conduct my experiments and write up.

I would like to acknowledge the CAPE technical staff, Bob Gordon, Frank Weerts, Tony Allen, Leigh Richardson, Peter Jones and Trevor Berry. I know that sometimes you did not understand what I was looking for but thank you for your advice and getting the job done.

The scholarship which was granted to me by the New Zealand Aid is gratefully acknowledged, I would have not done this work without it. Furthermore, I sincerely thank my supervisor for supporting me financially after my New Zealand Aid scholarship expired.

I thank God for my family; wife Bridget Kaira, sons Siwa, Mbachi, Anipa and daughter Elisa Mbobe. Bridget, you are lovely and beautiful wife. My children, you inspire me to work hard and be your role model. Mum (Elisa) and Dad (Jonas), I miss you and wish you were alive so that I could repay you. You worked so hard to get me this far, in the midst of poverty. Be assured, I will pass on your values.

TABLE OF CONTENTS

LIST OF TABLES

LIST OF FIGURES

Nomenclature

Abbreviations

A_i aromatic compound i

CFB circulating fluidised bed

CME canola methyl ester

C14:0 14 carbon atoms and zero double bonds in between carbon – carbon atoms

C16:0 14 carbon atoms and zero double bonds in between carbon – carbon atoms

C18:1 18 carbon atoms and one double bond in between carbon – carbon atoms

C18:2 18 carbon atoms and two double bonds in between carbon – carbon atoms

C18:3 18 carbon atoms and three double bonds in between carbon – carbon atoms

DESP dry electrostatic precipitator

DFB dual fluidised bed

ECN Energy Centre of the Netherlands

ESP electrostatic precipitator

H_{OG} height of gas phase transfer units

IC Internal combustion

IPA isopropyl alcohol

L litre

LHV low heating value MJ/Nm^3

L/G liquid to gas flow rate ratio

MS mass spectrometer

N_{OG} number of gas phase transfer units

OLG oil based gas washing

PAHs poly-aromatic hydrocarbons

ppmV parts per million volume mg/L

RME rapeseed methyl ester

RPS rotation particle separator

S-B steam to biomass

TREC Tar RECduction with char

UC University of Canterbury

UV ultraviolet

VTT Technical Research Centre of Finland

WESP wet electrostatic precipitator

[-] dimensionless quantity

Symbols

α liquid phase parameter of the overall volumetric mass transfer coefficient in the scrubber, [-]

β gas phase parameter of the overall volumetric mass transfer coefficient in the scrubber , [-]

β' gas phase parameter of the overall volumetric mass transfer coefficient in the stripper, [-]

δ solubility parameter, $(J/m^3)^{0.5}$

δ_1 solubility parameter of CME, $(J/m^3)^{0.5}$

δ_2 solubility parameter of the tars, $(J/m^3)^{0.5}$

δ_d dispersion parameter contribution to solubility parameter of CME, $Pa^{0.5}m^3$

δ_h hydrogen bonding parameter contribution to solubility parameter of CME, $Pa^{0.5}m^3$

δ_p polar parameter contribution to solubility parameter of CME, $Pa^{0.5}m^3$

ε_{LoB} operating void space in the packing. [-]

ρ density, kg/m^3

ρ_i density of component i, kg/m^3

ρ_G density of the carrier gas, kg/m^3

ρ_L density of the inert liquid, kg/m^3

ρ_{Lm} density of the liquid mixture or solution, kg/m^3

ρ_{tar} density of collection of tar components, kg/m^3

ρ_w density of the water, kg/m^3

φ parametric coefficient of the overall volumetric mass transfer coefficient in the scrubber, [-]

φ' parametric coefficient of the overall volumetric mass transfer coefficient in the stripper, [-]

φ_1 volume fraction of CME in the prediction of tar solubility in CME, [-]

μ viscosity, kg/m.s

μ_G viscosity of the carrier gas, kg/m.s

v_{01} molar volume of CME at 298.15K, m^3/mol

v_{02} molar volume of naphthalene at 298.15K, m^3/mol

v_1 molar volume of the CME an elevated temperature T, m^3/mol

v_2 molar volume of the naphthalene at an elevated temperature T, m^3/mol

v_i molar volume of component i in CME 298.15K, m^3/mol

v^L_2 molar liquid volume of naphthalene

Δ characteristic constant for the correction of polarity, cal/cm^3 or J/m^3

ΔH_1 Heat of vaporisation of naphthalene at 298.15 K. J/mol

ΔH_2 Heat of vaporisation of naphthalene at an elevated temperature, J/mol

ΔH^f Heat of melting naphthalene, J/mol

Δp Pressure drop, N/m^2

a area per unit volume of packing, m^2/m^3

a_0 first parameter for the density of CME as a function of temperature, [-]

a_1 second parameter for the density of CME as a function of temperature, [-]

a_2 parameter for the density of CME as a function of temperature and tar concentration, [-]

b_o first parameter for the viscosity of CME as a function of temperature, [-]

b_1 second parameter for the viscosity of CME as a function of temperature, [-]

A Heat transfer surface area, m^2

A^* first characteristic constant determined by properties of naphthalene

B^* second characteristic constant determined by properties of naphthalene

c_L specific heat capacity of CME, kJ/kg.K

c_w specific heat capacity of water, kJ/kg.K

c_{SF} gas velocity of flooding, m/s

D column diameter, m

d_i inside tube diameter

D_L CME diffusivity, m^2/s

d_s diameter of the sphere of the same surface as a single packing particle, m

E_ρ Cohesive energy density

f fugacity, N/m^2

f_2 fugacity of the model tar (naphthalene), N/m^2

f_o flooding percent

f^{oL} fugacity of the pure liquid model tar (naphthalene) for solubility of in polar solvents, N/m^2

f^{L}_{pure2} fugacity of the pure liquid model tar (naphthalene) for solubility in non polar solvents, N/m^2

f^{G}_{2} fugacity of pure gaseous model tar (naphthalene), N/m^2

Fu	product of packing factor and its conversion, m^{-1}
G	gas molar flow rate per area, kmol.m^2.s
G'	gas mass flow rate per area, kg/m^2.s
G_m	gas molar flow rate, kmol/s
G_{min}	minimum gas molar flow rate, kmol/s
H_{21}	Henry's law coefficient for the transfer of model tars (naphthalene) in CME
H_{OG}	overall gas phase height of transfer units
H_{OL}	overall liquid phase height of transfer units
k	equilibrium coefficient in the stripper, mol/mol
k(T)	equilibrium coefficient in the stripper as a function of temperature, mol/mol
k_X	liquid phase molar transfer coefficient, kmol/m^2.s
k_Y	gas phase molar transfer coefficient, kmol/m^2.s
K_X	overall liquid phase molar transfer coefficient, kmol/m^2.s
K_Y	overall gas phase molar transfer coefficient, kmol/m^2.s
K_Xa	overall volumetric liquid phase molar transfer coefficient, kmol/m^3.s
K_Ya	overall volumetric gas phase molar transfer coefficient, kmol/m^3.s
L	liquid molar flow rate per area, kmol.m^2.s
L'	gas mass flow rate per area, kg/m^2.s
L_m	gas molar flow rate, kmol/s
m	equilibrium coefficient in the scrubber, mol/mol

M	Molar mass, kg/kmol
m(T)	equilibrium coefficient in the stripper as a function of temperature, mol/mol
M_1	molar mass of first tar component, kg/kmol
Mair	molar mass of air, kg/kmol
m_G	mass flow rate of the gas, kg/s
M_i	molar mass of the ith tar component, kg/kmol
m_L	mass flow rate of the liquid, kg/s
m_W	mass flow rate of water, kg/s
N	mass transfer rate, $kmol/m^2.s$
n_o	safety factor, [-]
N_{OL}	overall number of gas phase transfer units, [-]
p	total pressure, N/m^2
p_i	partial pressure of the ith component, N/m^2
Q	heat load, W
Qtank	heat requirement for heating CME in the tank, W
R	universal gas constant, J/mol.k
R^2	square of the regression coefficient, [-]
S	stripping factor, [-]
S_a	separation factor for the scrubber, [-]
S_S	separation factor for the stripper, [-]

S_{CG} Schmidt number for the gas, [-]

S_{CL} Schmidt number for the liquid, [-]

T Temperature, K

t_1 inlet temperature of the tube side of a heat exchanger, K

t_2 outlet temperature of the tube side of a heat exchanger, K

T_1 inlet temperature of the shell side of a heat exchanger, K

T_2 outlet temperature of the shell side of a heat exchanger, K

T_C critical temperature, K

T_{in} inlet temperature, K

T_m temperature at melting point, K

T_{out} outlet temperature, K

Tr_1 inlet reduced temperature, [-]

Tr_2 outlet reduced temperature, [-]

U Overall heat transfer coefficient, $W/m^2.K$

u_W linear velocity of cooking water, m/s

u_{GF} gas velocity at flooding point. m/s

V_G volumetric flow rate of the gas

x mole fraction solubility of naphthalene in CME, mol/mol

x(T) mole fraction solubility of naphthalene in CME as a function temperature, mol/mol

X liquid phase mole tars per mole CME, mol/mol

X^* equilibrium liquid phase mole tars per mole CME, mol/mol

X_1 liquid phase mole tars per mole CME at the top column, mol/mol

X_2 liquid phase mole tars per mole CME at the bottom column, mol/mol

X_{in} inlet liquid phase mole tars per mole CME, mol/mol

X_{out} outlet liquid phase mole tars per mole CME, mol/mol

x_2^{ideal} ideal mole fraction solubility of naphthalene in CME, mol/mol

X^*_{out} outlet liquid equilibrium mole tars per mole CME, mol/mol

X^*_{in} inlet liquid equilibrium mole tars per mole CME, mol/mol

Y gas phase mole tars per mole CME, mol/mol

y_1 mole fraction tars at the top of the column, mol/mol

y_2 mole fraction tars at the top of the column, mol/mol

Y gas phase mole tars per mole CME, mol/mol

Y^* equilibrium gas phase mole tars per mole CME, mol/mol

Y_1 gas phase mole tars per mole CME at the top column, mol/mol

Y_2 gas phase mole tars per mole CME at the bottom column, mol/mol

Y_{in} inlet gas phase mole tars per mole CME, mol/mol

Y_{out} outlet gas phase mole tars per mole CME, mol/mol

Y^*_{out} outlet gas equilibrium mole tars per mole CME, mol/mol

Y^*_{in} inlet gas equilibrium mole tars per mole CME, mol/mol

Z height of packing, m/m

z_2 gas phase compressibility factor of the model tar (naphthalene), [-]

Chapter 1 Introduction

This PhD thesis presents my research on removal of tars contained in a producer gas produced in a biomass gasifier at the Department of Chemical and Process Engineering, at the University of Canterbury, Christchurch, New Zealand. The gasifier is a 100 kW laboratory scale gasifier with dual fluidized beds which consists of a bubbling fluidised bed (BFB) and a circulating fluidised bed (CFB) (Bull, 2008). The BFB is used to produce the gas by gasifying wood pellets with steam as gasification agent. While the CFB is used for combustion of solid char which is generated from the gasification to produce heat which heats up the bed material required for the endothermic reactions in the BFB. The gas can be used to fuel internal combustion (IC) engines, (commonly referred to as gas engines) coupled to a power generator. In addition, it can be used for hydrogen production, Fischer Tropsch (FT) synthesis, chemical synthesis and synthetic natural gas (SNG) synthesis. However, the gas contains some dust, tars, acidic and alkaline impurities which hinder the use of the gas for downstream applications.

The key aspects of this study are the determination of the design parameters for a tar removal system and the performance test of the system. In order to determine the design parameters and test the system, literature review is firstly thought about biomass tars and the methods of removing them from biomass producer gas. A suitable tar removal system is then selected to determine its design parameters and test its performance. In selecting the system, particular attention is paid to two successful gas cleaning technologies, one based at the Energy Centre of the Netherland (ECN) and the other at Guessing in Austria.

At ECN and Guessing plants, a wet scrubber is used to remove the tars from the producer gas and then the removed tars are burned in combustor of the gasifier. In the case of the ECN plant, the scrubbing liquid is regenerated and recycled for reuse in the scrubber. However, the Guessing technology consists of only one tar removal unit in which the scrubbing liquid is not regenerated. In the Guessing system, a proportion of the spent liquid is reused with the remaining proportion of the spent liquid being fed to a combustor of the gasifier for combustion. In the same time, some amount of fresh liquid is injected to replace the spent one.

The ECN scrubber consists of three separation units where the tars are firstly removed from the gas in the collector and then in the scrubber using thermal oil. In the third unit, the tars are removed from the thermal oil by heated air which is fed to the combustor with the absorbed tars being burned. The present study envisages the use of only two separation units in which the tars are firstly removed from the gas in the scrubber by using canola methyl ester (CME) biodiesel and then removed from CME in the stripper by using heated air. The CME (which is a type of methyl ester biodiesel) is chosen based on its sustainability and its similarity with rapeseed methyl ester (RME) which is the scrubbing liquid for the Guessing tar removal system. However, the literature on the solubility of the tars in CME is scarce and design parameters are lacking. As a result, thermodynamics and theories on gas-vapour solubility are to be used in this study to predict the solubility of the tars in CME. Once the solubility has been theoretically predicted, the design parameters such as the ratio of liquid to gas flow rates, the molar transfer coefficients can be determined. In addition, the equilibrium coefficient for the transfer of the tars from CME into the air in the stripper is also calculated and its design parameters determined.

In order to validate the underling theories for the prediction of tar solubility and to obtain design parameters, a test system was designed and constructed which consists of the scrubber and stripper. The working principles of the test system are based on the solubility of the tars. On one hand, the separation of the tars from the gas in scrubber is enhanced by increasing the solubility of the tars in CME. On the other hand, the transfer of the tars from the CME is enhanced by the reducing the solubility of the tars in CME. Therefore, the CME is cooled down before it contacts with the gas in the scrubber and it is heated up before contacting with the heated air in the stripper. In this way, the CME is confined in a closed loop in which it is heated up and cooled down as it circulates between the scrubber and the stripper.

1.1. Objectives of the Project

The objectives of this PhD project are to make contributions to solutions for two predicaments facing the supply of energy worldwide. One of the predicaments is the ever-diminishing supply of fossil fuel resources. The other is the increased awareness of the harmful environmental effects of heavy fossil fuel consumption. It

is estimated that almost 13TW of power which is mostly fossil fuel based is consumed worldwide (Argonne-National-Laboratory, 2005). In addition, the study of Begley has reported that by the year 2050 energy demand is expected to increase by 50 - 320% depending on the veracity of conservation of resources in that time (Begley, 2009).

In view of the two predicaments, scientists and engineers have recently been exploring alternative energy resources and developing technologies for converting these resources. One of the readily available alternative energy resources is biomass of agricultural and woody residues. The technology of biomass gasification has shown promising future in commercialisation to convert biomass to a combustible gas. The gas, consisting H_2, CO, CO_2, CH_4 and other hydrocarbons can then be used for production of power, hydrogen, FT gas, SNG and chemicals.

However, one of the major technical obstacles in the commercialisation of the biomass gasification technology is the gas cleaning to get rid of the tars. Tars which are one of the impurities in the combustible gas have been the major impediment to the use of the gas. Therefore, extensive research has been focused on the removal of the tars. The objectives of this research are to select, modify and design a tar removal system based on literature review and thermodynamic models, test its performance then obtain its design parameters for practical system design. More specifically the objectives of this project include:

(i) Selecting a tar removal system from successful current systems and modify it to consist of two separation units, one for tar absorption using CME (scrubber) and the other one for tar removal from the loaded CME by heated air (stripper).
(ii) Design a test system based on (i) above
(iii) Predicting solubility and equilibrium coefficients of the tars in the CME solvent as a function of temperature.
(iv) Obtaining desirable operation conditions and gas to liquid flow rate ratios both in the scrubber and in the stripper.
(v) Obtaining molar transfer coefficients for the design of both units (scrubber and stripper).
(vi) Testing the performance of the test system.

(vii) Design a practical system based on the results of the test system

1.2. Outline of the Thesis

This thesis contains seven chapters in which Chapter 1 is the project introduction as described above. Chapter 2 presents an extensive literature review in which various studies on tar removal from the biomass gasification producer gas will be discussed. In this chapter, definition of the tars and their formation are also described as well as a brief account of biomass gasification processes. Furthermore, the effect of operating parameters of the gasifier on the reduction of the tar content in the producer gas is also assessed.

Based on the literature review, a method for tar removal will be envisaged and modified in Chapter 3 which includes a scrubber for tar absorption by solvent (CME) from the producer gas and a stripper for tar release from the loaded CME by heated air. Details of this modified system will be presented and theories on prediction of the tar solubility in the CME and other needed properties will be explored. Chapter 3 ends with the specifications of the auxiliary units of the system. In Chapter 4, the equilibrium coefficients are predicted and then the two separation units are designed and constructed. In addition, preliminary experiments and their results are described.

The detailed experiments for the removal of the tars by using CME in the scrubber and heated air in the stripper are described separately in Chapter 5 for the scrubber and in Chapter 6 for the stripper. Chapter 5 will also present a new method for determination of tar concentration in the CME and in the gas. In both chapters, determination of molar transfer coefficients based on total tar concentration will also be presented. Chapter 6 also contains the redesign of the test system based on the state of the art off-gas quality using the determined design parameters. It also validates the benefit of recycling CME from the stripper to the scrubber by comparing with current successful systems. The validation shows only a small makeup is required to counter against tar accumulation in the system. Finally, Chapter 7 presents the general discussion and conclusion for the study. In addition, it also provides the recommendations for future work.

Chapter 2 Literature Review

There is a lot of literature on the removal of tars in gas cleaning of biomass gasification producer gas for two main reasons. Firstly, it is because the presence of the tars in the producer gas is the major obstacle in the commercialisation of the gasification technology. Secondly, there are many designs of the reactor (gasifier) which are used in the gasification technology. Due to there being a variety of gasifier designs, tars of varying concentrations and compositions in the producer gas are generated. Table 2.1a shows types of the gasifiers and the concentration of the tars generated in the producer gas.

Table 2.1a: Type of a gasifier and their tar output levels

Gasifier type	Tar output (g/Nm^3)	Example of the gasifier type	Tar output (g/Nm^3)
Updraft **(a)**	10 - 200	KTH **(b)**	25 - 124
		Harboøre **(c)**	80 - 100
Downdraft **(a)**	0.02 - 4	IISc/Dasag **(d)**	0.05 - 0.075
		KARA **(d)**	0.05 - 1
		Viking **(e)**	< 1
Air Blown circulating fluidised Bed **(a)**	2 - 20	MILENA gasifier **(f)**	10 - 20
		UMSICHT gasifier **(g)**	2 - 10
		JGSEE gasifier **(h)**	~10
Dual fluidised bed **(a)**	1 - 15	100 kW gasifier,Vienna **(i)**	2 - 2.1
		Guessing **(j)**	2 - 2.5
References: (a) (Brown, 2003), **(b)** (Skoulou et al., 2009), **(c)** (Hamelinck et al., 2004), **(d)** (Hasler et Nussbaumer et al., 1999), **(e)** (Hofmann et al., 2007), **(f)** (Zwart et al., 2009), **(g)** (Umsicht, 2009), **(h)** (Pipatmanomai, 2011), **(i)** (Pfeifer et al., 2004) and **(j)** (Hofbauer, 2002)			

In order to use the producer gas for electricity generation in IC engines, chemical synthesis, fuel cells and as FT gas or SNG, the producer gas must be of specific quality. As is the case for the designs of the gasifiers, there are varieties of designs of process units for the end use of the gas and hence they have varying tar tolerance levels as shown in Table 2.1b.

Table 2.1b: Tolerance levels of tar various downstream process units

Downstream unit (and their general tar tolerance levels)	General Tar levels (g/Nm^3)	Where applied	Feed gas quality, (mg/Nm^3)	Reference
IC engine **(k)**	< 0.6	Guessing CHP	10 - 40	1
		OLG	10	2
		UMSICHT gasifier	< 50	3
		IISc gasifier	50	4
		HTAG gasifier (KTH)	< 100	5
Gas turbine engines **(l)**	< 5	Jilin Province (China)	~1000	6
		Varnamo gasifier	< 5000	7
		ARBRE gasifier (UK)	100 - 500	8
		ECN micro-turbine	200	9
Biomass gasification fuel cell **(m)**	< 1	ECN fuel cell	200	10
		BIOCELLUS	104 - 338	11
		Rome 'La Sapienza	< 1	12
		Viking gasifier	< 5	13
Fischer tropsch (FT) synthesis reactor **(n)**	< 1	Guessing CHP	< 20	14
		ECN FT synthesis	200	15
		VTT plant	5	16
Synthesis natural gas (SNG) **(o)**	0.2	Guessing CHP	< 20	17
		VTT plant	5	18
		ECN plant	200	19

References: (k)(Babu, 1995), **(l)**(Hasler et Nussbaumer et al., 1999), **(m)**(Hasler et Nussbaumer et al., 1999), **(n)**(Hamelinck et al., 2004), **(o)** (Zwart et al., 2009), **1**(Hofbauer, 2002), **2**(Zwart et al., 2009), **3**(Ising et al., 2002), **4**(Dasappa et al., 2004), **5**(Kalisz et al., 2004) **6**(Henderick et Williams et al., 2000), **7**(Toosen et al., 2008), **8**(Belgiorno et al., 2003), **9**,**10**,**15**,**19**(Zwart et al., 2009) **11**(Schweiger, 2007), **12**(Pino et al., 2006), **13**(Pierobon, 2010), **14,17**(Babu, 2006) and **16**,**18**(Kurkela, 1989)

It is worth noting that Table 2.1b only shows the general tolerance levels of tars in various units as tar tolerances are normally specified by manufacturers of units. For instance, a Jenbacher IC engine requires that the tar dew point be 5^oC below the gas temperature and that the levels of tar components of Benzol and naphthalene be specified in milligrams per 10kw power (Jenbach, 2009). Another IC engine that is commonly used for converting producer gas into power is the Caterpillar IC engine. The Caterpillar engine is used to produce electricity where total tar levels at inlet point is about $10mg/Nm^3$ and dew point of 2^oC (Zwart et al., 2009). The third engine that has been reported to be powered by producer gas is the

Guascor engine which requires that the dew point be less than 5^{o}C and the tar concentration be less than 3mg/MJ (Guascor, 2005).

Similarly, various manufacturers of units for gas turbine, fuel cell, FT reactor and SNG have their operation specifications. Some few examples of where these units are applied and their tar tolerance have been shown in Table2.1b.

2.1. An Overview of Biomass Gasification and Tar Formation Processes

Biomass gasification is a process that converts biomass which is a carbonaceous material into carbon monoxide, hydrogen, carbon dioxide, methane and negligible amounts of some other higher molecular weight hydrocarbons. In the conversion, the biomass is reacted at high temperatures in excess of 700^{o}C (Bridgwater, 2001), without combustion but with a controlled amount of oxygen and/or steam. The products of gasification are collectively called producer gas which can be used as a fuel for heating and power generation as well as the synthesis of liquid fuels.

Biomass gasification takes place in a reactor called the gasifier. There are two distinct processes which take place in a gasification process, namely pyrolysis, and gasification. Pyrolysis is the process which is responsible for tar formation and it will be discussed later. On the other hand, gasification starts with solid-gas type of reactions in which solid biomass is consumed by steam (H_2O) to form CO, H_2 and CH_4:

Primary: $C_{(s)} + H_2O_{(g)} \rightleftharpoons CO + H_2$

Secondary: $C_{(s)} + 2H_2O_{(g)} \rightleftharpoons CO_2 + 2H_2$

These reactions are endothermic and proceed slowly and are favoured by higher temperatures. Therefore, they can be controlled by changing the steam to biomass ratio of the gasification process (Franco et al., 2002). In an operation of higher steam to biomass ratio, the gasification environment is saturated with hydrogen so much that unconverted biomass undergoes further reaction called

hydrogenation which involves the exothermic conversion of carbon in a hydrogen rich environment to methane (CH_4):

$$C_{(s)} + 2H_2 \rightleftharpoons CH_4$$

Further, the presence of the carbon dioxide (CO_2) gives rise to the so called Boudouard reaction which is an endothermic reaction of solid carbon with CO_2 to form carbon monoxide (CO):

$$C_{(s)} + CO_2 \rightleftharpoons 2CO$$

As regards energy consideration, CO_2 is an energy sink. As a result, the gasification process is designed and operated to consume as much CO_2 as possible by increasing the gasification temperature.

The solid-gas phase reactions are much slower than the gas-gas phase reactions. Therefore, the solid-gas phase reactions are more often used to model thermodynamic equilibrium of the gasification process than the gas-gas reactions (Franco et al., 2002). On the other hand, gas-gas phase reactions occur very rapidly everywhere in the reactor and determine the constituents and composition of the gasification producer gas (Probstein et Hicks et al., 2006). These reactions include the steam-methane reforming reaction where methane and water vapour (H_2O) are highly exothermically converted to carbon monoxide and hydrogen:

$$CH_4 + H_2O_{(g)} \rightleftharpoons CO + 3H_2$$

Then the excess water vapour undergoes the popular exothermic water-gas shift reaction to convert carbon monoxide into carbon dioxide and hydrogen.

$$CO + H_2O_{(g)} \rightleftharpoons CO_2 + H_2$$

The water gas shift reaction is predominantly responsible for the gas composition in the steam gasification at temperatures between 730 - 830 °C (Franco, Gulyurlu et al. 2002). On the other hand, Boudouard reaction and the solid – gas reactions predominantly determine the gas composition at temperatures above 830 °C (Frannco et al., 2002).

As described in the reactions for the gasification, the endothermic reactions are favoured by higher temperatures. In the case of a DFB gasifier, the higher temperatures are created by the circulating bed material which carries heat from the combustion chamber where char is combusted. The heat carried by bed material initiates the gasification process as it enables the devolatilisation or pyrolysis of the biomass in the gasification chamber of the DFB gasifier. Both the combustion and gasification processes produce tars (Higman et Burgt et al., 2003).

The tars have been defined in different ways in literature which may cause some confusion both in research and development, and in practical applications. For example, some of the definitions of tars are as follows:

(i) Historically, tars were defined as an operational parameter for boilers, transfer lines, and internal combustion engines; being largely organic compounds from gasification that condensed under operating conditions of these units at their inlet devices (Milne et al., 1998).

(ii) Tars have been defined as organics produced under thermal or partial-oxidation regimes or rather gasification of any organic material (Rabou et al., 2009).

(iii) The Biomass Technology Group (BTG, The Netherlands) defines tars as the mixture of chemical compounds which condense on metal surfaces at room temperature (Anonymous, 1995).

(iv) Tars are considered to be the condensable fraction of the organic gasification products and are largely aromatic hydrocarbons, including benzene (Dayton, 2002).

(v) In this study, tars are defined as all organic compounds with molecular weight larger than that of benzene with the exclusion of soot and char. This definition has been widely accepted and applied (Milne et al., 1998).

The tars can be produced in gasification of various types of biomass including woody biomass, agricultural residues and bio-solid wastes. The full process of the biomass gasification includes two steps: initial devolatilization or pyrolysis and subsequent gasification. In the initial devolatilization process, the biomass gets de-volatilised to yield the gases, tars and char as shown in Figure 2.1 (Shafizadeh et Lai et al., 1972; Bradbury et al., 1979; Shafizadeh, 1982). In the

subsequent gasification process, a series of reactions occur among the volatile gases, gasification agent, char and tar which produce the producer gas.

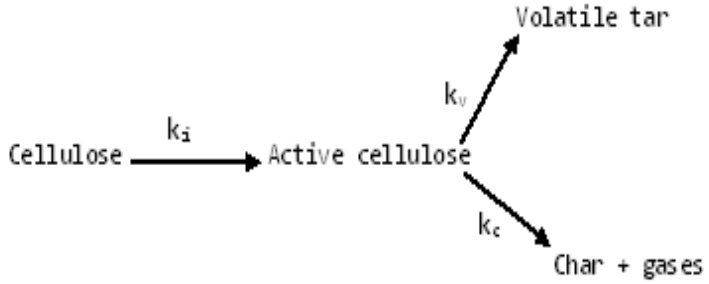

Figure 2.1: Mechanism of tar formation in biomass devolatilization (Shafizadeh et Lai et al., 1972; Bradbury et al., 1979; Shafizadeh, 1982).

The volatile components of the biomass generated in the initial devolatilization process can be vaporized at temperatures as low as 600°C (Morf et al., 2002). The initial vapours are made of permanent gases and larger condensable molecules called primary tars. In the subsequent gasification reactions, some of the heavy molecular weight compounds (primary tars) may be cracked at 700 - 850°C, producing secondary compounds (phenolics and other mono-aromatics) (Morf et al., 2002). At higher temperatures, tertiary conversion to poly-aromatic hydrocarbons (PAHs) starts and the soot formation is observed simultaneously (Morf et al., 2002). All these reactions (cracking, partial oxidation, re-polymerisation, and condensation reactions) take place in the gas phase between permanent gases and tar vaporized species. They can react even inside the biomass particle unless it has a diameter less than 1mm (Morf et al., 2002). The surface of the char formed by de-volatilization of the original particle catalyses those reactions. This tar formation pathway can be visualised as reported in Figure 2.2.

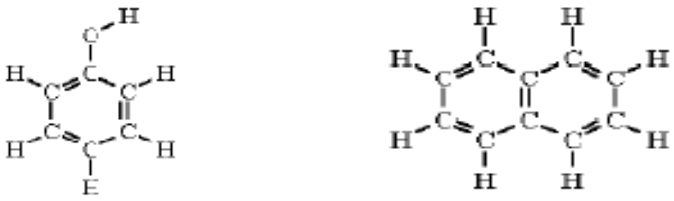

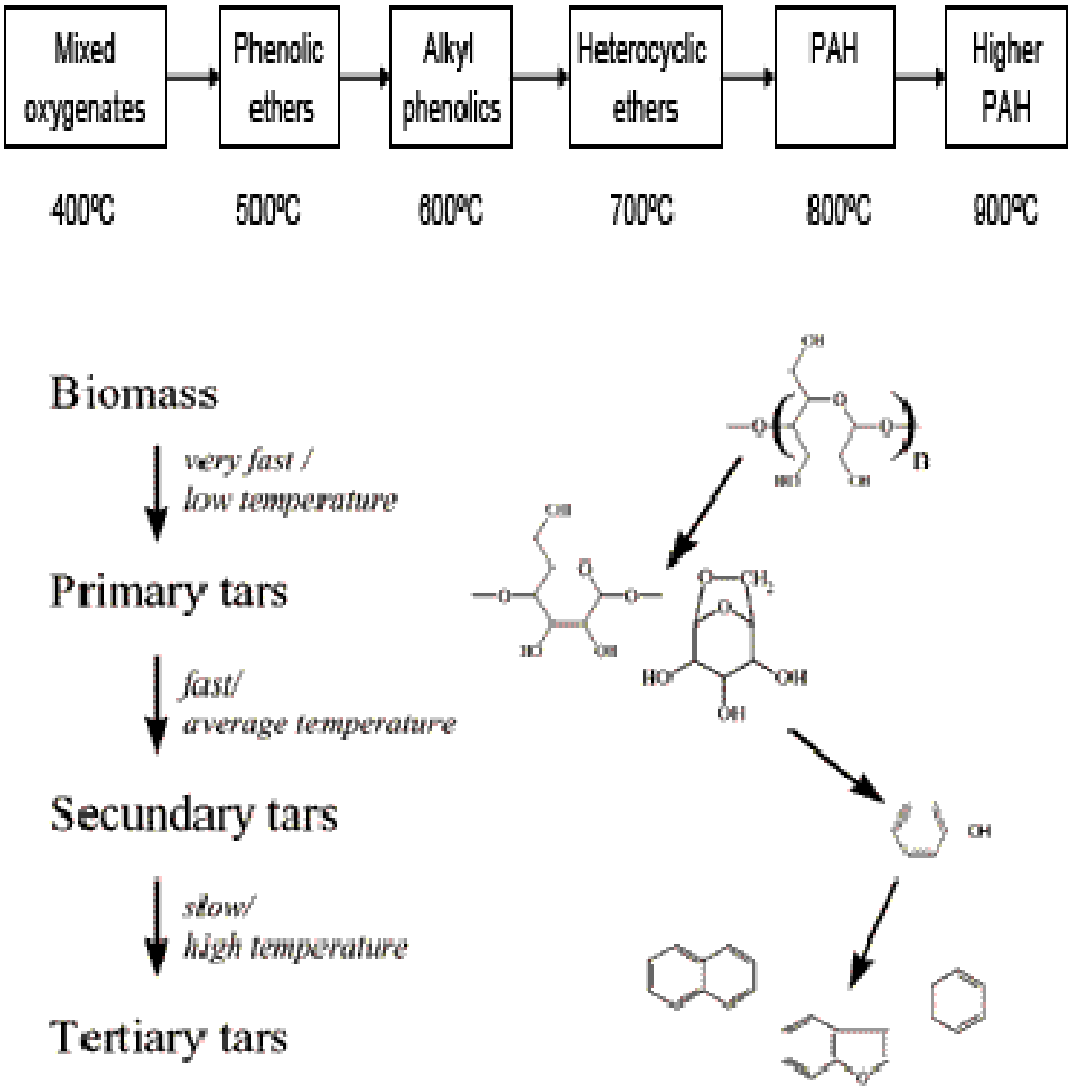

Figure 2.2: Tar formation scheme in the whole gasification process (Morf et al., 2002)

In some literature, the tars have been classified according to their solubility in water and condensation. The classification enables the understanding of the tars to be easy in terms of their physical and chemical properties. Table 2.2 shows how the tars can be classified into five classes.

Table 2.2: Classes and descriptions of tars (Kiel et al., 1999; Devi et al., 2005)

Class	Description
1	**Heaviest** tars that condense at high temperatures even at very low concentrations
2	**Heterocyclic** compounds (e.g. phenol, pyridine, cresol): Compounds that generally exhibit high water solubility due to their polarity
3	Aromatic compounds(1 ring e.g. xylene, styrene, toluene): **light** hydrocarbon not important in condensation and water solubility
4	**Light** polyaromatic hydrocarbons [PAH] (2 ~ 3 ring PAH compounds e.g. naphthalene, fluorine, phenanthrene): Condense at relatively high concentration and intermediate temperature
5	**Heavy** polyaromatic hydrocarbons (4 ~ 7 ring PAH compounds e.g. fluoranthene, pyrene, up to coronene): These compounds condense at relatively high temperature at low concentration

The last four classes of the tars described in Table 2.2 are often contained in the producer gas downstream gasifier. Therefore they should be considered in the design, the test and investigation of a tar removal test system.

A thermodynamic parameter called dew point is a useful tool for trouble shooting, optimisation and control of processes for tar removal in gasification producer gas cleaning. Dew point can be thermodynamically defined as the temperature at which the real total partial pressure of the tars equals their saturation pressure. Literally, it is the temperature at which the tars condense when the gas is cool down. The dew point of a tar component varies with its molecular size and concentration (Boerrigter et al., 2005). The effect of tar concentration in the gas on the tar dew point is shown in Figure 2.2a.

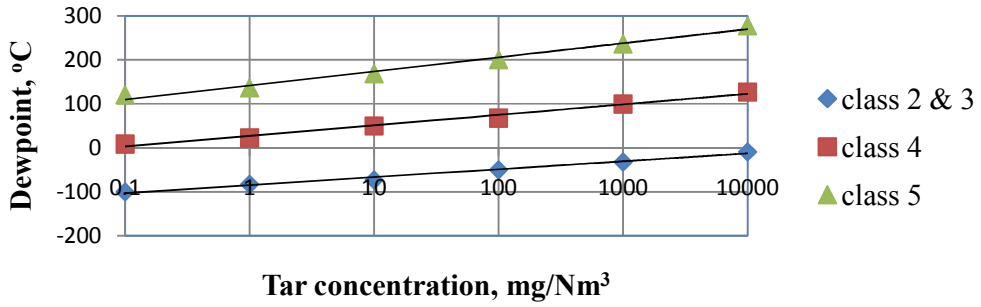

Figure 2.2a: Effect of tar concentration on tar dew point (Boerrigter et al., 2005)

Figure 2.2a shows that tar dew point increases with tar concentration. Therefore, the presence of class 2 and 3 tars in the gas would not cause problems to

an IC engine and gas turbine even if the gas tar concentration was 10g/Nm^3, typical of the raw gas quality of the UC gasifier. This is because the gas inlet temperature to an IC engine is about 40^oC (Buhler et al., 1997). As a result, such members of class 2 and 3 as phenol, pyridine, cresol, xylene, styrene, toluene and benzene would not be considered to be tars.

The producer gas of biomass gasification has a potential for power generation in IC engine and synthesis of FT gas, chemicals, SNG and as well as for use in fuel cell. However, this potential is hindered by the presence of the tars inherent in the gas. As tars have a relatively low boiling point, they condense when the temperature is reduced; therefore, the tars cause numerous problems in the application of the gas such as fouling, plugging, clogging and blocking of equipment as shown in Figure 2.3.

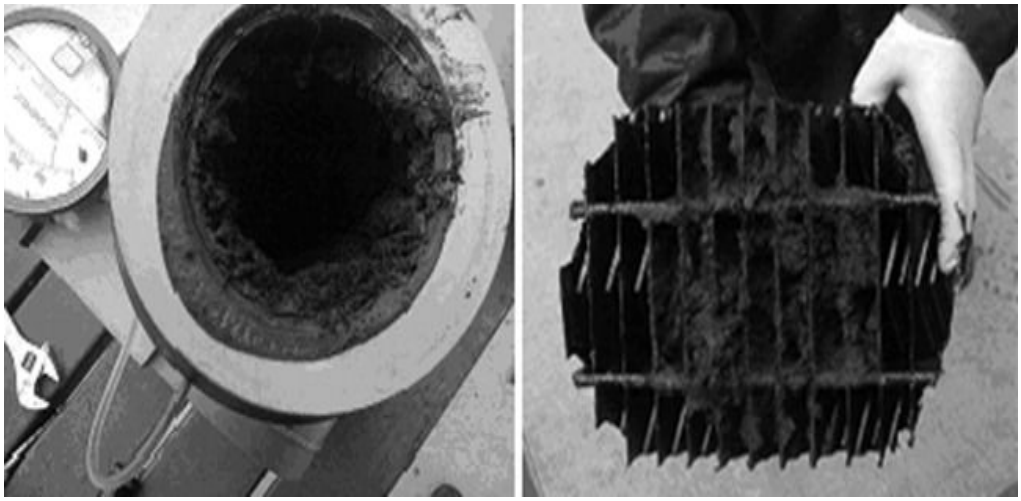

Figure 2.3: Plugging of piping and fouling of equipment (Zwart et al., 2009)

The above discussion of the biomass gasification process suggests that some operation parameters can be regulated in order to inhibit or reduce the formation of the tars during biomass gasification. These parameters include gasification temperature, steam to biomass feeding ratio in the steam-blown gasification, bed materials in fluidised bed gasifier, producer gas residence time in the gasifier and gasifier type, and are collectively called primary measure of tar reduction. However, the reduction of tars as function of gasification conditions needs to be looked at collectively. It has been reported (Delgado et al.,1995) that in a fluidised bed gasifier, catalytic bed material of dolomite with good porosity and particle size could reduce

tars to 0.5 g/Nm^3 from 10 – 200 g/Nm^3 tar in raw gas at steam gasification temperature of 780 ^oC and steam-biomass ratio of 1.The upper limit of the tar levels reported here (Delgado et al., 1995) are rather too higher and typical values for pyrolysis. It is likely that these tar levels were generated with gasifier operating at low temperatures, typical of pyrolysis operating temperature, below 600^oC (Kinoshita et al., 1994).

2.2. Primary Measures of Tar Reduction in Biomass Gasification

The primary measures of tar reduction are measures taken inside the gasifier to reduce tar level in the producer gas. The effects of these measures on tar reduction are subsequently discussed.

2.2.1. Effect of Gasification Temperature

It has been reported that gasification temperature has effects on the producer gas composition and the tar formation. According to the results presented in Figure 2.4 (Herguido et al., 1992), tar yield from the steam gasification of wood chips decreases with increasing gasification temperature and this effect is more significant above 750°C.

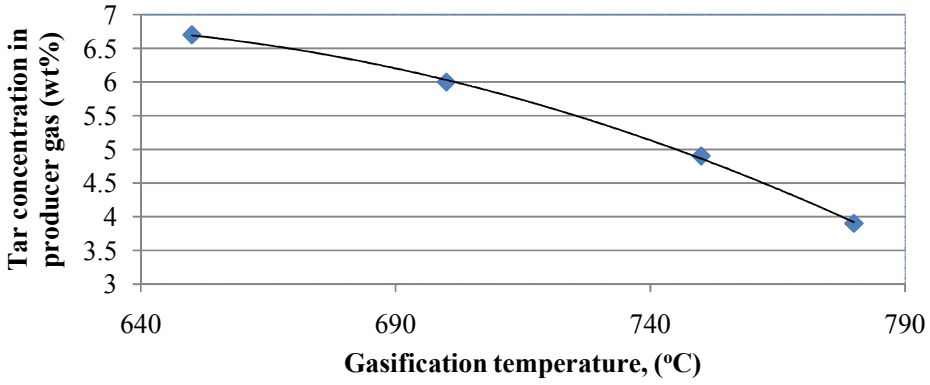

Figure 2.4: Effect of gasification temperature on tar concentration in the producer gas in steam biomass gasification (Herguido et al., 1992)

The results presented in Figure 2.4 can be explained based on the initial pyrolysis and subsequent gasification reaction pathways where the temperature has significant effect as shown in Figure 2.5 (Shafizadeh, 1982). As the major compounds in the biomass are cellulose and hemicelluloses (Hosoya et al., 2007), the analysis of Shafizadeh (Shafizadeh, 1982) on cellulose gasification can be applied to the biomass gasification.

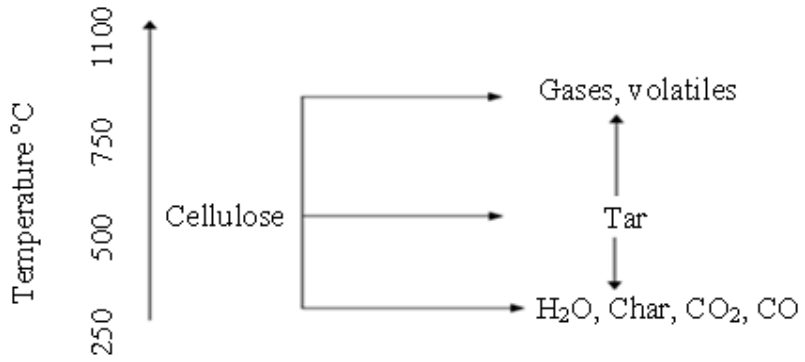

Figure 2.5: Effect of temperature on the conversion of cellulose to different products (Shafizadeh, 1982)

According to Shafizadeh (Shafizadeh, 1982), low temperatures of less than 300 ^{o}C are characterised with incomplete conversion of cellulose resulting into excess char, water vapour, carbon dioxide and carbon monoxide (Shafizadeh, 1982). However, at temperatures above 500 ^{o}C the conversion is complete resulting into gases and volatiles, mainly low molecular weight hydrocarbons (Shafizadeh, 1982).

In the steam biomass gasification, the addition of steam at temperatures higher than 500 ^{o}C promotes chemical reactions where conversion of the volatile gases to hydrogen and carbon monoxide occur. Among these reactions, carbon monoxide reacts with water vapour to form hydrogen in water-gas shift reaction (Shafizadeh, 1982). At high temperatures, char (carbon) reacts with carbon dioxide to form carbon monoxide in the Bourdourd reaction (Shafizadeh, 1982).

At temperatures of around 750°C, large molecular weight or polycyclic aromatic hydrocarbons (PAH) are produced as organic vapours which on heating produce low molecular weight volatile and, on cooling, large chain PAH. Consequently, high gasification temperatures above 850 ^{o}C, as shown in Figure 2.4, promote conversion of tars into lighter molecular weight gases and volatiles in the

producer gas. However, conflicting results have been reported (Shafizadeh, 1982) at temperatures above 850 ^{o}C as regards tar conversion to permanent gases and other volatiles. In this regard, Shafizadeh (Shafizadeh, 1982) reported that there was an increase in the amount of naphthalene at gasification temperature of 900 ^{o}C using birch wood as biomass and air gasification agent when a temperature range of 700 - 900 ^{o}C was examined. Similarly, Brage (Brage et al., 1997) reported that, in the gasification of birch wood, an increase of 2 - 8 g/Nm^3 naphthalene was observed when gasification temperature was increased from 700 to 900 ^{o}C. In both of the above reports, the amount of oxygenated and substituted 1-ring and 2-ring aromatics was found to be drastically reduced with the increase in gasification temperature. These results can be due to fact that naphthalene is reportedly a very stable compound such that it needs a catalyst to break down. The thermal decomposition of naphthalene starts at 1100 – 1200°C (Jess, 1996). Its complete decomposition occurs at much higher temperature of around 1400°C (Jess, 1996). However, it converts completely at a much lower temperature of 750°C in the presence of a Ni-MgO catalyst (Jess 1996).

2.2.2. Effect of Air Preheating and Air Flow Rate in Air-Blown Biomass Gasification

In biomass gasification with air as gasification agent, the temperature of feeding air may have some effects on the producer gas composition and tar concentration. It has been reported that preheating air used in the gasification of woody biomass reduces the amount of tar in the producer gas with supporting data given in Table 2.3 (Bhattacharya et Dutta et al., 1999). However, preheating the air can increase the energy efficiency and energy output. The high temperatures after pre-heating can also increase the gasification temperature which tends to cause destruction of inner wall lining of the gasification column and create ash fusion problems.

Table 2.3: Tar levels in producer gas from air gasification of woody biomass with and without preheating of the fed air (Bhattacharya et Dutta et al., 1999)

Air temperature after preheating (^oC)	Air flow rate (*l*/min)	Tar content (mg/Nm^3)	
		With preheat	Without preheat
210	140	3.88	28.23
250	120	8.54	17.74
295	100	20.96	40.81

The results in Table 2.3 further imply that higher air flow rates would enhance the reduction of tar content in the producer gas. These results can be verified by the observation of Houben's team (Houben et al., 2005) that at moderate temperatures and in presence of hydrogen and radicals (i.e. chemically reactive fragmented compounds), tars are cracked which prevents tar polymerisation. However, air flow rate and preheating should regulated such that air flow rate should be reduced while temperatures of pre-heating increased to inhibit combustion while enhancing gasification. The gasification equivalence ratio is within 0.2 and 0.4 (Beenackers et van Swaaiji et al., 1984).

2.2.3. Effect of Steam-Biomass Feeding Rate (S-B) Ratio in the Steam-Blown Biomass Gasifiation

In the biomass gasification with steam as gasification agent, the ratio of steam to biomass feeding rates (S-B) also influences the producer gas composition and tar content, generally. According to the results of Herguido's team as depicted in Figure 2.6 (Herguido et al., 1992), the concentration of the tars in the gas is reduced with increasing the S-B ratio. However, this finding is in contrary with the observation of Rabou's steam (Rabou et al., 2005) that recycling of liquid tar and water mixture to the gasifier inhibited tar destruction while the moisture content in the producer gas was increased by 20% and the gasification temperature was reduced by 20 ^oC. Therefore, there must be an optimum S-B ratio for the tar reduction.

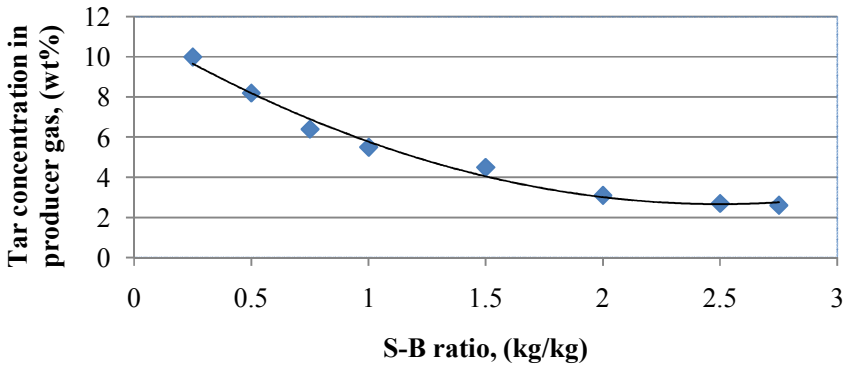

Figure 2.6: Effect of steam to biomass feeding rate ratio on tar concentration in the producer gas in steam biomass gasification (Herguido et al., 1992)

The results presented in Figure 2.6 are consistent with the observations of Orio's team et al. (Orio et al., 1997) who found that tars from steam gasification have more phenolic and C-O-C bonds which are easily converted by steam reforming reactions than those from air gasification process. Similarly, Perez's team (Perez et al., 1997) found that pure steam produces more phenolic tars which are easy to be catalytically converted than those from biomass gasification using mixture of steam and oxygen as the gasification agent.

The effect of steam-biomass ratio on tar formation can be better interpreted if it is considered in relation with gas composition and gas heating value as shown in Figure 2.7 and Figure 2.8.

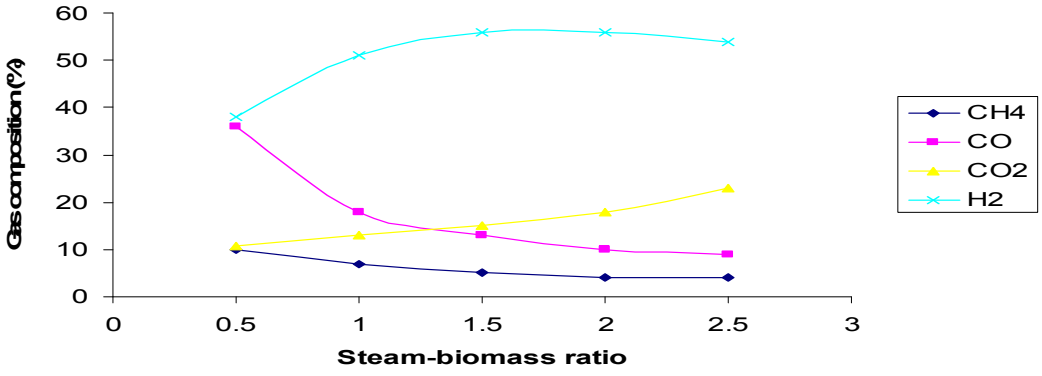

Figure 2.7 : Effect of steam to biomass feeding rate ratio on gas composition in steam biomass gasification (Herguido et al., 1992)

Figure 2.7 shows the results from steam biomass gasification in dual fluidised bed gasifier which has similar structure to the UC gasifier (Bull, 2008). The gasifier consists of two columns, one being the bubbling fluidised bed as gasification column and the other called the circulating fluidised bed as combustion column. In the gasifier, the siphon and chute designs are carefully designed as these structures also have an effect on the producer gas composition. The siphon is the structure for sealing the gas transfer between the gasification column and the combustion column. The chute is the pathway for the solid char and bed materials to move from the gasification column to the combustion column. Therefore, any inter-column leaking of gases will increase the content of N_2 and CO_2 in the producer gas.

Figure 2.7 shows that the H_2 content and CO_2 content increase while the CO content decreases with increasing the steam to biomass ratio. The hydrogen increase can be explained by the enhanced water-gas shift reaction due to the increased water vapour which results when the steam to biomass rate ratio is increased. The steam to biomass rate ratio has insignificant influence on the CH_4 content.

The low heating value (LHV) is defined as the heat released by complete combustion of a given fuel when the water vapour as resultant product exists in gas state. LHV is used as a gas quality parameter as high LHV is desired for the producer gas. Figure 2.8 shows that the LHV is decreased when the steam to biomass rate ratio is increased. However, the reasonable way of assessing the effect of steam to biomass ratio on the producer gas' low heating value is to consider the total LHV as the LHV changes with increasing steam reforming reactions which increase the composition of hydrogen in the producer gas.

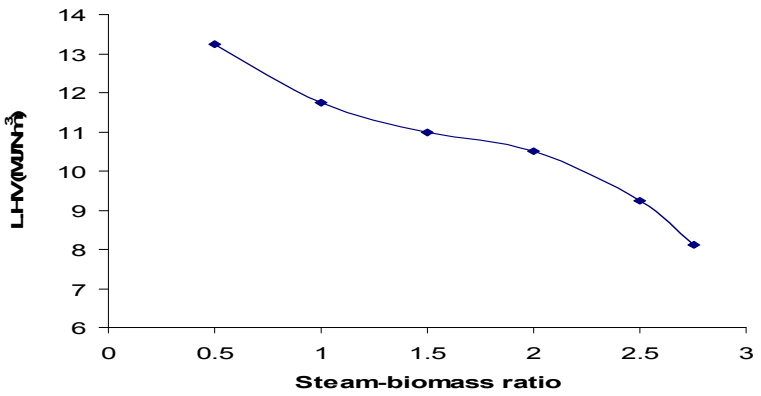

Figure 2.8: Effect of steam to biomass feeding rate ratio on lower heating value (LHV) of the producer gas from steam biomass gasification (Herguido et al., 1992)

However, based on Figure 2.8, the decreases in the LHV with increasing the steam to biomass rate ratio can be attributed to the increase in the CO_2 levels in the gas, as shown in Figure 2.7. As CO_2 is inert, it dilutes the gas and thus reduces the LHV of the gas.

2.2.4. Effect of Producer Gas Residence Time in the Gasifier

The general effect of producer gas residence time on tar concentration at an operating temperature of 900 ^{o}C was investigated by Houben (Houben, 2004) and the results are shown in Figure 2.9. The tar concentration was measured by solid phase absorption (SPA) method (Houben, 2004).

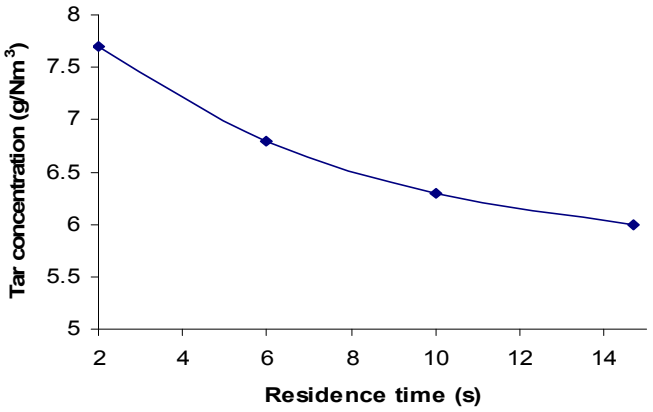

Figure 2.9: Effect of producer gas residence time on tar concentration in the producer gas (Houben, 2004)

The results in Figure 2.9 were obtained from experiments conducted in air biomass gasification in a downdraft fixed bed gasifier. However, the trend from the study could be applied to a more general situation where the producer gas is cracked at high temperatures.

From Figure 2.9, it is seen that tar concentration decreases with increasing producer gas residence time. Therefore, an optimised residence time needs to be determined as longer residence time theoretically enhances the complete tar conversion but in this case the gasifier size is significantly increased or impractical in circulating fluidised bed gasifier.

2.2.5. Effect of Bed Additives or Catalytic Bed Materials

In a fluidised bed gasifier, bed material may be used to crack the tars where the bed material is in contact with the producer gas. The effect of bed material on the tar reduction has been extensively studied and reported (Milne et al., 1998; Dou et al., 2003; Kimura et al., 2006). In the study, the common catalysts being used are:

- Ni-based catalysts,
- Calcined dolomites and magnesites,
- Eolites,
- Olivine
- Iron

- Limestone
- Magnetites
- Zeolites
- Iron ore
- Calcite
- Quartz
- Ash
- Mixtures of many of the above with silica sand.

The effectiveness of dolomite catalysts to cracking tars was studied by Devi's team (Devi et al., 2005) who reported that the conversion of the tars into simpler hydrocarbons, carbon, CO, H_2 and H_2O was mainly in the bed temperature range of 800 - 900 ^oC at atmospheric pressure. These operating conditions are easily attainable in the UC gasifier. Therefore, the incorporation of these additives into bed material would easily be done.

The key factor for the choice of a catalytic bed material is the suitability for application in the gasifier and the target use of the producer gas. If the producer gas is to be used in an IC engine, particular attention should be paid to the removal of both light tars and heavy tars because their dew points are normally above the engine feed temperature. However, in this case the removal of GC-undetectable tars heterocyclic tars and light aromatic tars is less critical as the dew points of these types of tars are less than -9 ^oC (Kiel et al., 1999) at atmospheric pressure.

According to Devi's team (Devi et al., 2005) in a fluidised bed gasifier with dolomite added in sand as bed material, the conversion of light tars and heavy tars is about 55% and 90% at a bed temperature of 900 ^oC. Corella's team (Corella et al., 1988) reaffirmed the suitability of using dolomite as bed material but if the calcined dolomite is added, the tar content could be reduced from 6.5 wt% to 1.3 wt% tars. Similar results were reported by Narva'eh's team (Narva'ez et al., 1996) that the reduction of tars by 40% was achieved by using 3% calcined dolomite catalyst as the bed material.

Some research findings have been documented where in-bed catalysts have performed selectively. Bilbao's team (Bilbao et al., 1998) recorded that 50 wt% of Ni-Al catalyst in sand as the bed material could yield a producer gas with hydrogen

content of 62% but considerably decreased the methane content as well as tar content. Rapagna's team (Rapagna et al., 2000) found that olivine catalyst reduced the average tar content by 94% which was 2.4 g/Nm^3 compared to original tar content of 43 g/Nm^3 with only ordinary sand. Rapagna's team (Rapagna et al., 1998) reported, in another document, that further reduction of tar content in the producer gas was possible to a level of 0.3g/Nm^3 using sand and a catalyst.

In-bed catalyst can affect gas composition and tar yield (Devi et al., 2002). This is because the tars can be cracked at much lower temperatures (600 - 800°C) than would otherwise be possible (1000 °C plus) (Brown, 2003). Different bed materials have been tested at Guessing Austria with toluene as a model tar to select a suitable catalytic bed material (Rauch, 2004) as shown in Figure 2.9a.

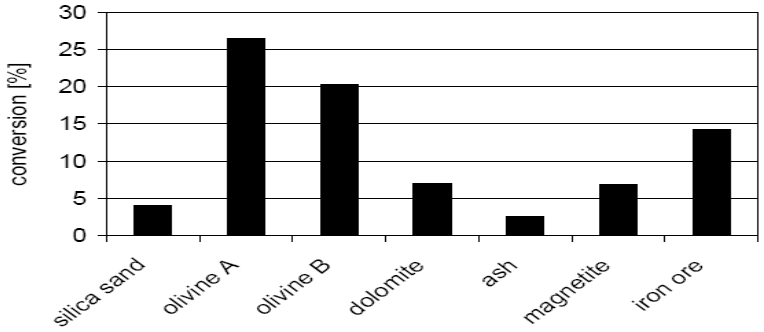

Figure 2.9a: Performance of various catalysts at converting toluene as model tar (Rauch, 2004).

Figure 2.9a shows that olivine A was the best in-bed catalyst. This result would be useful if toluene was the most abundant tar component in the producer gas of the DFB Guessing gasifier. In case of the UC gasifier, naphthalene is the most abundant tar component (Bull, 2008). On the other hand, naphthalene has been used in a similar manner as was used by Rauch, 2004 and (Bolhar-Nordenkkampf et Hofbauer et al., 2004). Therefore, naphthalene would be used to test its reduction by various in-bed catalysts for the case of the UC gasifier.

Although in-bed catalysts have been reported to be generally successful at reducing total tar concentration, there are specific drawbacks in using these catalysts. For example, nickel based catalysts have been widely tested in gasifiers and shown to be successful (Sutton et al., 2001). However, they are susceptible to severe

deactivation by carbon deposition and H_2S poisoning. Nevertheless, the deactivation would not arise in a DFB gasifier as the deposited carbon can easily be burnt off by the circulating bed material, especially in the combustion zone. Therefore, using nickel would be advantageous as they not only reduce tar levels but also increase gas yields and reduce ammonia levels (Devi et al., 2002).

The effect of in-bed nickel based catalysts were investigated at a 100 kW DFB gasifier operating at 850^{o}C and atmospheric pressure whose results are shown Figure 2.9b (Rauch et al., 2004).

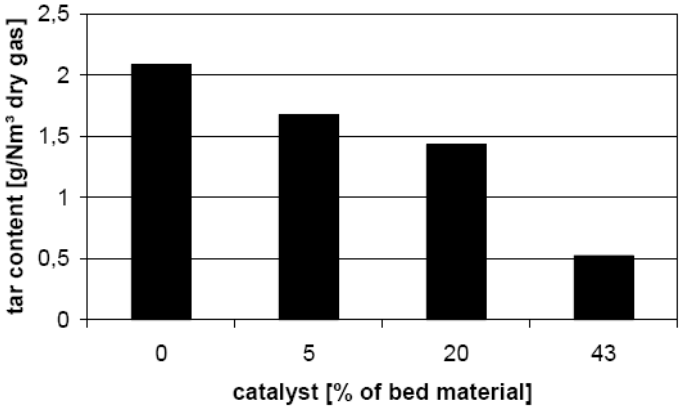

Figure 2.9b: Effect of in-bed nickel based catalysts on tar reduction (Rauch et al., 2004).

Figure 2.9b shows that increasing the percent of the nickel catalyst in the bed material increase the tar reduction levels as the concentration of the tars in the gas is reduced. However, increased amount of catalyst in the bed material may cause problems such as attrition, entrainment and agglomeration.

Besides nickel based catalysts, a combination of olivine and calcite has been tested with great success. Olivine has good attrition resistance and tar reduction, and so does calcite. Olivine catalysts are very successful at steam reforming methane and tars (Devi et al., 2002). Although steam reforming methane reduces the heating value of the producer gases, it increases the hydrogen to carbon monoxide ratio which is good for liquid fuel synthesis. The effect of in-bed catalysts on tar reduction and composition of the producer gas were investigated tabulated in Table 2.3a (McKinnon, 2010).

Table 2.3a: Average producer gas composition using olivine/calcite mixtures as bed materials, compared with values for greywacke and pure olivine (McKinnon 2010).

Gas	Greywacke	Olivine	Olivine + 25% Calcite	Olivine + 50% Calcite
H_2	21.2%	26.1%	29.5%	40.0%
CH_4	14.2%	13.0%	11.6%	12.0%
CO	36.9%	32.6%	28.1%	20.2%
CO_2	21.5%	22.8%	25.9%	23.4%
C_2H_4	5.2%	4.5%	4.1%	3.3%
C_2H_6	1.0%	0.9%	0.9%	0.9%
H_2:CO	0.57	0.80	1.05	1.98

In a nut shell, in-bed catalysis can help to reduce tar levels in the producer gas. However, the choice of the catalyst is so important that it can affect the smooth operation of the gasifer. In this regard, the criterion for the choice of catalytic bed materials is that they should be economically available, attrition resistant, active and selective to only reduce tar levels. Attrition of bed material in a fluidized bed is directly proportional to gas and particle velocities (Devi et al., 2002). That leaves the problem of agglomeration as one of the problems that an in-bed catalyst can cause, as mentioned above. However, studies have found that the problem of agglomeration can be circumvented by adding limestone (say 25 %) and silica sand (say 75 %) to the bed material (Devi et al., 2002). In view of the criteria for the choice of a catalyst, the Ni/Mo catalyst has not been used widely because of its vulnerability to being poisoned by sulphur, chlorine and alkali metals. Although the Ni/Mo catalyst is said to be most effective at low temperatures below 650 ^{o}C, the tars levels at gasification temperature below 650^{o}C are very large and which makes downstream tar removal problems very difficult to solve (Kinoshita et al., 1994).

2.2.6. Effect of Free Radicals in Air and Oxygen Biomass Gasification

Free radicals are formed when covalent bonds of light tars are broken by high energy. In the case of the UC gasifier, it is energy carried by the bed material. The formation of the radicals should be avoided by regulating the gasification

temperature as it yields increased levels of heavy tars due to the polymerization of the radicals with light tars especially naphthalene.

Houben's team (Houben et al., 2005) investigated the effects of radicals on tar cracking using naphthalene as model tars, and found that at moderate temperatures of about 500 ^{o}C and high levels of hydrogen gas and radicals, polymerization of naphthalene and soot formation were inhibited in favour of cracking of naphthalene into permanent gases. However, at the same temperatures, higher air-biomass ratio in excess of 0.2 inhibited the cracking but promoted polymerization and soot formation. The phenomenon of 1-2 ring tar polymerization and soot formation was explained by a mechanism of two pathways:

- Direct aromatic radical combination e.g. two benzene rings making biphenyl.
- A series of H-abstraction or acetylene addition.

The reaction process of the inhibition of polymerization and soot formation could be summarised as follows $A_i^{\cdot} + H_2 \rightarrow A_iH + H^{\cdot}$ where $A_i^{\cdot}$ and $H^{\cdot}$ are aromatic and hydrogen radicals, and A_iH H_2 are aromatic and hydrogen molecules. This process shows that the aromatic radicals are neutralised before they can be combined together or with acetylene to form heavy tar compounds or soot respectively. Therefore, the observation and results of Houben's team (Houben et al., 2005) can be used for optimisation of controlled combustion temperature in the air or oxygen biomass gasification to avoid radical formation which yield increased tar levels.

2.3. Secondary Measures of Tar Reduction in Biomass Gasification

Secondary measures of tar reduction are those taken downstream gasifier to reduce tar levels in the gas such as secondary bed filter, plasma tar removal technology, scrubbers, secondary catalytic cracking, secondary tar reforming and so on. These are discussed in the subsequent subsections of Chapter 2 and have been classified as physical and chemical measures of tar reduction.

2.3.1. Physical methods of Tar Reduction in the Producer Gas

In the physical downstream tar removal methods for tar reduction from the biomass gasification producer gas, the tars are removed from the gas without

involving a chemical reaction. In other words, the tars are just transferred from one phase to the other without changing their chemical nature. These methods can be classified as wet processes, dry processes or wet/dry processes. In the wet processes, the tars are transferred from the producer gas into liquid phase through gas absorption by solvent, tar condensation and separation by filtration or centrifugation. The dry processes use filters to separate dust and in the process the tars are removed as they condense and/or get absorbed on the dust. The wet/dry process is a combination of these two processes. The details of these tar removal technologies are described in the subsequent subsections.

2.3.1.1. Tar Removal by Cooling/Scrubbing Columns

The removal of tars is performed in a unit where a cooling tower is coupled with wet aqueous scrubber (Watanabe et Hirata et al., 2004). The unit is normally located after the cyclone where the dust is firstly removed from the producer gas after the producer gas exits from the gasifier. After the cyclone, the gas is further cleaned in a scrubber in which the gas is in contact counter currently with cooling water. The used water is then recycled and cooled in a cooling tower as shown in Figure 2.10.

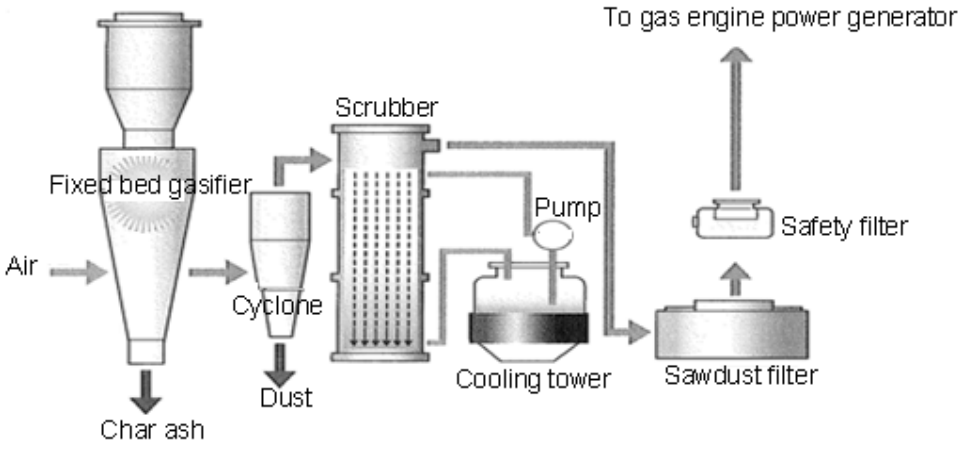

Figure 2.10: Schematic diagram of a gasifier and tar removal by cooling/scrubbing towers (Watanabe et Hirata et al., 2004)

The gas then exits the scrubber onwards to the sawdust filter where some remaining tars and water vapour are removed before being fed into an IC engine.

The immediate concern with the technology depicted in Figure 2.10 is the problem of wastewater treatment. In addition, the quality of the producer gas would not be suitable for most of end use rather for power generation in IC engine or gas turbine engine. However, the tars retained in the sawdust can be recycled to the gasifier as energy source. Moreover, the state of the art for tar removal downstream gasifier by wet scrubbing is the use of non-aqueous scrubber which avoids wastewater treatment problems.

2.3.1.2. Tar Removal by Venturi/cyclone Scrubbers

The schematic diagram for the operating principles of a venturi/cyclone scrubber is shown in Figure 2.11.

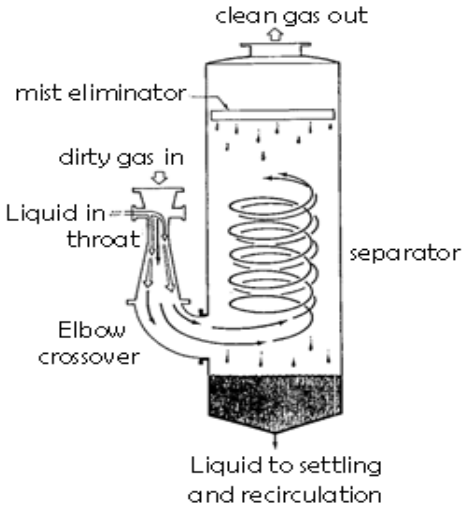

Figure 2.11: Operating principles of venturi/cyclone scrubber, adapted from (Dutta, 2007)

As shown in Figure 2.11, the raw producer gas is firstly accelerated into the venturi to its maximum velocity at the throat where it is sucked into a column where the gas is in contact with downward flowing liquid. The effect of gas sucking into the liquid forms foamy dispersion of gas in the liquid and the mixture flows down to

column bottom and then goes to a separator. In the separator, the dispersion mixture swirls into a cyclone where the gas escapes from the liquid and thus the gas and liquid are separated. Any entrained mist in the gas is then removed by the mist eliminator.

In a similar technology, the venturi scrubbers without downstream cyclone has been used to reduce the tar content in the producer gas of biomass gasification with the efficiency ranging 51 – 91% (Milne et al., 1998). In order to achieve high efficiency, the velocity of the gas at throat was 56m/s and the pressure drop through the throat was almost 4kPa (Milne et al., 1998). In their study, the tar concentration produced by an updraft rice husk gasifier was reduced by 20 times from 80g/Nm^3 to 4g/Nm^3.

In another similar setup, a combination of cooling tower and venturi scrubber was used in a closed system for tar removal and dust separation. The system operated at slightly vacuum of 1.4 kPa, a liquid to gas mass flow rate ratio of 1 and the tar concentration at the exit was lower than 10 ppmv (Fernandez, 1997).

Since the use of the venturi requires high velocities of the gas, the technology is unsuitable for application where the gasifier operates at atmospheric pressure.

2.3.1.3. Tar Removal by Granular-Bed Filters

Granular-bed filter system for gas cleaning consists of a dust-laden gas chamber, a granular filter bed, and a clean-gas chamber. The material for the bed may be sand, gravel, coal, coke, pebbles, or packing of various shapes (Guzhev, 1971). They can be designed with bed in horizontal, vertical, or inclined position. The bed might be fixed, moving by gravity, or rotating. Sometimes the design allows for the regeneration of the bed material by unloading and replenishing the bed, partial regeneration by vibration, partial regeneration by reverse-flow purging, or complete regeneration by washing the bed. Some filters have been designed according to the retaining grids, whether sieve, louver, tubular, or made up of rotating sprockets. Others have been design according to the number of trays with filter bed which could be one-tray or multi-tray. There are also other designs based on the operating cycle, whether periodic or continuous operation (Guzhev, 1971).

Granular-bed filters have been used for the removal of both tars and dust from gases. For instance, 80 to 95%w/w efficiency of dust and 60 to 95%w/w of tars have been removed in a granular bed filtration from biomass gasification producer gas (Sharan et al., 1997).

Recently, a concept of removing tars from the producer gas of biomass gasification by using a moving bed granular filter has been developed at Energy Centre of the Netherlands (ECN) (van der Drift et al., 2005). The concept is called TREC-module which stands for the Tar REduction with Char.

In the TREC-module operating at 900^{o}C, a moving granular bed is trapped in a fixed bed and the gas is allowed to flow across the bed. The bed is always moving to avoid high pressure drops. In addition, the filter is especially designed to make char particles partly settled on the top of the bed so that their concentration is evenly distributed in the bed. The schematic diagram showing the movement of the bed and the gas is shown in Figure 2.12.

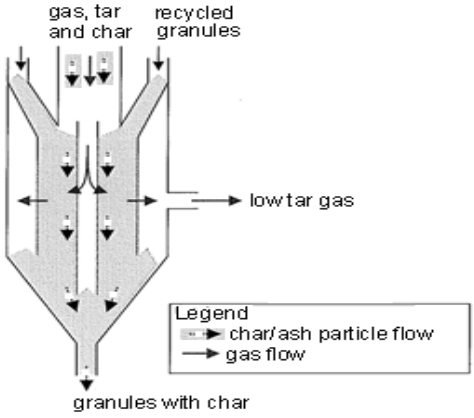

Figure 2.12: Schematic diagram of the TREC-module for the removal of tars and particles downstream a gasifier (van der Drift et al., 2005)

The TREC-module is placed in downstream of a fluidised bed gasifier at ECN. It is designed to trap char particles and therefore serves as a high-temperature filter. In addition, it acts as a reactor in which the composition of raw producer gas is altered after the TREC-module and the experimental results are given in Table 2.4.

Table 2.4: Typical product gas composition before and after TREC-module (van der Drift et al., 2005)

		Before TREC	After TREC
CO	Vol% wet	14	14
H_2	Vol% wet	5.6	10
CO_2	Vol% wet	13	13
CH_4	Vol% wet	4.2	3.5
C_{2-5}	Vol% wet	1.3	0.6
C_{6-7}	Vol% wet	0.4	0.3
H_2O	Vol% wet	18	12
Tar(C_{8+})	g/nm^3wet	10.6	2.4

Table 2.4 shows that the amount of the tars decreases significantly after the TREC-module. In addition, it has been reported that the phenol content in the gas is almost completely eliminated. The tar dew point has been calculated to be 170°C, a marked improvement from the original tar dew point of 350°C. The tar dew point of 170°C is induced by unconverted heavy tar compound of C_{16+} hydrocarbons.

In short, in the TREC-module, char and ash are entrained in producer gas containing tars and are carried until reaching a location where the producer gas disengages from char and ash in the downstream of the gasifier. The TREC-module helps in tar reduction because the tar is adsorbed onto the char/ash. The TREC-module also acts as a reactor in that the composition of the H_2 in the producer gas is increased because the steam reforming reaction is favoured by the high operating temperature of 900^oC. The development of this technology has been inhibited by the problems of destruction of inner wall lining and ash fusion because of its high operating temperature of 900^oC.

Similar results to those given in Table 2.4 were also reported for tar removal by filters of char at various temperature (El-Rub Abu, 2008). El-Rub Abu, 2008 used naphthalene as a model tar compound to investigate its removal by the char. The investigation was done off-line a gasifier as shown in Figure 2.13.

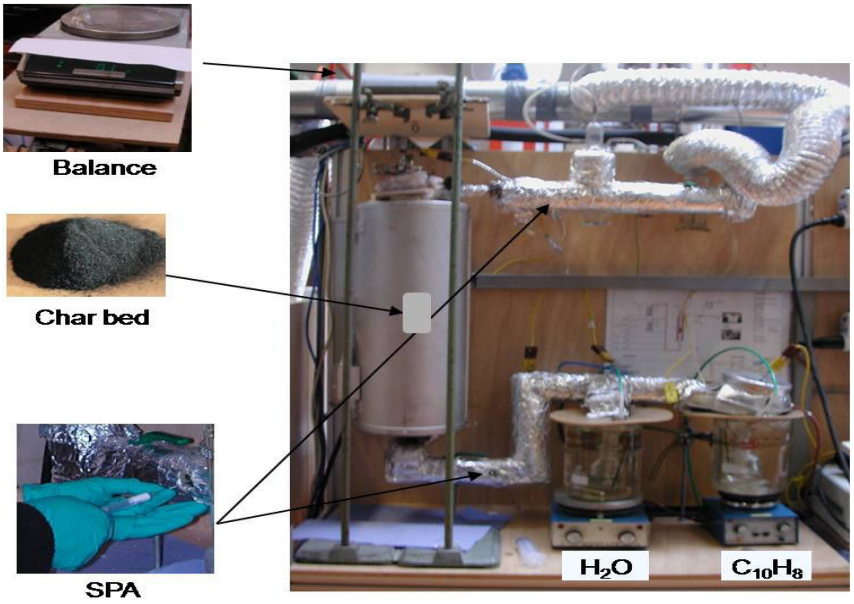

Figure 2.13: A Photograph of an experiment setup to investigate tar removal by char (El-Rub Abu, 2008)

The results of his investigation showed that simulated tar (naphthalene) could be removed with efficiency of up to 99.5% by char filter and the efficiency was found to increase with temperature as shown in Figure 2.14. It should be noted that the tar removal efficiency using the filter decreases with time when the tar loading increases. However, this result was not reported in the work of El-Rub Abu (El-Rub Abu, 2008).

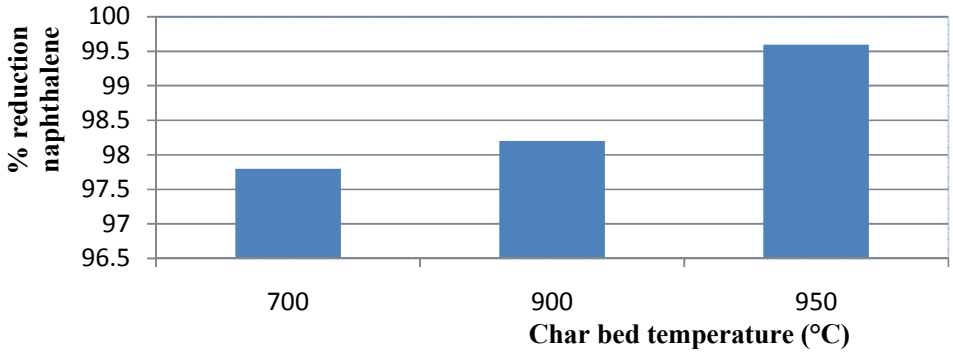

Figure 2.14: Effect temperature of the char bed on tar removal efficiency El-Rub Abu (El-Rub Abu, 2008)

This technology of tar reduction in the downstream gasifier cannot easily be applied unless a secondary process is incorporated which provides for recycling the char containing tar to the gasifier and replenishing the bed with fresh tar free char.

In the case of the TREC-module, it can effectively remove tars from the biomass gasification producer gas at high-temperatures. However, the cleaned producer gas may not be good enough for liquid fuel synthesis or use in an IC engine. An in-bed olivine catalyst is reported to be able to reduce the tar concentration to a range of 2-5g/Nm^3 in a dual fluidised bed gasifier (Proll et al., 2005). Therefore, further treatment of the producer gas would be needed when the gas is used for liquid fuel synthesis or in IC engine.

2.3.1.4. Tar Removal by a Rotational Particle Separator

A rotational particle separator (RPS) is designed principally for the removal of particles from gas. As mentioned earlier, the tars are often adsorbed by particles especially char and ash. Therefore, the RPS can remove tars when it removes the particles.

The working principle of the RPS is based on separation by centrifugation. The separation involves the application of a separation element which is cylindrical in shape and rotates around its symmetry-axis. The element consists of a large number of small channels, typically one millimetre in diameter, arranged in parallel to the symmetry and rotation axis. When fluid is led through the channels, the particles entrained in the fluid are driven by the centrifugal force to the walls. Since the radial distances for particles to move to the collecting surfaces of each channel are small, particles of small sizes are capable of being separated, such as ash and char adsorbed with tars. A schematic diagram for a setup of an RPS in a gas cleaning process is shown in Figure 2.15.

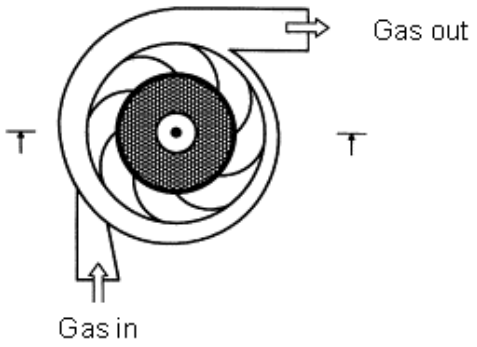

Figure 2.15: An illustration of gas flow through an RPS (Brouwers, 1997)

An RPS can be operated with fixed or variable rotation speed and is capable of removing tar aerosols. The particle laden cylinder channels can be cleaned by injecting compressed nitrogen from the top of the rotating filter element through a nozzle.

A certain design mode of an RPS was made at the Energy Centre of the Netherland (ECN). In this design, the RPS contains a rotating cylinder from which the central part is blocked and the outer ring is filled with narrow channels as shown in Figures 2.16.

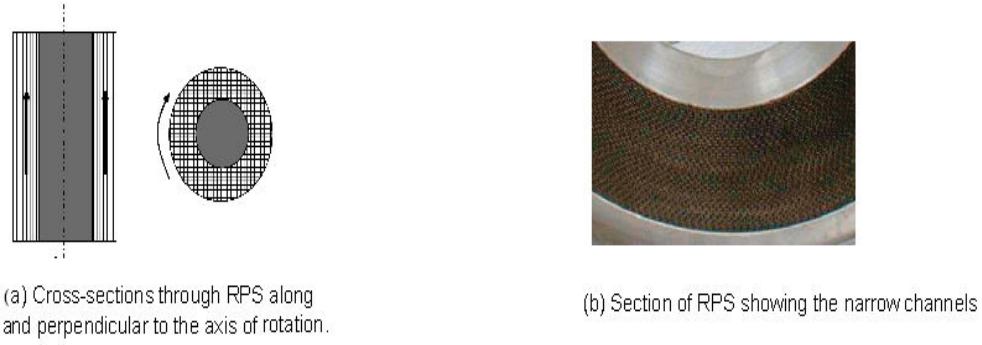

Figure 2.16: Illustration of core parts in the RPS designed by ECN (Rabou et al., 2009)

In a classic RPS, the gas flows through the narrow channels and the gas rotation generates a centrifugal force that drives particles or droplets contained in the gas to the walls. During the tests at ECN, the top of the RPS was continuously sprayed with water at rate of 200 *l*/h to flush tar droplets and dust from the channel

walls. The RPS operated at a rotation rate of 3000 rpm and a temperature of 40 – 50 °C. The gas flow rate was 190Nm^3/h which induced high pressure drop over the RPS. Tests were conducted by using 25% of the maximum flow rate and the tar content was reduced from 8 to 4.5 g/Nm^3 (Rabou et al., 2009).

The summary about the RPS tar removal technology is that the tar is adsorbed onto the char entrained in the gas and also the tar condenses as the gas temperature decreases. The adsorbed and condensed tar is separated from the gas by a centrifugal force which tosses the condensed tar and char/ash containing tar to the wall of the RPS. In some cases as in an operation at ECN, the water sprayer is plumbed on top of the RPS to enhance tar removal by dissolving them in the spray. Generally, tar removal by RPS is enhanced by high gas flow rate in which case the gasifier should be pressurised. Therefore, this technology cannot be applied at UC gasifier because it operates at atmospheric pressure. Otherwise, this technology can be used at UC gasifier if the producer gas is boosted downstream which increases the operating costs and therefore undesirable.

2.3.1.5. Tar Removal by a Fabric Filter

The use of fabric filters for flue gas dedusting in combustion processes is a mature and proven technology. Nevertheless, they have been used sparingly in gas cleaning of biomass gasification producer gas. Hasler and Nussbaumer have reported a study where two fabric filter units were tested with producer gases from an IISc/Dasag downdraft gasifier and a KARA downdraft gasifier in a laboratory scale. The tests were conducted by using one filter bag with a total filter surface of 0.31m^2 and the units were heated to 350°C which showed poor tar removal efficiencies because the operating temperature was below tar dew point of the gas. However, when the filter material made of ceramic fibre tissue was used, the system operated up to a temperature of 600°C at which tar would not condense, the efficiency improved. The schematic setup for their study is shown in Figure 2.17.

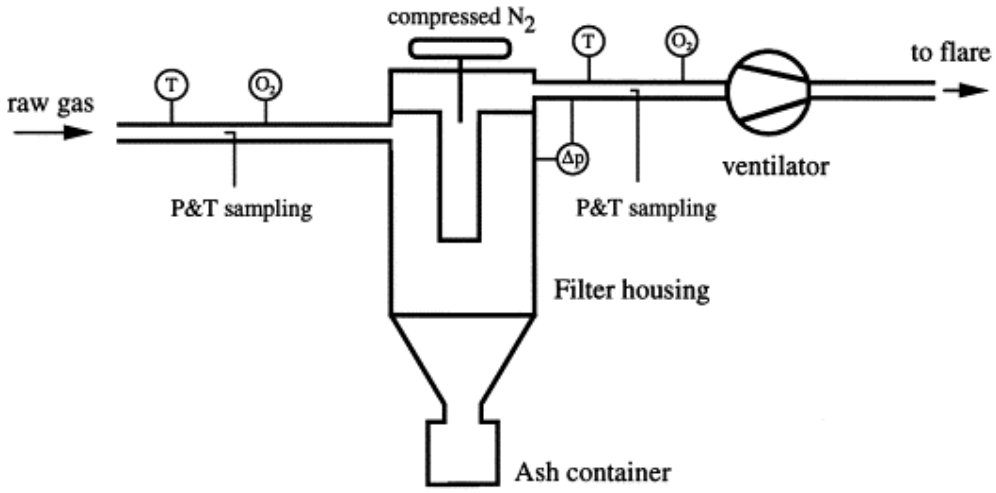

Figure 2.17: Schematic of the fabric filter unit for particle and tar removal studied at the IISc/Dasag gasifier (Hasler et Nussbaumer et al., 1999).

During their study, the fabric filter unit was fed with a slip stream of the raw producer gas from the IISc/Dasag gasifier. The sampling of the tars was made before and after the filter, and maximum 50% tar reduction was recorded. The clean gas passed a ventilator and a water seal as a fire safety precaution before it was flared in a swirl burner. The dedusting of the laden filter bag was made by back-flushing with a jet pulse of compressed nitrogen. Since the state of the art for tar reduction after a ceramic fibre is higher efficiency than 51 - 91% (Han et Kim et al., 2008), the tar reduction by this method was not satisfactory. The low tar reduction of 50% can be attributed to many factors such as the gas tar dew-point being higher than the filter operating temperature, polymerisation of the tars on the filter cake and tar desorption which had previously been adsorbed. However, these factors are mere speculations and thus need further investigation.

2.3.1.6. Tar Removal by an Activated Carbon Filter

The tar content in a producer gas can be reduced significantly by passing it through a fixed bed of a carbon filter in which the tars are adsorbed onto carbonaceous materials such as lignite coke or activated carbon.

Hasler and Nussbaumer (Hasler et Nussbaumer et al., 1999) conducted tests on tar adsorption by a carbon filter in a laboratory scale fixed bed with granular lignite coke as an adsorbent as shown in Figure 2.18.

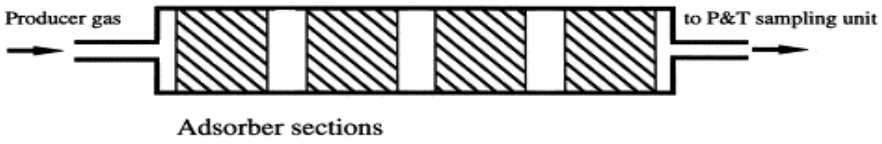

Figure 2.18: Schematic diagram of a laboratory scale fixed bed adsorber for tar removal from producer gas (Hasler et Nussbaumer et al., 1999).

The lignite coke was chosen because of its favourable cost and the good adsorption characteristics. For the adsorption test runs, the sieved coke fraction from 0.56 mm to 1.0 mm was used. Test runs were made with clean producer gas from the IISc/Dasag downdraft gasifier and after the RPS and the sand bed filter. The tar reduction was 50%, which was rather low as a combination of the cyclone, RPS and fixed bed adsorber in their order of series, can reduce the amount of tars in the gas with efficiency ranging 51 – 91% (Han et Kim et al., 2008) which is not good enough for downstream gas application.

2.3.1.7. Tar Removal by Wet Electrostatic Precipitators

Generally electrostatic precipitators are used to removal fine solids and liquid droplets, including aerosols.

An electrostatic precipitator (ESP) usually consists of a series of high voltage electrodes and corresponding collector electrodes which generate an electric discharge called corona discharge. Particles are charged by the corona discharge and subsequently separated from the gas stream under the influence of the electric field generated between the electrodes. An ESP can operate in a single or two stages. In a single-stage ESP, the electric field which is used to generate the corona discharge is also used to attract and hence remove the charged particles. In a two-stage ESP, charging and removal of the particles occurs in separate electric fields.

In a classic electrostatic precipitator such as the one shown in Figure 2.19, the charged particles are moved by a strong electrostatic field onto the collecting plates

where they agglomerate. There are dry ESP (DESP) and wet ESP (WESP). The collecting plates are cleaned by rapping and washed in DESP and WESP respectively.

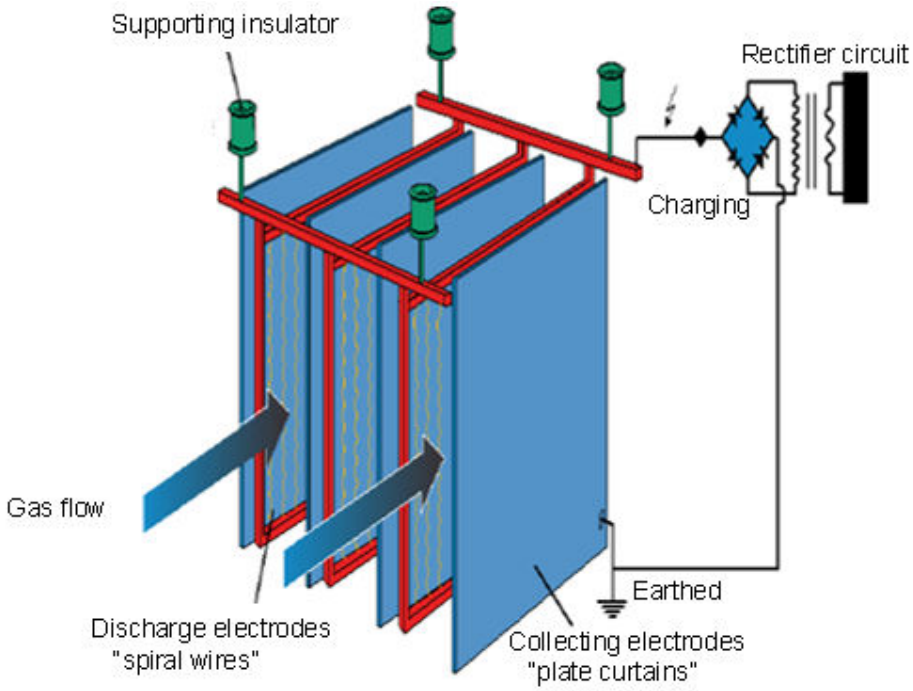

Figure 2.19: Schematic diagram of a classic electrostatic precipitator (Carlsson, 2008)

The performance of a WESP at removing the tars have been studied (Hedden et al., 1986) and reported elsewhere (Hasler et al., 1997). In this study, the tar separation efficiencies were between 0 and 60% and the gas moisture content was about 50 – 60%. There were operation problems such as the spark-over, tar and solid deposition on the collection plates.

In view of the low separation efficiencies and operation problems, the use of an ESP unit for tar removal was unattractive for the present study.

2.3.1.8. Tar Removal by a Wet Scrubber

The removal of the tars by using a wet scrubber involves the transfer of the tars between the gas and liquid phase. A solvent or scrubbing liquid is used to

dissolve the tars contained in the gas. As a result, the unit where the removal of the tars occurs is often called a solvent scrubber, gas absorber or gas absorption column.

Since the raw producer gas is a gas mixture of mainly CO, H_2, C_2H_2, C_2H_4 and tars, and is produced at temperatures ranging 650 – 800°C (Milne et al., 1998), the solvent should have special qualities. It should have low vapour pressure at operation temperature so that it does not easily vaporise during contacting with the gas. In addition, it should have high loading for the tars to reduce its recirculation rate, and it should be selective to prevent any possibility of co-absorption.

An example of a successful tar removal technology using the wet scrubber for tar removal can be found at Guessing biomass gasification plant in Austria. The schematic diagram of this technology is shown in Figure 2.20.

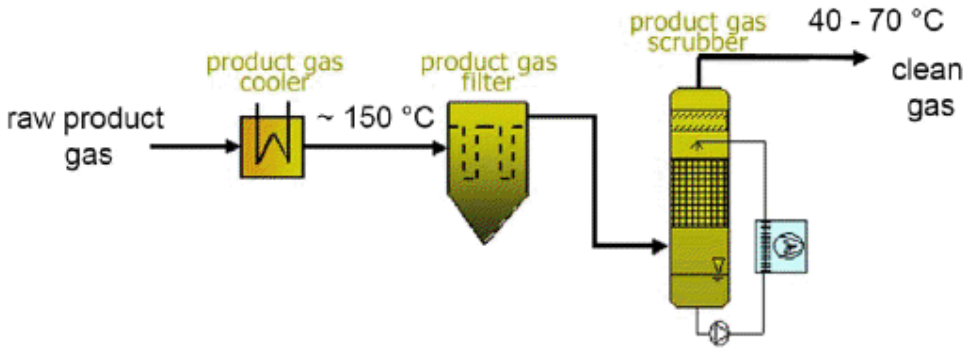

Figure 2.20: Schematic diagram of the cold gas cleaning involving RME tar scrubber (Hofbauer, 2002).

In this technology, the process of tar removal starts with the gas cooling with water from a temperature range of 850 - 900 ^oC to about 150 - 180 ^oC. This is followed with bag filtering to remove particulates and some tars. After the filter, the wet scrubber is used to absorb tars, ammonia and condensates by using a solvent called rapeseed methyl ester (RME). After separation of the condensates, a portion of tar loaded RME is fed to combustor of an indirect gasifier for recovery of the energy in the tars. The remaining tar loaded RME is blended with fresh RME for reuse in the absorber. High quality of producer gas with very low tar content has been achieved from the scrubber in the Guessing biomass gasification plant because the tar levels in

the feed producer gas are low after significant content of tars has already been removed by the gasifier's in-bed-olivine catalyst and filters. The tar concentration after the gasifier is approximately 2.5g/Nm^3 and the tar concentration in the producer gas exiting the scrubber is in the range 10 – 40mg/Nm^3 of dry gas which is highly suitable for application in an IC engine (Hofbauer, 2002).

Another successful technology for tar removal by using a wet scrubber has been developed and investigated at the Energy Centre of The Netherland (ENC) at Dahlman. This gas scrubbing technology is called OLGA, which stands for oil-based gas washing and its simplified flow diagram is as shown in Figure 2.21.

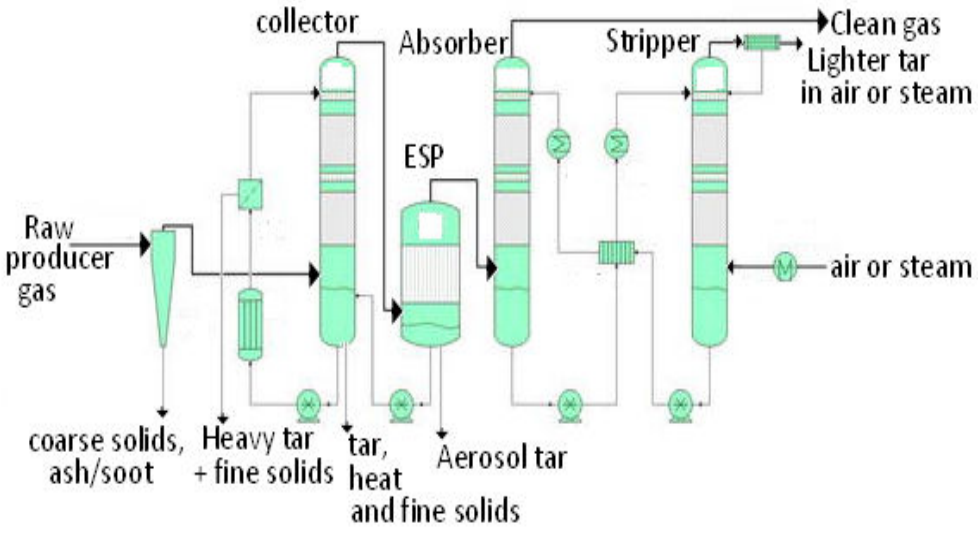

Figure 2.21: A simplified flow diagram of the OLGA (Zwart et al., 2009).

The OLGA reduces the tar dew point to -15 ^oC in the gas and removes all non tar contaminants (Rabou, 2005). The technology has a series of pre-treatment and gas cleaning before the scrubber which involve the use of a cyclone for ash and dust removal from the producer gas, a collector to cool the producer gas with thermal oil which condenses and collects heavy tars, followed by wet electrostatic precipitator to collect dust, water droplets and tar aerosols. In the scrubber, light tars are absorbed by the thermal oil. The spent oil exiting the scrubber is piped into the stripper where the oil is regenerated and tar is transferred into either steam or air for tar recovery. The cleaned gas exiting the scrubber is finally washed with water in an aqueous scrubber to cool it and remove acidic and alkaline impurities.

A recent report on the performance of the OLGA has revealed that the removal efficiency of 99% could be achieved with tar concentration reduced from 16.855 to about 0.2g/Nm^3 (Zwart et al., 2009). In addition, the phenol which was 0.4g/Nm^3 in the raw producer gas was also reduced to below detectable levels.

There are other removal technologies in the downstream of the gasifier which are non-physical methods. Although they are wet or wet-dry processes like the physical methods, the removal of the tars involve some chemical changes. Hence they are called non-physical tar removal methods.

2.3.2. Non-Physical Methods of Tar Reduction in the Gas

The non-physical methods are methods of tar reduction in which the chemical nature of the tars is changed. The tars are converted in different compounds such as simple hydrocarbons. In some situations, the heavy tars are broken down into light tar and fragments of benzene, toluene, xylene and so on. The process of non-physical tar reduction occurs by thermal, catalytic, steam or oxidative conversion.

2.3.2.1. Tar Reduction by Thermal Conversion

Tars can be thermally cracked at high temperatures. During the thermal cracking, the tars are converted to lighter molecular weight hydrocarbons which can be part of the producer gas. Based on the literature review, various attempts have been made in the development of this area of tar reduction technology although inclusive results have been reported.

(i) Temperatures in excess of 900°C are needed to thermally crack tars in a downdraft gasifier (Kaupp et al., 1983).

(ii) Temperatures lower than 1000 – 11000°C are inadequate for thermally cracking the tars and eliminating them (Parikh et al., 1987).

(iii) Thermal cracking of the tars to acceptable levels and reducing soots in the meantime require operating temperatures higher than 1100°C (Rensfelt et Ekstrom et al., 1988).

(iv) Thermal cracking of the tars might yield non-wettable and extremely fine soot (Rensfelt, 1996).

In view of the above listed observations, the removal of the tars by thermal cracking was not a viable alternative.

2.3.2.2. Tar Reduction by Conversion with Steam

Steam as gasification agent is discussed in Section 2.2.3 which shows that the tar content decreases with the steam to biomass feeding rate ratio. Steam has also been used for tar reforming at high temperatures to reduce the tar concentration in the producer gas. An example of tar reforming in the producer gas has been reported by Garcia and Hiuttinger (Garcia et Hiuttinger et al., 1989). In their study, it was found that there were low yields of the producer gas at temperatures up to 950°C. The yields were low because polymerization and condensation reactions were more favourable than the decomposition of the naphthalene into simpler hydrocarbons. As a result, more tars and carbonaceous residues were formed (Garcia et Hiuttinger et al., 1989). In a separate study of Jess (Jess, 1996) it was reported that steam has insignificant influence on the conversion of aromatic hydrocarbons(Jess, 1996). Further, Studies by Guanxing,s team (Guanxing et al., 1994) found that the combination of using dolomite as bed material with application of steam tends to increase the yields of naphthalene and other polycyclic aromatic hydrocarbon in the biomass gasification producer gas (Guanxing et al., 1994). However, other studies have shown that combination of steam and catalysts can break down the tars into permanent gases such carbon monoxide, methane, ethane and acetylene (Wang et al., 2010). In one of these studies, a laboratory scale apparatus was setup to investigate the steam reforming of biomass fuel gas, as shown in Figure 2.22 (Wang et al., 2010).

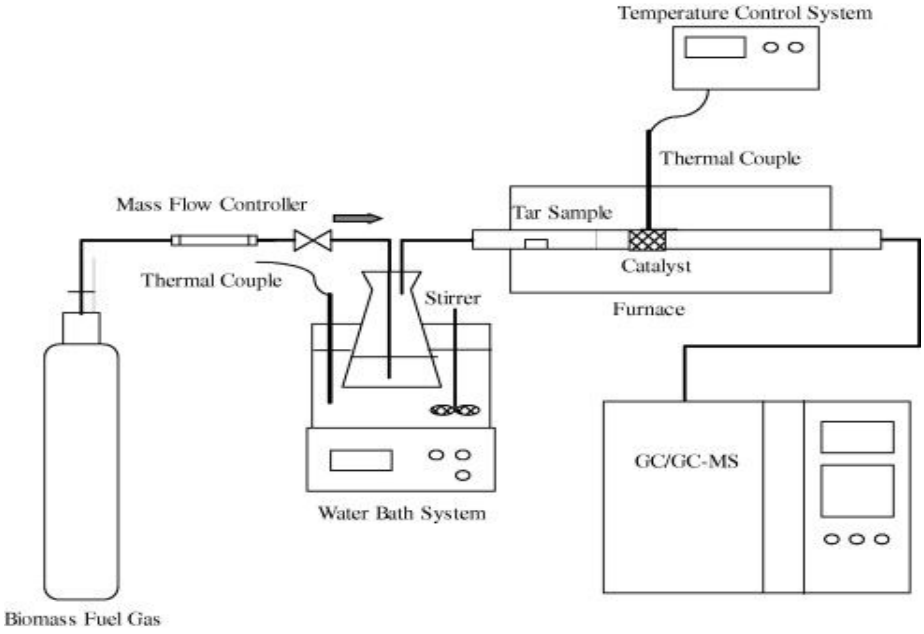

Figure 2.22: Schematic diagram of the experiment system for tar reforming (Wang et al., 2010)

In Figure 2.22, a simulated biomass gasification producer gas is fed into the system at a flow rate of 300 cm^3/min (standard) in which a quart fixed bed reactor was used with NiO-MgO solid solution cordierite monolith as catalyst. The apparatus was operated at a temperature of 750°C and the steam was injected at a steam to producer gas ratio of 5.2. During the steam reforming, some compositions of the gas components in the producer gas were changed and the full results are given in Table 2.5.

Table 2.5: Changes in the biomass gasification producer gas through steam reforming (Wang et al., 2010)

Producer gas component	Before reactor	After reactor
Hydrogen, H_2	0.01432 kg/m^3	0.0377 kg/m^3
Carbon monoxide, CO	0.1513 kg/m^3	0.063 kg/m^3
Methane, CH_4	0.1077 kg/m^3	0.0245 kg/m^3
Carbon dioxide, CO_2	0.4312 kg/m^3	0.4930 kg/m^3
Ethylbenzene, $C_6H_5CH_2CH_3$	112.24 µg/m^3	5.668 µg/m^3
Styrene, $C_6H_5CH{=}CH_2$	1.772 mg/m^3	80.84 µg/m^3
2-methyl-phenol, $C_6H_4(OH)CH_3$	10.69 µg/m^3	0
Naphthalene, $C_{10}H_8$	67.66 µg/m^3	0

This method of catalytic steam reforming of the raw biomass gasification producer gas could be desirable for the application of the gas in liquid fuel synthesis because high H_2 content is required to achieve the optimum H_2/CO ratio of 2. . The reactor for the catalytic steam reforming could be arranged in the downstream of the main gas cleaning units. However, the high temperatures at which the reforming occurs could be a hindrance.

2.3.2.3. Tar Reduction by Partial Oxidation

The reduction of the tars by partial oxidation has been reported. It has been reported (Beenackers et van Swaaiji et al., 1984) that addition of controlled oxygen to volatile vapours in downdraft gasifiers can achieve low tar contents (Beenackers et van Swaaiji et al., 1984). Another study shows that the addition of controlled oxygen to the second stage of a pyrolysis/cracker system preferentially oxidises the tars by converting them to carbon monoxide (Jensen et al., 1996). It also been concluded that partial oxidation at high temperatures can reduce the tars in the producer gas (Kaupp et al., 1983). However, the contact of the oxygen and the tars in the producer gas is limited. Moreover, in indirect gasifiers such as the dual fluidised bed gasifier, the direct contact of oxygen with the tars is impossible as the gasification agent is steam. Nevertheless, indirect gasifiers which use steam as the gasifying agent have an added advantage because they produce a lot of phenolic tars which are easily catalytically converted to hydrogen and carbon monoxide (Perez et al., 1997).The mechanism of tar reduction by partial oxidation has been investigated by Wang et al (Wang et al., 2008) who used naphthalene as a model tar which was added in the producer gas for controlled oxidation with a catalyst in a experimental rig shown in Figure 2.23.

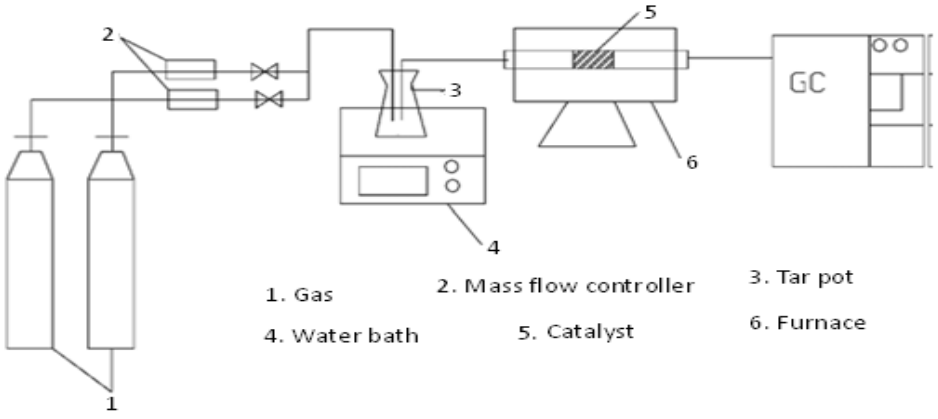

Figure 2.23: Schematic diagram of the partial oxidation tar reforming experiment (Wang et al., 2008)

In order to investigate the reduction of the naphthalene by partial oxidation, an oxygen/nitrogen gas mixture in a ratio of 95:5 and total flow rate of 60cm^3/min was added into the reactor. The reactor operated at the temperature 750°C and atmospheric pressure. The products of the reaction were analysed and it was found that 99% naphthalene was converted to hydrogen and carbon monoxide through the reactor (Wang et al., 2008). The mechanism for the conversion was postulated to be firstly, the oxidation of the gas components such as hydrogen, methane and carbon monoxide and then the production of the oxidation reformed the naphthalene to hydrogen, methane, carbon monoxide and carbon dioxide.

In the partial oxidation tar reduction, high temperature condition is required thus an external energy supply is needed. Although it could be more economical to use air for the partial oxidation but the contents of N_2 and CO_2 in the producer gas will increase, which is undesirable.

2.3.2.3. Tar Reduction by Catalytic Cracking

The tar reduction by using catalysts in the gasifier has been discussed in Section 2.2.5 where a catalyst was added to the bed material. However, the tar levels in the producer gas from biomass gasification in this way are still higher than the required levels either for use in IC engine or for liquid fuel synthesis. This section

will be focussed on the use of catalysts in the downstream tar cracking after the gasifier.

A study has been carried out to investigate the removal of tars in a secondary catalytic bed as shown in Figure 2.24 (Pfeifer et Hofbauer et al., 2008). In this study, a slip stream of producer gas was firstly taken from a commercially operated gasification plant after the filter to remove the dust. Then the dust-free slip stream of producer gas was fed to the test rig at a flow rate 0.7Nm^3/h and electrically heated to 900°C for tar cracking within a bed of nickel-based monolith catalysts.

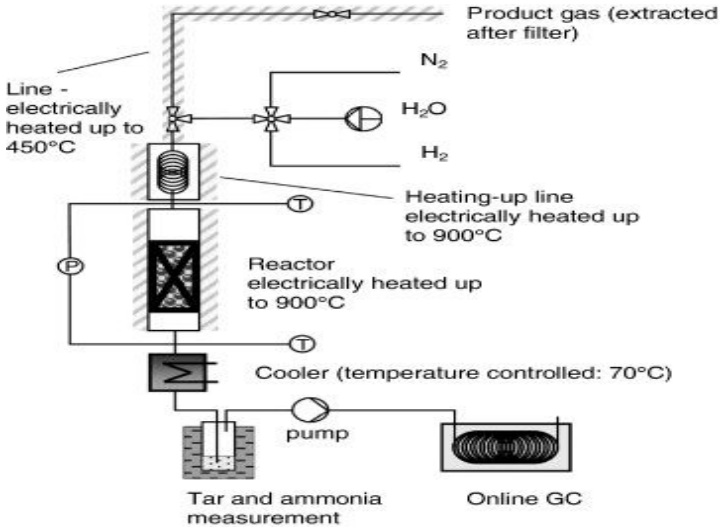

Figure 2.24: Schematic diagram of the side-stream test rig for catalytic cracking of tars (Pfeifer et Hofbauer et al., 2008)

By measuring the tar contents before and after the system, it was found that the tars were almost completely eliminated and a considerable content of ammonia was also decomposed. Although the study of Pfeifer and Hofbauer was successful at reducing the tar levels in the gas downstream gasifier, their technology has not been commercialised. However, a similar approach has been undertaken to develop a technology at the Technical Centre of Finland (VTT) aimed at reducing tar levels in the gas downstream gasifier and the technology has been commercialised.

The technology at VTT is commercially viable and research has been undertaken there to show that nickel-based catalysts are very efficient in decomposing tars in the producer gas at 900°C (Simell et al., 1996). Besides, from

the work of Simell's team (Simell et al., 1996) the producer gas containing dust was efficiently purified from tars and ammonia with nickel monolith catalyst. In their study, the reactor operated at temperatures of over 900°C and pressure of about 5 bar to completely decompose the tars and convert 80% of ammonia. The gas from a pilot scale fluidised bed gasifier was continuously fed into the reactor for 100 hours without any sign of catalyst deactivation and poisoning under those operating conditions.

2.3.2.4. Tar Reduction by Plasma Technology

Plasma technology is a tar removal method where an electric discharge between electrodes, called corona discharge, contains energetic electrons, ions and radicals which break down tar components contained in the gas. Nair's team have demonstrated the removal of the tars by this method as illustrated in Figure 2.24a (Nair et al., 2004).

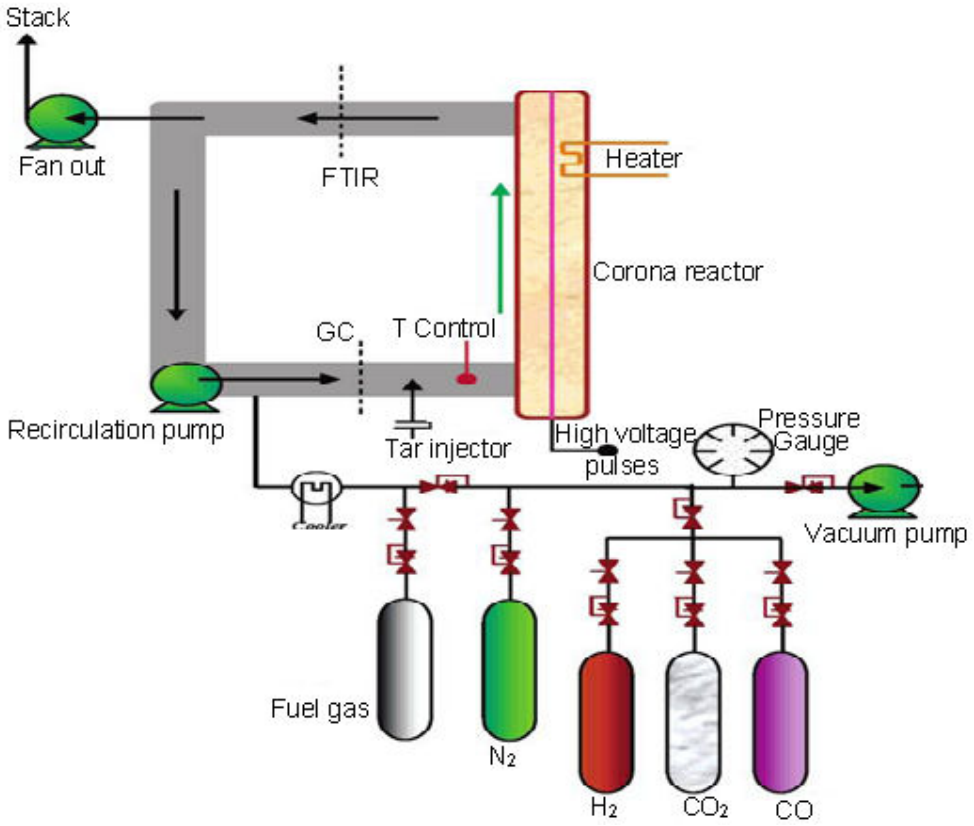

Figure 2.24a: Tar removal by Plasma Technology (Nair et al., 2004)

The reactor for the experiment was of a diameter and length of 0.25 and 3m respectively and was part of the loop where gases were circulated. The results

showed that energy density of about 400 J/*l* was required to break done naphthalene. Naphthalene was a model tar component that was simulated into a gas mixture of 12% CO_2, 20% CO, 17% H_2, 1% CH_4, and the rest N_2. The reactor operated at a pressure of 1 bar and a temperature of 200 °C. Naphthalene was 100% broken down to CO and formaldehyde. In addition the following observations were made:

(i) The naphthalene conversion increased slightly with increasing energy density

(ii) The naphthalene conversion increased continuously with increasing reactor temperature

Although the plasma method has the capability of 100% tar conversion and can be used downstream the gasifier, it operates at high temperature and requires the use of external power input. Due to high temperature and energy requirements the plasma technology was undesirable for tar removal in this study.

Similarly, the technology of catalytic thermal cracking of the tars contained in the producer gas was not appealing because it requires high temperatures in excess of 900°C. The exit temperature of the gas produced by the UC gasifier is in the range 700 – 750°C (Bull, 2008; McKinnon, 2010).

2.4. Combined Methods for Tar Reduction

From the above discussion, each tar removal method has its advantages and disadvantages. In most cases, the tar content in the producer gas is still higher than the required level using a single method. Therefore, a combination of two or more separation methods can be used in order to effectively reduce the tar content to the required level. The individual tar removal methods can be selected based on the properties of the tars and required tar levels. Some of the properties which have been used to select these methods are polymerization and condensation. It has been shown that 2-ring polycyclic aromatic hydrocarbons (PAHs), such as naphthalene, polymerize to form larger ring PAHs in air at temperatures in excess of 900°C (Chen et al., 2009). Therefore, thermal cracking of the tars is not a viable method in this case. On the other hand, some tar components have been found to condense at as high temperatures as 350°C (Rabou et al., 2009). The condensation point of different tar components is different thus it can only be determined individually. Therefore, a

more useful term, called dew point, is commonly used for description of condensation of tars in the producer gas. The knowledge of the tar dew point is important for the operators of the installations. The dew point is positively related to the tar concentration (g/Nm^3 or mg/Nm^3) in the producer gas; therefore, these two terms are all used in this field. However, to keep consistency and for ease of measurement, the tar concentration is normally measured and presented in practice and thus used in this thesis. It should be noted that even at very low level of tar concentration, the tar dew point might be high enough to adversely affect the downstream application of the producer gas.

Combination of different gas cleaning methods also needs to consider the temperature effect which is related to the dew points of tars and water vapour. For instance, Figure 2.25 shows the temperature range for separation of different impurities in the producer gas as the process temperature decreases. As the producer gas is cooled down, different impurities ranging from dust through heavy tars, light tars, polycyclic aromatic tars and NH_3 to HCl are progressively removed. The dust is separated initially; wherein some heavy tars are removed together with the dust as they get adsorbed or condense on the dust.

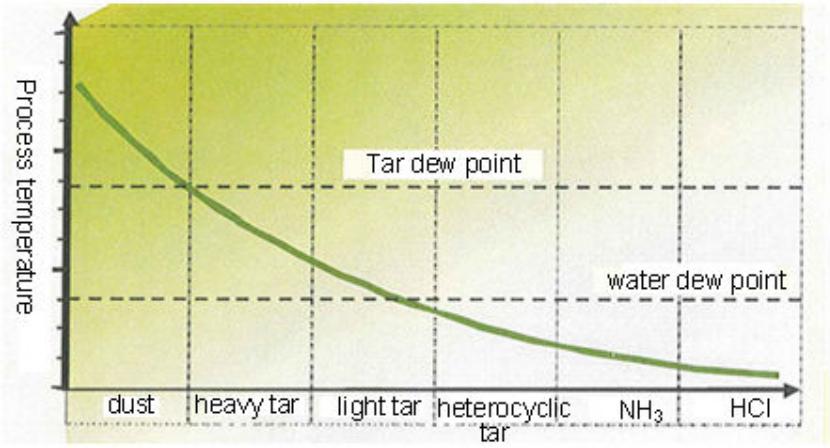

Figure 2.25: An illustration of the temperature effect on removal of different impurities from the biomass gasification producer gas (Boerrigter, 2002).

After all the heavy tars have been removed, the removal methods of the lighter tars and polycyclic aromatic tars are strongly dependent on their dew points (van der Drift, 2009). The types of tar removal methods and their separation efficiencies are shown in Figure 2.26.

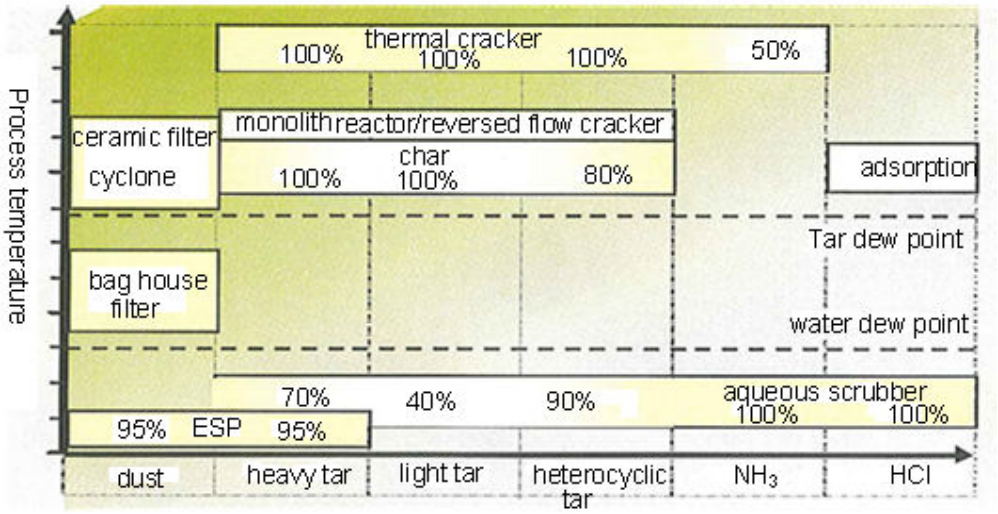

Figure 2.26: Various methods and their efficiencies for removal of tars and other impurities (Boerrigter, 2002).

Figure 2.26 shows that ceramic filters and cyclones can be used to remove dust at high gas temperatures. Ceramic filters have been reported to operate effectively at high temperatures as 650 - 850^{o}C (Hasler et Nussbaumer et al., 1999; Zevenhoven et Kilipinen et al., 2001). In fact Figure 2.26 shows generally, gas cleaning process beginning from when the gas emerges the gasifier up to the end use of the gas. The first process being the dust removal by ceramic filters and cyclones at high temperatures or bag house filters at moderate temperatures. Once the gas has been de-dusted, it can then be cleaned further by removing the tars downstream the gasifier using physical methods such as thermal cracking. Thermal cracking can remove 100% of the tars by breaking them to simple hydrocarbons at temperatures ranging 900 – 1290^{o}C (van Heesch et al., 1999). However, thermal cracking of the tars is very energy intensive and was thus disregarded in this study. Similarly, the use of high temperature filters was not appealing because filters which operate in temperatures above 750 ^{o}C are susceptible to bending and alkali attack which render them ineffective, in addition to the operation being equally energy intensive (van Heesch et al., 1999). Other than thermal cracking, catalytic cracking can also be employed for tar reduction as shown in Figure 2.26. Clearly it shows that thermal cracking and as well as catalytic cracking can reduce tar concentration of all sorts of tars from heavy tar to light tars and finally heterocyclic tars. It is worth noting that there are not many state of the art systems currently where thermal cracking and

catalytic cracking are used as secondary measures for tar reduction. Mostly, these methods are used as primary measure of tar reduction. Figure 2.26 also highlights the use of an aqueous scrubber as being effective at removing 90% of heterocyclic tars and 100% ammonia and acid impurities. As a result, the aqueous scrubber helps to significantly reduce tar dew point as well as the water dew point. Therefore, it would be advantageous to employ an aqueous scrubber downstream especially if the producer gas is to be applied in an IC engine where dew point is an operation parameter. However, aqueous scrubber would work fine if primary measures are so well taken that 100% of heavy tars and light tars are eliminated in the gasifier and the producer gas is cooled down below water saturation temperature before entering the scrubber (Zwart et al., 2009). An alternative gas cleaning system which can take advantage of successive primary measures of tar reduction to employ an aqueous scrubber as a secondary measure is shown in Figure 2.27.

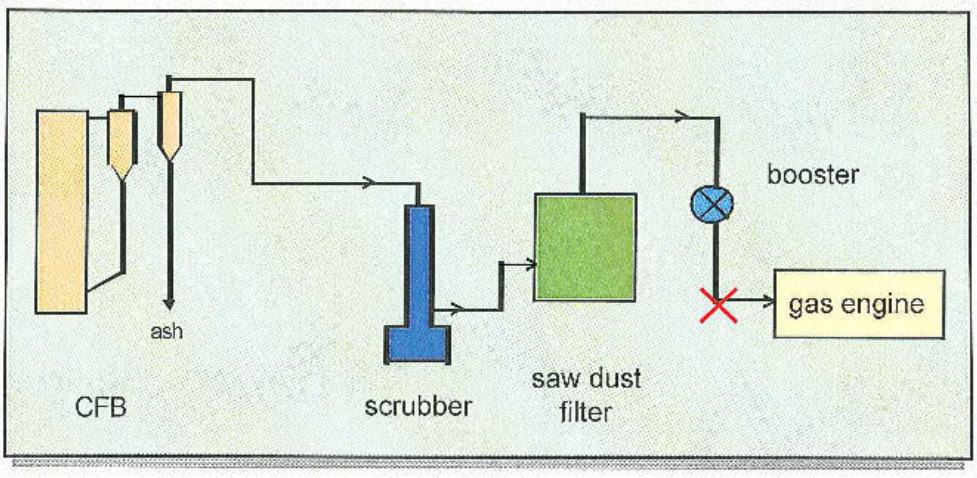

Figure 2.27: Schematic diagram of a simple combination of different tar removal units for gas use in an engine (Boerrigter, 2002; Zwart et al., 2009)

Figure 2.27 shows a simple combination of different gas cleaning units used to remove tars and other impurities in the producer gas at the ECN (Boerrigter, 2002). The product gas was generated from a circulating fluidised bed (CFB) gasifier with tar levels in the gas range 10 – 20 g/Nm^3 (Zwart et al., 2009). In this gas cleaning system, the heavy tars which stuck on particles were firstly removed together with ash in the cyclone. Further downstream, the gas was cleaned in a scrubber in which water was used to get rid of some remaining heavy tars and light tars, as well as NH_3. The sawdust filter was then used to remove tar aerosols before

the cleaned gas was fed into the engine. The water from the scrubber was treated in a settling tank to separate the heavy tars and then in a candle filter for further cleaning, and finally the water was fed into a stripper to remove NH_3. As a result, most of the water was reused in the scrubber (Rabou et al., 2009).

In the scrubber, acid was added to the water to remove NH_3 more effectively from the producer gas. In the water stripper, a base was added to drive NH_3 from the water. The cleaned gas contained 2.3g/Nm^3 tars which was considered high for using the gas in the engine. However, tar levels reduced from 0.6 to 0.2 g/Nm^3 when the same system was used for cleaning of biomass gasification producer gas generated from a fixed bed gasifier. The engine in this case operated on the cleaned gas for a period of 6 h without any problem.

More complicated combination is expected to clean the producer gas to a lower level of tar concentration, but the challenges are the costs and complexity for construction and operation. An example is shown in Figure 2.28 in which an additional cyclone, a second scrubber and an ESP are added to the existing system as shown in Figure 2.28.

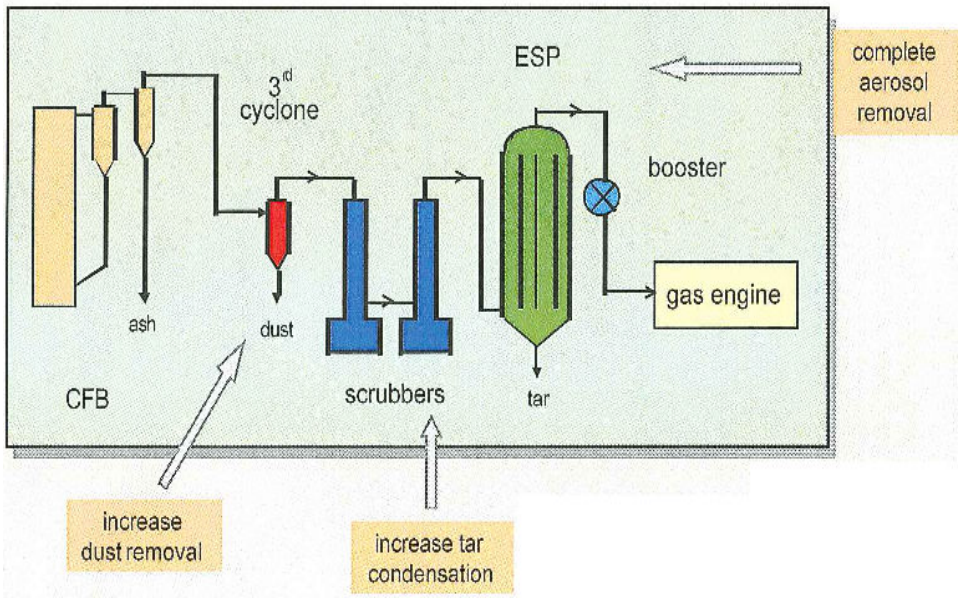

Figure 2.28: Schematic diagram with additional units to those shown in Figure 2.26 (Boerrigter, 2002; Zwart et al., 2009)

The addition of the three units enabled more efficient tar removal from the gas. Further, the efficiency of the second scrubber at removing both the tars and NH_3

was enhanced by cooling down the water before feeding to the second scrubber. In this combination of units, the best results for the tar removal were recorded as a tar reduction from 10 to 1.4g/Nm^3 when the CFB gasifier operated at 880°C. However, the tar levels were still unacceptable for the gas application in an IC engine. In addition, there were other operation problem; the pipe between the scrubbers got clogged by tars and dust (Rabou et al., 2009).

The combination of the units in Figure 2.28 required further improvement in order to further reduce the tar concentration in the producer gas for its application in the engine. The improvement which was made is illustrated in Figure 2.29 (Rabou et al., 2009).

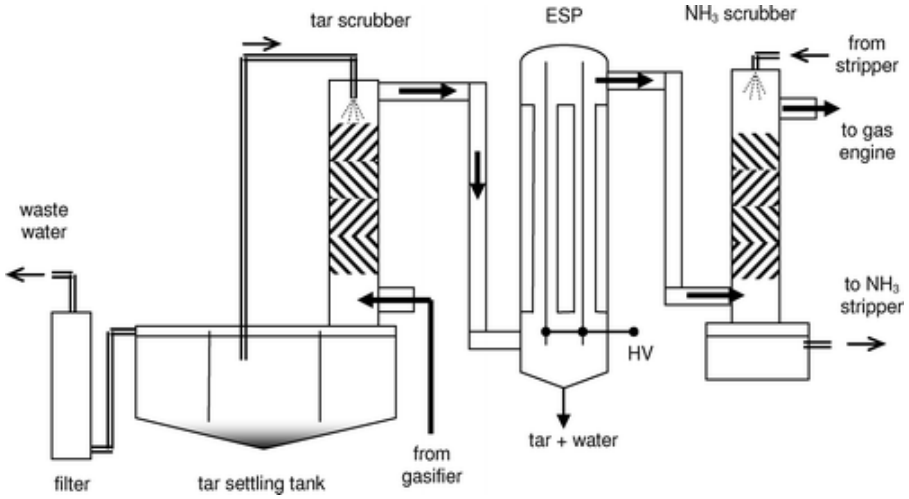

Figure 2.29: Schematic diagram of the 3rd improvement on tar removal methods at ECN (Rabou et al., 2009)

In the improvement shown in Figure 2.29, the ESP was placed between the two scrubbers to reduce the tar loads to the downstream scrubber. Although the downstream scrubber was principally meant for the removal of ammonia, some tars were also removed in this unit. In addition, the tar settling tank was modified by enlarging and subdividing it to improve the settlement. In order to enhance the removal of benzene, toluene, and some derivatives of naphthalene from the wastewater, the settling tank was insulated and heated thereby reducing the solubility of these hydrocarbons. As a result of the improvement depicted in Figure 2.29, the product gas was cooled from 300 to 25 °C when the 18°C water was used in the tar scrubber. Additionally, the tar concentration downstream the ESP was reduced to

0.7g/Nm^3 with tar dew point of 21°C. The combination of units shown in Figure 2.28 was effective at removing the tars. However, the units suffered severe fouling. The fouling was evident when pressure drop over the units increased drastically due to the clogging by the tars. An after-test inspection showed some naphthalene deposited on the cooler parts of the scrubber. Following these changes, the final improvement was made which is now popularly called the OLGA (Figure 2.30) which has been briefly discussed in Section 2.3.18.

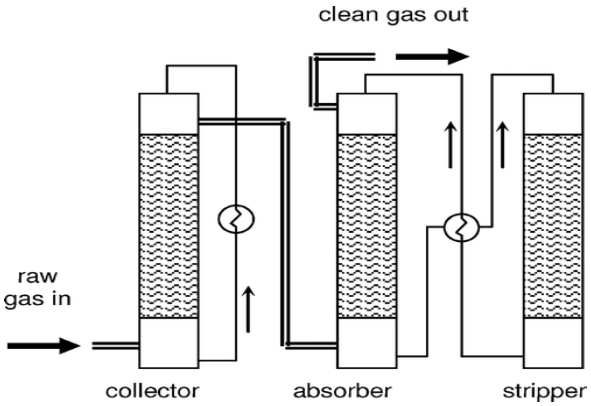

Figure 2.30: A simple flow scheme of the OLGA tar removal system (Rabou et al., 2009).

The working principle of the OLGA and its success were derived from the realisation that the mixing of the dust, tar and water should be removed in advance before the tar removal. This was found in the trials using systems shown in Figures 2.27 to 2.29. In this regard, the prevention of mixing water, dust and tars could be partially achieved by cleaning the gas using a suitable liquid solvent in the scrubber operating above the water vapour dew point of the producer gas. Once this is achieved, tar condensation in downstream equipment can be prevented. This idea has been applied at ECN in the OLGA system as shown in Figure 2.29 in which the producer gas goes into a collector to quench the gas with oil and cool the gas down to a temperature above its water dew point. In the process, part of the tars condenses and mixes with the scrubbing oil. The next unit after the collector is the absorber which removes tar vapours of benzene and toluene by using thermal oil as solvent. A stripper is used to recover the tars absorbed in the scrubber using high temperature air to drive off the absorbed tars from the loaded oil. The tars removed in both the

collector and the stripper units are recycled to a combustor where the tar energy is recovered.

2.5. The Choice of the Tar Removal Method

Amongst the methods of tar reduction which have been reviewed, the use of wet scrubber is the most attractive one because it does not need the use of external heat energy and expensive catalysts. The only concern is the choice of the scrubbing liquid solvent. In previous studies (Hofbauer, 2002; Zwart et al., 2010), various types of scrubbing solvents have been tried to remove tars from the producer gas from biomass gasification. The results of these studies have been compiled and listed in Table 2.6.

Table 2.6: Performance of various solvents used for removing tars from biomass gasification producer gas

Scrubbing liquid	Total tar concentration		% Tar removal
	Before (g/Nm^3)	After (mg/Nm^3)	
RME **(a)**	2.5	15	99.2 – 99.6
Glycerol **(b)**	10 – 20	900	94
Thermal oil **(c)**	10 – 20	150	99
Water **(d)**	0.05 – 1	4500	10 - 25
Biodiesel **(e)**	10 – 20	6.3	58
RME**(f)**	10 – 20	8.4	44
References: **(a)** (Hofbauer, 2002) **(b)** (Zwart et al., 2010)			
(c) (Zwart et al., 2009) **(d)** (Hasler et Nussbaumer et al., 1999)			
(e) (Zwart et al., 2010) and **(f)** (Zwart et al., 2010)			

With reference to Table 2.6, water is not preferred solvent in scrubber which has been tried to remove the tars. However, water is a very good medium at removing dust from the gas. In a typical gas cleaning operation cited in Table 2.6, a maximum of 98% particulates were removed by water (Hasler et Nussbaumer et al., 1999). In order to achieve this level of separation of the particulates, the gas is firstly cooled down before feeding to the dust collector.

Although water shows poor removal efficient for tars, it has still been used for the tar reduction from the producer gas of biomass gasification for low temperature gasification processes. In these applications, the removal efficiency for total tar removal was as high as 80% (Zwart et al., 2009). This high tar removal efficiency

can be attributed to the fact that low temperature gasification produces polar tars. Since water is a polar solvent, the solubility of the polar tars in it would be high.

The other scrubbing liquid which have been used to remove the tars as listed in Table 2.6 are Rapeseed methyl ester (RME), thermal oil, glycerol and biodiesel which were tried in the OLGA system (Zwart et al., 2010). As seen from Table 2.4, RME was used as scrubbing liquid in two separate studies and two quite different results are reported. (Hofbauer, 2002) reported a tar removal efficiency of up to 99.6% whereas Zwart's team (Zwart et al., 2010) achived a tar removal efficiency of only 44%. Since Hofbauer used an indirect steam gasifier while that of Zwart's team (Zwart et al., 2010), a circulating fluidised bed air gasifier, the difference in the tar removal efficiency could be due to the different types of gasifiers as tar concentration in the raw gas would be significantly different. In addition, the temperature of the producer gas at the feeding point to the scrubber was also different in the two studies. In the study of Zwart's team (Zwart et al., 2010), the gas was fed at 350 °C while in the study of Hofbauer (Hofbauer, 2002), the feeding gas temperature was 160 – 180°C. A scrubbing liquid of high boiling point would enhance the solubility of the solute (tars) because of the low vapour pressure of the liquid hinder substantial vaporisation. On the other hand, scrubbing liquids of high vapour pressures at a given temperature reduce the transfer of the solute from the gas to the liquid because their vaporisation enables them to be saturated with the solute (tars) and hence reduce the driving force.

In pilot scale trials, both ECN-OLGA tar removal system (Rabou et al., 2009) and the Gussing plant RME scrubbing system have been successful for the removal of tars from the producer gas of biomass gasification (Hofbauer, 2002). In both of these technologies, wet scrubbing is employed and thermal oil is used as the scrubbing liquid. In view of the results shown in Table 2.6 and the other literature cited in Sections 2.3 to 2.4, a system for removing tars by a wet scrubber will be investigated. The system will be based on the ideas from the OLGA and Guessing's RME scrubber. However, CME biodiesel will be used as the scrubbing liquid. The choice of CME biodiesel is based on the results in Table 2.6 which shows the tar removal of 58% when biodiesel was used in the wet scrubber where the temperature of the gas was 350°C. This result needs further investigation because biodiesel and RME have similar physical and chemical properties although solubility properties are

not the same. Moreover, biodiesel can be used for higher temperatures than RME is used in the Gussing's RME scrubber. Since high gas temperatures reduce the solubility of the solutes in the scrubbing liquid, the use of the CME biodiesel is expected to have higher tar removal efficiency at low gas temperatures.

2.6. Basis of the Process Design for the Tar Removal System

The design of the OLGA tar removal system is based on the removal of naphthalene and phenols as the target tar components (Zwart et al., 2010). According to (Zwart et al., 2010) the concentration of naphthalene was one of the design parameters because naphthalene can cause crystallisation problems in the IC engine. However, (Zwart et al., 2010) noted that the naphthalene concentration of 40mg/Nm^3 does not cause problems in the IC engine. As such, their design was mainly focused on the concentration of phenols. In addition, the concentration of naphthalene was sufficiently low so that it does not cause any concern in IC engine. Therefore, their design was optimised to the removal of phenols. The main concern of phenols is the production of poisoned condense water and possibility of expensive wastewater cleaning.

According to the research team at the UC gasifier, naphthalene was the most abundant tar component in the producer gas from the point of view of the definition of tars. At the time of this research, the team's definition of tars excluded all class 2 and 3 tars as the research was focussed on gas cleaning for power generation. However, the focus of the research has now shifted to the synthesis of liquid fuels. The abundance of naphthalene can be evidenced by the laboratory results for the characterization of the tar components in the producer gas from the UC gasifier as shown in Table 2.7. It can be seen clearly in Table 2.7 that naphthalene is the most abundant tar component in the producer gas that was produced at the UC gasifier on 21st February 2008. However, the amounts of acenaphthylene are close to those of naphthalene and as such it should be regarded as an equally abundant tar component. Naphthalene has been solely chosen as the model tar component for the design of the test system because of its more adverse effects on process units than those of acenaphthylene.

Table 2.7: Characterisation of tar components in UC's producer gas

Gasifier tests performed on 21/2/08 and samples analysed by Hills Lab on 21/2/08

Sample Name:	Sample #2c	Sample #4	Sample #5
Lab No:	468037 / 3	468037 / 5	468037 / 6
Units:	µg/167µg total tar	µg/335µg total tar	µg/345µg total tar
Acenaphthene	7.2	9.2	8
Acenaphthylene	40	84.4	87.7
Anthracene	8.1	13.8	13.9
Benzo[a]anthracene	2.7	4.5	4.7
Benzo[b]fluoranthene	2.4	4.1	4.4
Benzo[a]pyrene (BAP)	2.1	3.8	4.3
Benzo[g,h,i]perylene	0.9	1.2	1.2
Benzo[k]fluoranthene	0.9	1.6	1.7
Chrysene	2.5	4	4.2
Dibenzo[a,h]anthracene	0.5	0.7	0.8
Fluoranthene	6	10.1	11.2
Fluorene	16.3	28.7	29.1
Indeno(1,2,3-c,d)pyrene	1.1	1.5	1.7
Naphthalene	44.7	114	118
Phenanthrene	23.8	41.2	40.8
Pyrene	7.5	12.1	13

Contrary to the results in Table 2.7, Figure 2.31 which was obtained using the gas from UC gasifier in 2009 shows that phenol is relatively more abundant than naphthalene (McKinnon, 2010). However, phenol cannot be regarded for the design of the test system because it has been disregarded as a tar component by the definition of the tars as discussed earlier on in section 2.6 of this chapter. Now that the research team will focus on using the gas for liquid fuel synthesis, the removal of phenol will have to be considered especially in the performance of the test system by sampling and analysing levels of phenol.

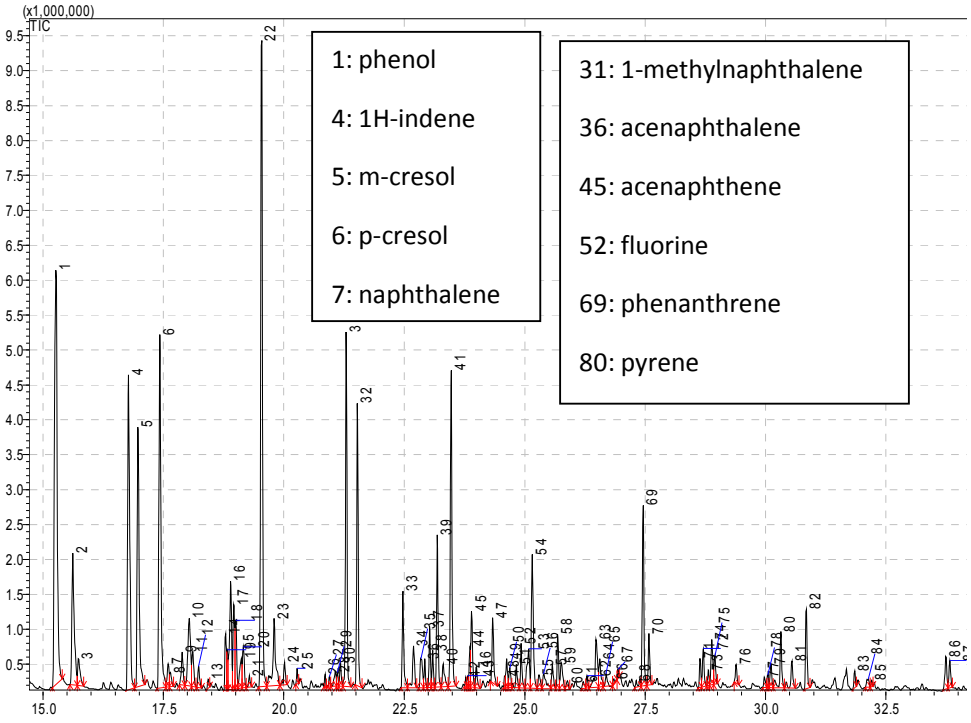

Figure 2.31: Some components in a UC gasifier tar sample (McKinnon, 2010).

In the design of the test system for tar removal using a wet scrubber, the use of water as solvent should also be avoided due to the problem of wastewater treatment. Instead, CME biodiesel should be used to absorb naphthalene, phenol and other heavy molecular weight hydrocarbons. The loaded CME can then be contacted with hot air in a stripper operated at temperature range of 220 – 230^{o}C and atmospheric pressure. In this way, the condensed water, phenol, naphthalene and other hydrocarbons (smaller than naphthalene) can be vaporised. As a result, the CME can be regenerated and be reused in the scrubber.

Since the heavy PAHs such as fluorine, phenathrene, pyrene and so on have lower vapour pressure than naphthalene, they are not expected to be vaporised from the CME. However, they would not be in the producer gas which is fed to scrubber as they would be cracked in the gasifier. In addition, the heavy tars would have condensed onto the dust during gas cooling and be retained as filter cake as the gas passed through the filter.

In view of naphthalene and CME being the basis for the design of the tar removal test system, literature on the naphthalene as a solute and CME as a solvent

for the system design and investigation should be sought. In this regard, the comparison between RME and CME is shown in Table 2.8.

Table 2.8: Constituents and their molecular formulas and Compositions for RME and CME biodiesels (Yuan et al., 2005)

CME			RME		
Name	Molecular Formula	%wt	Name	Molecular Formula	%wt
methyl myristate	$C_{15}H_{30}O_2$	0.1	methyl myristate	$C_{15}H_{30}O_2$	0
methyl palmitate	$C_{17}H_{34}O_2$	3.9	methyl palmitate	$C_{17}H_{34}O_2$	2.7
methyl stearate	$C_{19}H_{38}O_2$	3.1	methyl stearate	$C_{17}H_{34}O_2$	2.8
methyl oleate	$C_{19}H_{36}O_2$	60.2	methyl oleate	$C_{19}H_{36}O_2$	21.9
methyl linoleate	$C_{19}H_{34}O_2$	21.1	methyl linoleate	$C_{19}H_{34}O_2$	13.1
methyl linolenate	$C_{19}H_{32}O_2$	11.1	methyl linolenate	$C_{19}H_{32}O_2$	8.6
Methyl erucate	$C_{23}H_{44}O_2$	0.5	Methyl erucate	$C_{23}H_{44}O_2$	50.9

Table 2.8 shows that the most abundant methyl ester in CME is methyl oleate (being 60.2%wt) which is 21.9wt% in RME. On the other, the most abundant ester in RME is methyl erucate (being 50.9%wt) which is only 0.5wt% in CME. Using the data in Table 2.8, the molecular weight for CME and RME are 294.89 and 323.79. Therefore, RME is a larger molecule than CME which means that the tar solubility in RME should be higher than that in CME at the same temperature and pressure. However, the relative tar solubility can be conclusively decided if the tar solubility in CME can be predicted and then compared with the reported tar solubility in RME. The reported solubility of tars produced during biomass gasification is 0.5kg/kg in RME at 50^{o}C and atmosphere pressure (Proll et al., 2005). Moreover, the use of the molecular size to tell solubility is not conclusive especially when dealing with gas solubility.

The solubilities of model tar (naphthalene) in RME and CME have been compared and discussed in Chapter 3. In addition, the densities and viscosities of both RME and CME and how they affect tar (naphthalene) solubility have been compared and discussed in Chapter 4. In the comparison, the densities have been

used to determine the cohesive energy densities, which are related to gas solubility, so that the solubility of naphthalene is conclusively defined (Barton, 1983).

Chapter 3 Description of a Tar Removal Test System, Prediction of Tar Solubility and Specification of the System's Auxiliary Units

3.1. Introduction

This chapter contains the description of a test system, prediction of tar solubility in CME and specification of the system's auxiliary units for tar removal from the gasification producer gas. The test system consists of a scrubber and stripper for scrubbing tars from raw producer gas by absorption using CME biodiesel and stripping the tars by using air. The tars absorbed by the CME in the scrubber are then released out of the CME into air in the stripper. In this way, the CME is confined in a closed loop and the tars are carried away by the hot air and their energy can be recovered if the tar-loaded air is fed to the combustion unit of the UC gasifier. The schematic diagram for the tar removal system is shown in Figure 3.1.

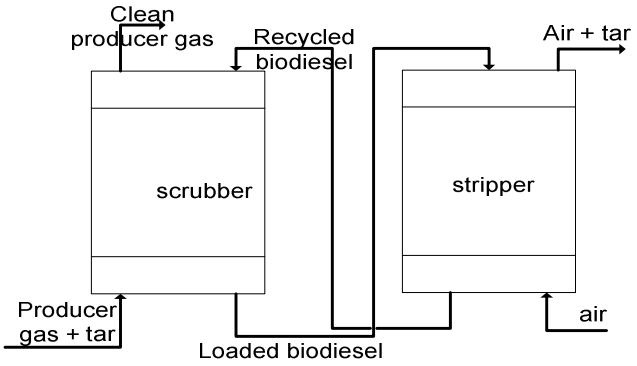

Figure 3.1: Schematic diagram of the test system for tar removal.

The tar removal test system is to be used for the UC gasifier which is operated at atmospheric pressure with temperatures of the emerging producer gas ranging from 973 – 1073 K (Bull, 2008). In the test system, the producer gas is firstly cooled down to prevent vaporising of the CME which is used in the scrubber. In addition, the effect of temperature on the solubility of the tars in the CME biodiesel is explored. Therefore, some basic property data of the tar-biodiesel system are needed for the design of the equipment and the operation of the system. The data will

also be used to optimise the operation conditions (temperature, gas to solvent flow rate ratio) in both the scrubber and the stripper.

The data in open literature on the solubility of the tars in CME is not found. As a result, thermodynamics and theories are used to predict the solubility of the tars (represented by subscript 2) in the CME (represented by subscript 1). The prediction of the tar solubility is based on a theory described by the following equation (Prausnitz et al., 1999):

$$\frac{1}{x_2} = \frac{f^{L}_{pure2}}{f^{G}_{2}} \exp\left[v^{L}_{2}(\delta_1 - \delta_2)^2 \varphi_1^2 / RT\right] \qquad (3.1a)$$

where:

x_2 is the mole fraction solubility of the tars, mol/mol,

δ_1 is the solubility parameter of the CME, $(J/m^3)^{0.5}$,

δ_2 is the solubility parameter of the tars, $(J/m^3)^{0.5}$,

v^{L}_{2} is the molar liquid volume of the tars, m^3/mol,

φ_1 is the volume fraction of the CME,

f^{L}_{pure2} is the fugacity of pure liquid tars, N/m^2,

f^{G}_{2} is the fugacity of pure gaseous tars, N/m^2,

R is the universal gas constant, J/mol·K, and

T is the absolute temperature of CME, K.

The parameter φ_1 is defined as follows:

$$\varphi_1 = \frac{(1 - x_2)v_1}{(1 - x_2)v_1 + x_2 v_2} \qquad (3.1b)$$

In which v_1 and v_2 molar volumes of naphthalene and CME (mol/m^3)

Equation (3.1a) is applied to non-polar gases/vapours in non-polar solvents. In order to use it in systems involving polar solvents such as CME biodiesel, Equation 3.1a was modified to the following equation (Yen et McKetta et al., 1962):

$$-\ln x_2 = \frac{v_2^L \varphi_1^2}{RT}\left[\delta_1^2 + \delta_2^2 - 2\delta_2\left(\delta_1^2 + \Delta\right)^{0.5}\right] + \ln f^{oL} \qquad (3.2)$$

In which Δ is the characteristic constant which is used as a correction factor for polar solvents, J/m^3, and f^{oL} is the fugacity of pure liquid tars, N/m^2.

In using Equation (3.2), f^{oL} is the saturation pressure of the tars which is approximated by the Clausius-Clapeyron equation (Barton, 1983). In the system where the gases or vapours follow the Ideal Gas Law, the above equation can be re-arranged as follows (Barton, 1983):

$$\ln x_2^{ideal} = \frac{\Delta H^f}{RT_m T}\left(T - T_m\right) \qquad (3.3)$$

In which ΔH^f is the heat of fusion of the tars, J/mol, T_m is the melting temperature of the tars, K, and x_2^{ideal} is the solubility of tar vapours in CME, mol/mol.

Equations (3.1b) to (3.3) were used to predict the solubility of the tars as a function of temperature.

3.2. Prediction of the Solubility of the Tars in CME Biodiesel

In order to predict the tar solubility in CME, the properties of the tars and the CME appearing in Equations (3.1a) to (3.2) are firstly determined. Since naphthalene has been determined to be the most abundant components of the tars in the producer gas (Bull, 2008), the solubility parameters and molar volumes of the naphthalene are used to represent the of tars. The solubility parameters and molar volumes are normally given in literature at room temperature, 298.15 K. However, these

parameters can be modified by the following relation at elevated temperatures (Barton, 1983):

$$\delta_2 = \sqrt{\frac{\Delta H - RT}{v_2}} \tag{3.4}$$

In which ΔH is the heat of vaporization and the rest are as defined earlier. In the case of naphthalene, the heat of vaporization at an elevated temperature can be estimated by using the Watson Equation as follows (Watson, 1943):

$$\Delta H_2 = \Delta H_1 \times \left(\frac{1 - T_{r2}}{1 - T_{r1}} \right)^{0.38} \tag{3.5a}$$

In which ΔH_1 is the heat of vaporization of naphthalene at 298.15 K, J/mol, ΔH_2 is the heat of vaporization of naphthalene at an elevated temperature, J/mol, and T_{r1} is the reduced temperature of naphthalene at 298.15 K and its critical temperature (T_C) in Kelvin, given as follows (Barton, 1983):

$$T_{r1} = \frac{298.15}{T_C} \tag{3.5b}$$

T_{r2} is the reduced temperature of naphthalene at an elevated temperature (K) and its critical temperature (K), given as follows (Barton, 1983):

$$T_{r2} = \frac{T}{T_C} \tag{3.5c}$$

The molar volume of naphthalene at an elevated temperature T (K) can be calculated from the molar volume at room temperature (v_1), as follows (Smith et al., 1996):

$$v_2 = v_1 \times \frac{T}{298.15} \tag{3.6}$$

In order to calculate molar volumetric fraction, the molar specific volume for naphthalene and CME biodiesel is needed. The molar volume of CME was estimated by using the properties of its constituents because CME is a mixture of six (6) methyl

esters. The properties of these constituents (methyl esters) are shown in Table 3.1 (Barton, 1983; Yuan et al., 2005).

Table 3.1:Constituents properties at 298 K for the estimation of molar volume of CME

Name	Molecular Formula	Weight, %	Polar parameter ,$Pa^{0.5}m^3$ (δ_p)	Molar volume, m^3/mol (v_i)
methyl myristate	$C_{15}H_{30}O_2$	0.1	4470	0.303
methyl palmitate	$C_{17}H_{34}O_2$	3.9	5430	0.338
methyl palmitate	$C_{17}H_{34}O_2$	3.9	5820	0.374
methyl oleate	$C_{19}H_{36}O_2$	60.2	5210	0.368
methyl linoleate	$C_{19}H_{34}O_2$	21.1	4730	0.361
methyl linolenate	$C_{19}H_{32}O_2$	11.1	5130	0.354

The data in Table 3.1 was used to estimate molar volume of CME at elevated temperatures as follows (Barton, 1983):

$$v_l = \sum_{all} v_i \times \frac{T}{298.15} \tag{3.7}$$

In which the summation applies to the sum of the molar volume contribution by each of the constituent as shown in Table 3.1 and 'i' stands for the i^{th} constituent of the CME.

In the end, the solubility parameter of the CME can be determined as a combination of the polar parameter (δ_p), dispersion parameter (δ_d) and hydrogen bonding parameter (δ_h)(Barton, 1983). The δ_p and δ_h parameters are attributed to the carbonyl group contained in each of the constituents, as such they are of the same magnitude of 240100 $Pa^{0.5}m^3$ and 7000 $Pa^{0.5}m^3$, respectively (Barton, 1983). After the estimation of the parameters of the constituents, the solubility parameter of the biodiesel can be estimated as follows (Barton, 1983):

$$\delta_l = \sqrt{\delta_d^2 + \delta_p^2 + \delta_h^2} \tag{3.8}$$

Ultimately, the prediction of the solubility of the naphthalene in CME requires the correction for polarity described as the characteristic constant, Δ. A study has been undertaken in which Δ has been correlated with δ_1 for gas solubility in 10 polar solvents as shown in Figure 3.2 (Yen et McKetta et al., 1962).

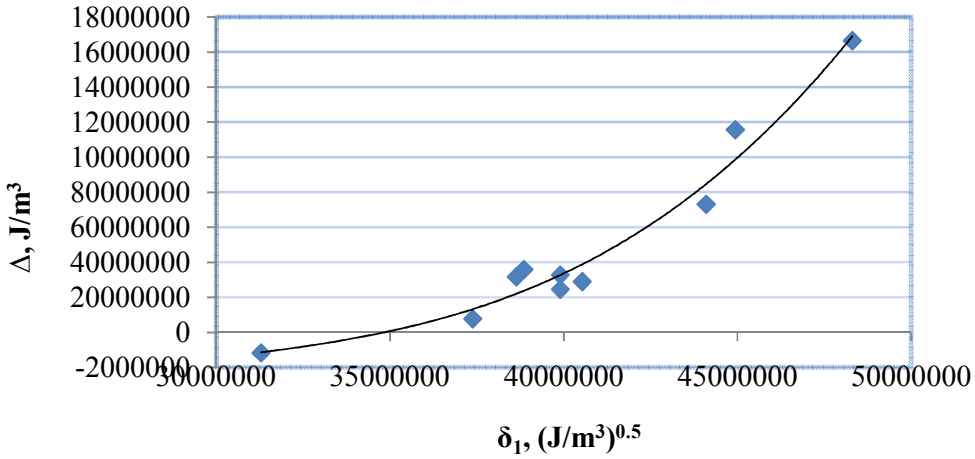

Figure 3.2: Correlation of Δ with δ_1 for gas/vapour solubility in polar solvents (Yen et McKetta et al., 1962).

The incorporation of the correction factor (Δ) into Equation (3.2) transforms it to a non-linear form which requires a mathematical program to solve it for x_2. As a result, a Matlab program is used to predict the solubility of the naphthalene in the biodiesel as a function of temperature and the results are shown in Figure 3.3.

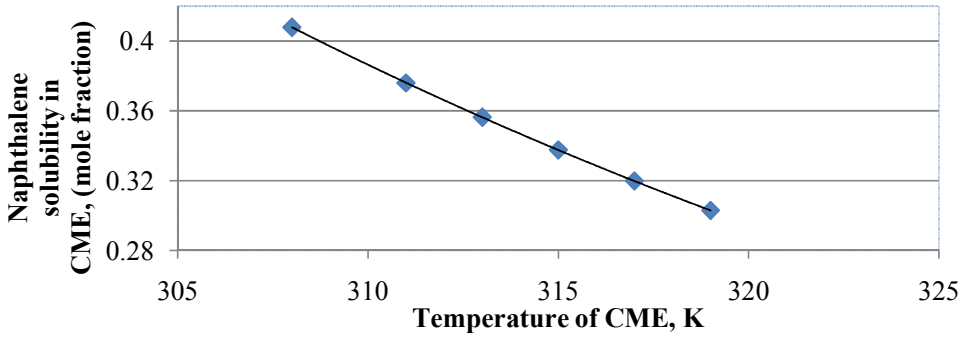

Figure 3.3: Predicted naphthalene solubility in CME as a function of temperature of CME.

Figure 3.3 shows that the solubility of naphthalene in CME decreases as the temperature of CME is increased. As a result, lowering the temperature of the CME

before it contacts with the gas containing naphthalene would enhance the solubility of the naphthalene in the CME. On the other hand, increasing the temperature of the naphthalene-loaded CME would decrease the solubility of the naphthalene. Furthermore, contacting the heated naphthalene-loaded CME with a hot gas would further decrease the solubility as well as enhance the transfer of the absorbed tars into the hot gas (air or nitrogen).

Figure 3.3 can be used to compare the solubility of model tar (naphthalene) in CME with those of real tars in RME as a way of validating the prediction of naphthalene solubility in CME. Literature has crudely reported the solubility of biomass tars in RME at 1 atmosphere and 50^{o}C to be 0.5kg/kg which is equivalent to 0.4842 moles tars per mole tar-RME solution. Using Figure 3.3, the naphthalene solubility at 1 atmosphere and 50^{o}C is 0.272 moles naphthalene per mole naphthalene-CME solution which is less than that of RME because CME is a smaller size molecule than RME. Generally, the solubility of naphthalene should be higher in a larger size molecule (RME) than in a smaller size molecule (CME). By the concept molecular size and the predicted and literature solubility values, the two solubilities compare closely.

In this study, a tar removal test system was built as a separate system from the gasifier, thus, the producer gas would be simulated by a readily available inert gas, nitrogen. The nitrogen would act as a carrier gas for the naphthalene which would be in vapour state at elevated temperatures. Since naphthalene exists in solid state at room temperature, it would be vaporised in a vaporiser. Figure 3.4 illustrates the tar removal test system which is based on the concept of Figure 3.1. In Figure 3.4, the nitrogen is used to represent the producer gas and CME is used as a solvent in the scrubber, and the tars are released from the CME by hot air in the stripper.

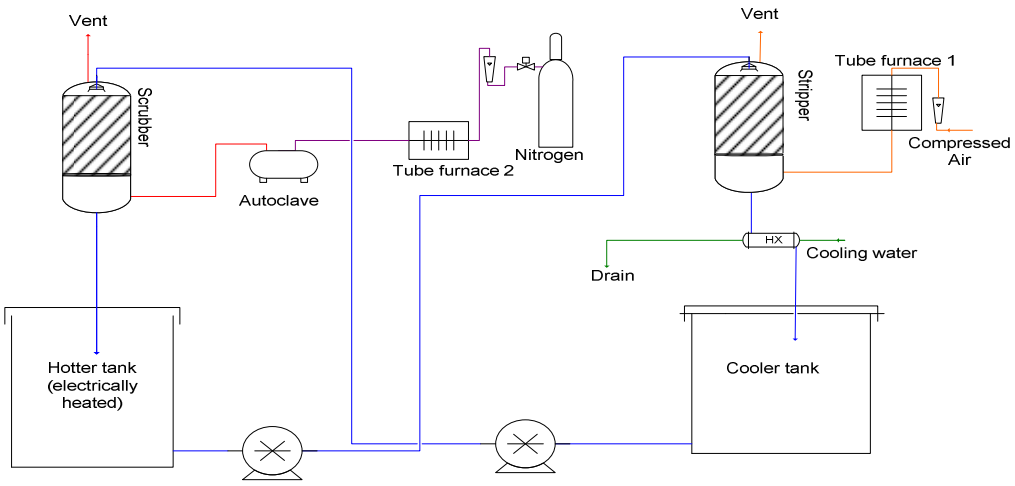

Figure 3.4: A complete schematic of the test system for the tar removal.

In the above system, the nitrogen is preheated in the tube furnace and the solid naphthalene is vaporised in the autoclave. The nitrogen is preheated to about 673 K by the Tube Furnace 2 which has a heating capacity of 1.5kW. The autoclave has built-in heating elements with power output of 3.5kW in which the naphthalene can be heated to a temperature in excess of 493 K which is the boiling point of naphthalene (Aldrich, 2010). As a result, the naphthalene is vaporised and carried away by the nitrogen gas from the autoclave into the scrubber. In order to prevent the naphthalene from re-crystallising, the pipe line from the nitrogen bottle to the scrubber is heated by heat-trace elements.

In operation, the CME is circulated in a closed loop through the scrubber and the stripper. After the stripper, the CME is cooled down and discharged into the cooler tank. A pump is used to deliver it into the scrubber where it contacts with the hot gas stream of nitrogen loaded with naphthalene vapours as tars. After the scrubber, the tar-loaded CME is discharged into a tank for heating. The heated tank has three sets of heating elements to control the CME temperature. Another pump is used to deliver the loaded CME to the stripper where it contacts with hot air which is heated by Tube Furnace 1 with a heating capacity of 1.5kW. In order to ensure that naphthalene is effectively transferred from the CME into the hot air, the air is heated to temperatures up to 528 K.

3.3. Specification and Selection of the Cooler and Heater

In order to achieve the target temperatures for the CME, the cooler and heater have to be specified so that they would provide or remove suitable amount of heat for the liquid phase. These temperatures are necessary in order to achieve the optimum efficiencies of the scrubber and the stripper. As it has been observed, low temperatures of the biodiesel promote high scrubbing efficiency. On the other hand, high temperatures promote high stripping efficiencies. In order to specify these units, an energy balance for each unit was conducted.

In taking the energy balance involving the stripper, its operating temperature was specified to avoid explosions as the liquid phase contacted with the hot air. In this regard, the temperature of the Tube Furnace 1 was specified so that the temperature of the heated air entering the stripper was well below the auto-ignition of biodiesel which is in the range 515 – 528 K (Shibata et al., 2008). Since the heat capacity of CME is much higher than that of air, especially at moderate temperatures (Goodrum, 1996), the temperature rise of the liquid phase over the stripper can be considered negligible.

In the case of energy balance involving the scrubber, the temperature of nitrogen stream containing naphthalene at the inlet point was specified typical to that cited in literature (Hofbauer, 2002). The temperature of the liquid stream entering the scrubber is governed by the heat exchanger (cooler) located below the stripper in Figure 3.4. The liquid stream inlet temperature to the scrubber was optimised to a value at which the cooler was capable of delivering. Consequently, the size of the cooler was specified so that the required temperature can be achieved. In order to specify the cooler, its heat load (Q) was firstly quantified as follows:

$$Q = m_L c_L (T_1 - T_2) \tag{3.9a}$$

$$Q = m_w c_w (t_2 - t_1) \tag{3.9b}$$

In which m_L is the mass flow rates of the liquid stream, kg/s, m_w is the mass flow rate of the cooling water kg/s, c_L is the heat capacity of the liquid stream, J/kg.K, and c_w is the heat capacity of the cooling water, J/kg.K.

The temperature of the cooling water entering the cooler was set at 288 K, which is the average temperature of water supplied by Christchurch City Council in New Zealand (Holdings, 2006). The cooling water is designed to flow inside the tubes while the liquid stream (CME) flows outside the tubes of the cooler. In addition, the cooler is insulated and thus it can be assumed that all of the heat provided by the liquid stream (CME) would be transferred to the cooling water. Therefore the temperature of the cooling water exiting the cooler is determined as follows:

$$t_2 = \frac{m_L c_L}{m_w c_w}(T_1 - T_2) + t_1 \qquad (3.10)$$

In Equation (3.10), the mass flow rate of the CME stream is obtained from the liquid to gas ratio for the design of the scrubber and stripper. The heat capacity of the CME stream is obtained from literature for a methyl ester biodiesel which contains 60.2wt% methyl oleate (as shown in Table 3.1) as one of its constituents (Goodrum, 1996). It would be justifiable to use the literature heat capacity for pure methyl esters as the concentration of the naphthalene (solute) in the liquid stream both in the scrubber and in the stripper would be very low. On the other hand, the mass flow rate of the cooling water can be determined by using the typical shell and tube fluid velocity. For the water in the tubes, the recommended velocity ranges from 1.5 to 2.5m/s (Sinnott, 2005). Therefore, m_w can be estimated as follows:

$$m_w = 0.25\pi d_i^2 \rho_w u_w \qquad (3.11)$$

In which d_i is the inside diameter of the tubes, ρ_w is the density of the cooling water, kg/m^3 and u_w is the linear velocity of the cooling water, m/s. T_1 and T_2 can be set to be 353 and 303 K, respectively. The 353 K is the safe temperature at which most seals in the readily available pumps can operate properly, and 303 K is a reasonable temperature which the scrubber can be operated at. In addition, a standard tube inside diameter in the range 0.016 – 0.025m can be used (Sinnott, 2005). Based on the

above values, the water exiting temperature, t_2, is estimated be below 353 K. This water exiting temperature is appropriate in that the temperature profile of the cold stream (water) would not cross that of the hot stream. Therefore, ρ_w is evaluated at the average temperature of 288 and 353 K. After t_2 has been estimated, the size of the cooler in term of the cooling surface area (A) is estimated as follows:

$$A = Q\frac{\ln\left[(T_1 - t_2)(T_2 - t_1)^{-1}\right]}{U\left[(T_1 - t_2) - (T_2 - t_1)\right]} \qquad (3.12)$$

In which U is the overall heat transfer coefficient, $W/m^2.K$ and A is the cooling surface area, m^2,

According to Coulson, U for heat transfer between water and light organic oils is in the range 350 – 900 $W/m^2.K$ (Coulson et Richardson et al., 1996). Using this data, the heating area, A, was calculated to be in the range of 0.2 – 0.6 m^2. In this study, a heat exchanger with a heating area of 0.4 m^2 was selected. However, local manufacturers of heat exchangers do not make coolers of that area. As a result, two coolers of total area equalling 0.4 m^2 were bought from Savage Manufacturing Limited, Christchurch, New Zealand and used in the study (Parr, 2008), each had 48 tubes of 0.00523m inside diameter and 0.00056m thickness with 0.08m inside diameter shell.

The two coolers were plumbed in parallel to each other in order to meet the specification. The use of the two coolers helped to reduce the pressure drop over the stripper because the liquid phase was quickly drained by the two pipes which connected the coolers.

After the coolers have been specified and selected, the temperature of the liquid stream at inlet to the scrubber can be controlled by adjusting the flow rate of the cooling water. However, the temperature of the liquid stream at inlet to the stripper will only be fully controlled if the heat supplied to the heated tank is properly controlled.

In order to determine and control the heat supplied to the heated tank, the temperatures of the liquid stream in and out of the tank need to be known. The

increase in the temperature of the liquid stream over the scrubber is considered to be negligible. Therefore, the heating load in the heated tank will be determined by the required temperature of the biodiesel to the stripper. As discussed previously, it is necessary to increase the temperature of the biodiesel to enhance the stripping efficiency in the stripper. The amount of heat required for the heated tank (Q_{tank}) can be estimated as follows:

$$Q_{tank} = 1.2 m_L c_L (T_{out} - T_{in}) \tag{3.13}$$

In which T_{in} and T_{out} are the inlet and outlet temperatures of the liquid stream over the heated tank, respectively. The temperature of the CME in the heated tank is controlled by a PID controller. Besides, a 20% heat losses through the tank walls is assumed and incorporated in Equation (3.13), even though the heated tank and its discharge pipe are insulated with Kao-wool material.

The power required increases with the required outlet temperature of the biodiesel as shown in Figure 3.5. The temperature of the liquid stream discharge from the heated tank is designed at a maximum of 368 K and the liquid mass flow rate of 4.5l/min. However, it is also possible that the CME temperature at the inlet point of the stripper is higher than the controlled outlet temperature from the heated tank as the pipes connecting the heated tank and the stripper are heat-insulated and heated controlled.

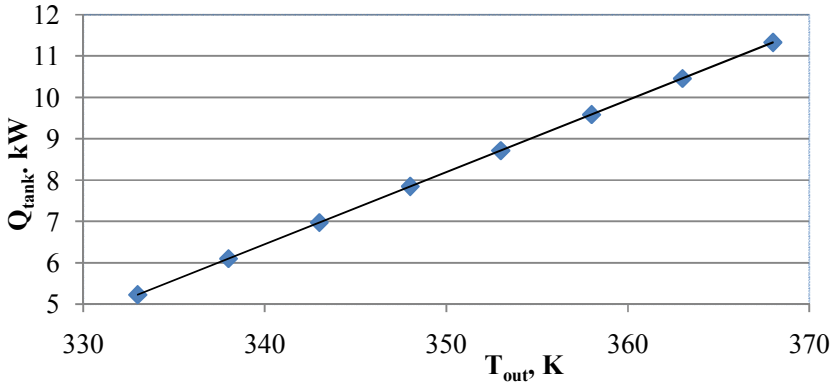

Figure 3.5: The amount of power required to heat up the CME from 330 to 368K at the CME flow rate of 4.5*l*/min.

After the specification of the auxiliary units for the system had been done, the scrubber and stripper were designed and preliminary experiment conducted on the system. The details for the design of the scrubber and stripper and the preliminary experiments are described in Chapter 4.

Chapter 4 Design of the Test System and Preliminary Experiments

4.1. Introduction

In this part of study, the test system consisting of a scrubber and stripper was designed and constructed on which preliminary experiments were conducted. In the scrubber, tars in the simulated producer gas were removed by CME as a solvent and in the stripper; the tars absorbed by the CME were released and carried away by hot air. In the design of these columns, the flooding point and pressure drop were firstly specified and later validated by experiments. In addition, the diameter and height of the packing in the two columns were estimated using the methods proposed by Sherwood (Sherwood et al., 1938; Lobo et al., 1945) for the predicted equilibrium coefficient. The design correlation involves density and viscosity of the gas and the liquid, equilibrium coefficient as well as the liquid to gas flow rate ratio. The density and the viscosity of the gas were obtained from the literature (Incropera et Dewitt et al., 2002). In the case of the liquid, the required properties were measured.

Over the years, the initial correlation proposed by Sherwood has been modified following more available experimental data. Leva used experimental data obtained from columns with packing materials of rings and saddles and extended the correlation by including lines of constant pressure (Leva, 1954). As a result, a chart which is now commonly called the generalised pressure drop correlation (Leva, 1954) was developed. The flooding curve in this chart has been conveniently used and accurately described by a polynomial regression (Benitez, 2002). This regression contains a quantity which is a product of the liquid to gas mass flow rate ratio and the gas to liquid density ratio.

In this work, the equilibrium coefficients for the scrubbing and the stripping process are predicted based on tar solubility in biodiesel, Henry's law coefficient and an equation of state. The Henry's law coefficient can be expressed as follows:

$$f_2 = x_2 H_{12} \tag{4.1}$$

In which f_2 is the fugacity of the tars in the gas phase, x_2 is the mole fraction of the tars in liquid phase and H_{12} is the Henry's constant for a given system where the tars are transferred between gas and liquid (CME) phases. Note that activity coefficient of the naphthalene in

CME was calculated by UNIFAC group method and found to be approximately 1(Gmehling et al., 1998). That is the reason it does not appear in Equation (4.1). On the other hand the use of the solubility rather than the equilibrium composition is based on the method for the experimental determination of the Henry's constant (Japas et al., 1992).

Equation (4.1) can be applied to dilute system, up to 10% (mol/mol) of the solute in both the gas and liquid phases (Iveson, 2000). If the total pressure (p) of the system is applied to Equation (4.1), it becomes:

$$\frac{f_2}{p} = x_2 \frac{H_{12}}{p} \tag{4.2}$$

The term H_{12}/p in the right side of Equation (4.2) is also called the equilibrium coefficient and term f_2/p defines the composition of the tars in the gas phase. In order to differentiate the expressions for the equilibrium coefficients in scrubber and stripper respectively, the following equation are adopted:

$$\text{For the scrubber,} \quad m(T) = \frac{f_2}{x(T)p} \tag{4.3a}$$

$$\text{For the stripper,} \quad k(T) = \frac{f_2}{x(T)p} \tag{4.3b}$$

In which m(T) and k(T) are the equilibrium coefficients as a function of temperature for the scrubber and stripper, respectively, f_2 is the fugacity of the tars and x(T) is the mole fraction solubility of the tars in biodiesel as a function of temperature.

In order to use Equations (4.3a) and (4.3b), the solubility of the tars was used which had been predicted following the procedure described in Chapter 3. The ratio of fugacity to total pressure was estimated by using the Soave-Redlich-Kwong equation of state, defined as follows (Zhou et Zhou et al., 2001):

$$\frac{f_2}{p} = z_2 - 1 - \ln\left(z_2 - B^*\right) - \frac{A^*}{B^*} \ln\left(1 + \frac{B^*}{z_2}\right) \tag{4.4}$$

where z_2 is the compressibility factor of the tars in the gas which is determined by using the Lee-Kesler correlation tables (Smith et al., 1996) and, A^* and B^* are

characteristic constants, which can be determined by using properties of the most abundant tar component, naphthalene, defined at its critical state.

Using Equations (4.3a) to (4.4) and the predicted solubility, the equilibrium coefficient is calculated as a function of temperature and the results are shown in Figure 4.1.

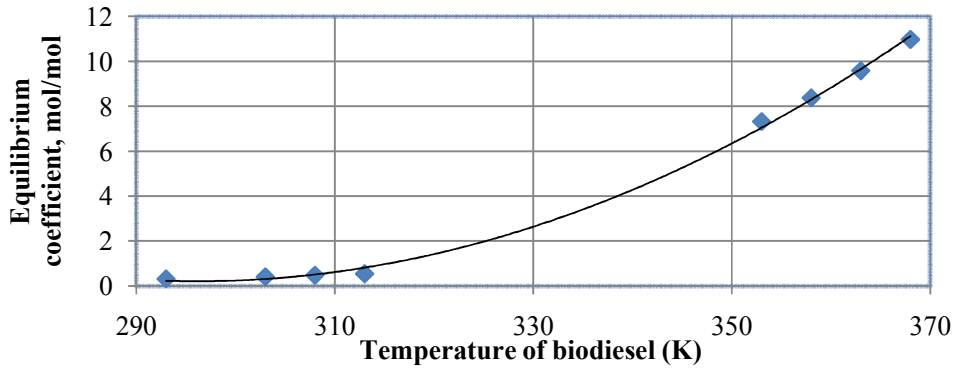

Figure 4.1: Calculated equilibrium coefficient of tars in the CME as a function of temperature.

In Figure 4.1, the equilibrium coefficient in the temperature region 293 – 313 K signifies the operation where tars are transferred from gas phase to the liquid phase. In that region the coefficient is less than 1 which means the tar solubility in CME is very much favoured. Conversely, the coefficient is greater than 1 in the region of temperature 353 – 368 K, implying that tar solubility in CME is not favoured. As a result, there are much more tars in the air than in CME. The region in between 313 and 368 K does not have data because the coefficients are not predicted in that region. However, the two regions are just connected by a best fit curve.

Once the equilibrium coefficient is known, the theoretical minimum CME biodiesel and air flow rate ratio can be determined in the scrubber from the operating line and the equilibrium curve. In this study, nitrogen is used as a simulated producer gas and its flow rate is fixed, therefore, the minimum CME flow rate can be calculated. By introducing a safety factor, the operational CME flow rate can be determined which is also the CME flow rate in the stripper as the CME circulates in an enclosed loop.

In the stripper, the maximum liquid to gas flow rate ratio is firstly found based on the operating line and the equilibrium curve. Then the CME flow rate determined from the scrubber is used as a fixed parameter for determination of the minimum air flow rate in the stripper. The determined flow rates are then used to optimise the liquid to gas ratio for the integrated system.

The liquid to gas flow rate ratio affects the temperature profiles over the columns both in the scrubber and stripper. In the scrubber, the gas is designed to enter at the bottom of the scrubber at temperatures of 433 – 473 K while the CME flows from the top of the scrubber at temperatures of 293 – 303 K. In the stripper, the hot air enters at the bottom of the stripper at 523 – 543 K and the CME enters the top of the stripper at temperature of 333 – 353 K. As the CME temperature varies both in the scrubber and stripper, the densities and viscosities of the CME are measured and correlated at different temperatures so that the data can directly be used in the practical design.

4.2. Measurement and Correlation of Density and Viscosity of the CME

Density and viscosity of the CME were measured at different temperatures to establish correlations as functions of temperature. The density was measured by the use of a density meter called the Anton Paar DMA60. Based on the measured data, the following correlation of density of tar free CME (ρ) as a function of temperature (T, K) was fitted:

$$\rho\left(\mathrm{kg/m^3}\right) = 1021.9 - 0.4568\mathrm{T}\left(\mathrm{K}\right) \tag{4.5}$$

The viscosity was measured by using a viscometer called the Haake Rotovisco RV 20. The correlation of the viscosity of tar free biodiesel (μ) as a function of temperature (T, K) was fitted as follows:

$$\ln\mu\left(\mathrm{kg/m.s}\right)) = \frac{2402}{\mathrm{T}\left(\mathrm{K}\right)} - 12.7 \tag{4.6}$$

In order to reflect the effect of the tar concentration on the density and viscosity of the CME, the above properties were measured at different temperatures

and tar concentrations. The densities of tar laden CME (ρ_m) and tar concentrations (x) at temperatures of 293.15, 298.15 and 303.15 K are as shown in Table 4.1.

Table 4.1: Densities of tar laden CME at 293.15, 298.15 and 303.15 K

293.15 K		298.15 K		303.15 K	
ρ_m (kg/m^3)	x (mol/mol)	ρ_m (kg/m^3)	x (mol/mol)	ρ_m (kg/m^3)	x (mol/mol)
887.83	0.003686	885.7	0.003591	884.14	0.00358
887.62	0.001476	885.49	0.001467	883.85	0.001462
887.73	0.002655	885.61	0.002713	883.97	0.002703
888.01	0.005596	885.89	0.005636	884.25	0.005617
887.49	0.000148	885.37	0.000147	883.73	0.000146

The data in Table 4.1 was used to analyse the effect of tar concentration on the density of tar laden CME. This effect is shown in Figure 4.2 which shows a linear trend with high R^2 values.

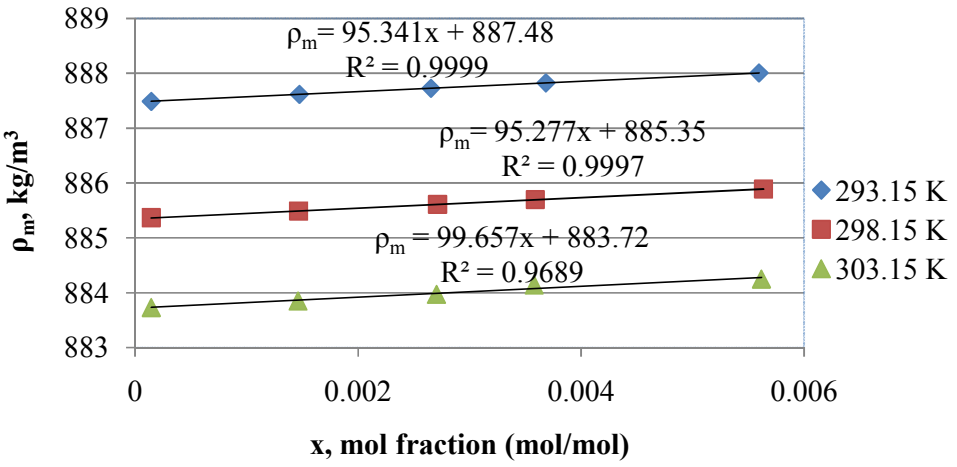

Figure 4.2: Effect of tar concentration on the density of tar laden CME at 293.15, 298.15 and 303.15 K

On the other hand, the R^2 values for the relation between temperature and tar concentrations were determined to be very low. Therefore, a multiple linear regression was used to correlate density of the tar laden CME (ρ_{LM}) with tar concentration (x_m) and temperature (T) as follows:

$$\rho_{LM}\left(\text{kg/m}^3\right) = 67.43x_m\left(\text{kg/kg}\right) - 0.3723\text{T(K)} + 996.45 \qquad (4.7)$$

The densities calculated by Equations (4.7) compared very closely with those which were measured and shown in Table 4.1

With regards to viscosity, it was found that the effect of tar concentration on the biodiesel viscosity was inconsistent thus no significant correlation could be established. This inconsistent phenomenon is clearly demonstrated in Figure 4.3.

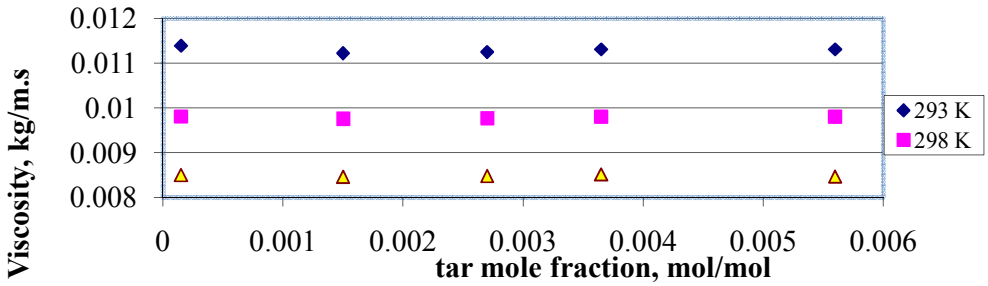

Figure 4.3: Inconsistent effect of tar mole fraction on viscosity of tar-CME solution

4.2.1. Density and Viscosity Correlations

Based on the above trends for CME properties as a function of both temperature and tar fraction, more general correlations are proposed for determination of biodiesel density and viscosity as follows:

Pure density (ρ), $\rho = a_1 T + a_0$ (4.8a)

Mixture density (ρ_m), $\rho_m = a_2 x + a_1 T + a_0$ (4.8b)

Viscosity (μ) $\ln\mu = \frac{b_1}{T} - b_0$ (4.9a)

Equations (4.8a), (4.8b) and (4.9a) are used to reformulate Equations (4.5), (4.6) and (4.7) to cover variations of both temperature and tar concentration. The experimental data are fitted to the proposed correlations by the least-squares method to obtain the coefficients (a_0, a_1, a_2, b_0 and b_1). In order to ascertain the applicability of the correlation, the data is statistically analysed and the results of the analysis are shown in Table 4.2.

Table 4.2: Analysis of the measured density and viscosity of pure biodiesel

Parameter	Coefficients			R^2
Pure density	a_o: 1021.9±9.9	a_1: -0.4568±0.037	-	0.9844
Mixture density	a_o: 996.5±9.4	a_1: -0.3723±0.032	a_2: 67.43±0.13	0.9207
Viscosity	b_o: -12.7±0.1	b_1: 2402±33	-	0.9997

Although, Equation (4.7) can be used for a wide range of temperatures and tar compositions, it has only been tested at the temperatures ranging 293.15 - 303.15 K. Therefore, its use at other temperatures would be satisfactory after it has been validated experimentally at those temperatures. Equation (4.7) was validated over that narrow range of temperature because that was the region of interest in this study.

The R^2 values shown in Table 4.2 show that the fitting is satisfactory. However, the effect of temperature on the density residuals is analysed to test the biasness of the correlation as shown in Figure 4.4.

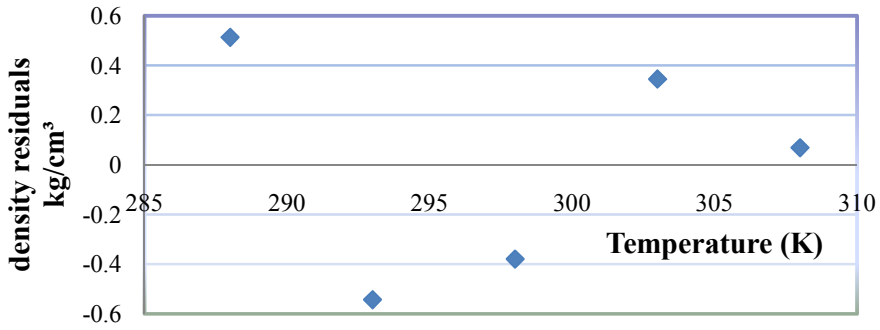

Figure 4.4: Plot of density residual against temperature

Figure 4.4 shows that the correlation is biased towards density because the residuals are uniformly distributed away from the temperature axis but towards density axis. Similarly, the data plot of natural log of viscosity residual against inverse of temperature is done to test the biasness of the correlation as shown in Figure 4.5. From Figure 4.5, it is seen that the model is unbiased because the residuals are randomly distributed.

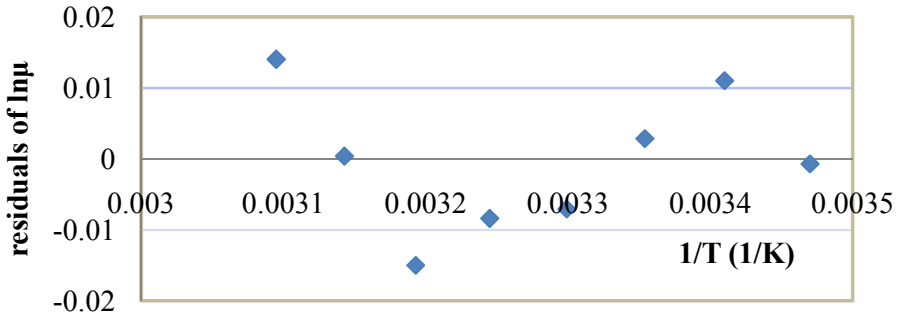

Figure 4.5: Plot of residuals of natural log of viscosity of CME against inverse of absolute temperature.

Since RME, unlike CME, has been used for tar removal successfully (Proll et al., 2005), the ability of CME to remove tars from producer gas can be explored by comparing the density and viscosity of RME with those of CME. The comparison is shown in Table 4.2a where literature values for RME and measured values, in this study, for CME have been used.

Table 4.2a: Densities and viscosities of RME and CME at 1 atmosphere and 25^{o}C

Property	RME (Rashid and Anwar 2008)	CME
Density (kg/m^3)	880	886
Viscosity (kg/m.s)	0.005298	0.00962

Table 4.2a shows that CME is denser and more viscous than RME which can not conclusively be used to compare the solubility of model tar (naphthalene). However, their densities and that of naphthalene can be used to assess the naphthalene solubility in CME and RME. The densities can be used to determine the cohesive energy density which is related to solubility (Barton, 1983). Table 4.2b can be used to determine the cohesive energy densities of CME, RME and naphthalene. In Table 4.2b, ΔH_{vap} is the heat of vaporization at 25^{o}C and 1 atmosphere for a component of either CME or RME and M is the molar mass (kg/k-mole) of the particular component and Σ is the summation of the contributions of ΔH_{vap} from each component, which result in the ΔH_{vap} for either CME or RME.

Table 4.2b: Heat of vaporization of constituents of biodiesel at 298 K and 1bar

		CME		RME	
Name	M	%mol	ΔH_{vap}, (kJ/mol)	%mol	ΔH_{vap}, (kJ/mol)
Methyl oleate	296	59.98	65.50	21.82	23.83
Methyl linoleate	294	21.16	23.11	13.14	14.35
Methyl myristate	242	0.1219	0.1106	0	0
Methyl palmitate	270	4.260	4.260	2.949	2.949
Methyl stearate	298	3.068	3.350	2.771	3.026
Methyl linolenate	292	11.21	12.24	8.685	9.485
Methyl erucate	352	0.4189	0.5346	42.64	54.42
			$\Sigma = 109.11$		$\Sigma = 108.06$

By using Table 4.2a, Table 4.2b, heat of vaporization and molar volume of naphthalene which are 43193 J/mol and 0.0001124m^3/mol at 298 K and 1 bar respectively, the cohesive energy densities of RME, CME and naphthalene can be determined as follows (Barton, 1983):

$$E_\rho = \frac{\Delta H_{vap} - RT}{v_m} = \frac{(\Delta H_{vap} - RT)\rho}{M} \qquad (4.9b)$$

In Equation (4.9b), R is the universal gas constant (J/mol.K), T is absolute temperature (K), V_m is molar volume (m^3/kmol), M is the molar mass, (kg/kmol), ρ is the density (kg/m^3) and E_ρ is the cohesive energy density (J/m^3). According to Barton (1983), substances which have similar or close values of E_ρ are miscible. In other words, a solute will dissolve in a solvent if its cohesive energy density is same or close to that of the solvent. In this study, the cohesive energy densities of RME, CME and naphthalene have been determined to be 0.29, 0.32 and 0.36GJ/m^3. Therefore, naphthalene is likely to be more soluble in CME than in RME but the difference in the solubilities might be small.

4.3. Liquid to Gas Flow Rate Ratio for the Scrubber

The scrubber is illustrated in Figure 4.6 with operation conditions shown at the top and the bottom of the column. If all of the concentrations of the liquid and the

gas are known, a straight line can be drawn between the conditions at the top and those at the bottom. This line is called operating line. Once this line is drawn, the liquid to gas flow rate ratio can be determined which is equal to the slope of the operating line. Based on the mass balances of tars both over the whole column and in part of the column, a linear relationship (defining the operating line) can be obtained between the tar concentration in the gas and that in the liquid at any location of the scrubber, as shown in Equation (4.10).

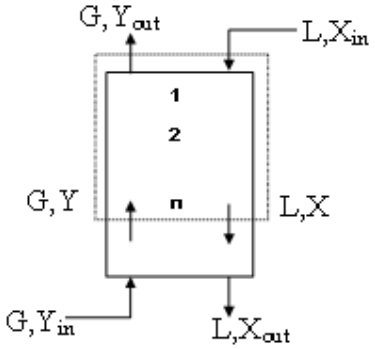

Figure 4.6: Schematic diagram for the scrubber column.

$$Y = \frac{L}{G}X + Y_{out} - \frac{L}{G}X_{in} \qquad (4.10)$$

In which X and Y are compositions in mole ratios of the tars in the liquid and gas phases, '**in**' and '**out'** denote inlet and outlet of the liquid and gas streams, and L and G are the liquid and gas phase molar flow rates (k-mol/m^2s), respectively.

However, in practice, the inlet conditions of gas and liquid as well as the target tar removal (or tar concentration of the outlet gas) are known, the outlet tar concentration in the liquid is affected by the liquid to gas flow rate ratio (L/G). In this case, the liquid to gas flow rate ratio needs to be determined first. In fact, the liquid to gas flow rate ratio (L/G) is the dominant factor for the column height required to achieve the required outlet concentrations of tars in the CME. At constant gas flow rate, the high ratio of liquid to gas flow rates will result in a shorter column height.

In a procedure to estimate the L/G for the scrubber, the minimum liquid to gas ratio (L_{min}/G) is firstly determined as follows:

$$\frac{L_{min}}{G} = \frac{Y_{in} - Y_{out}}{X^*_{out} - X_{in}} \tag{4.11}$$

In which X^*_{out} is the upmost liquid concentration which is attained in a long time and high tower, and is the equilibrium concentration corresponding to the inlet gas concentration as shown in Figure 4.7. Once the minimum liquid to gas flow rate ratio is known, a safety factor (n_o) is introduced to determine the actual gas to liquid flow rate ratio. The method to determine the actual L/G is as follows:

$$\frac{L}{G} = \frac{Y_{in} - Y_{out}}{X_{out} - X_{in}} \tag{4.12}$$

$$\frac{L}{G} = n_0 \frac{L_{min}}{G} = \frac{Y_{in} - Y_{out}}{X_{out} - X_{in}} = n_0 \frac{Y_{in} - Y_{out}}{X^*_{out} - X_{in}} \tag{4.13}$$

In which n_0 is chosen between 1 and 2, that is $1 < n_0 < 2$ (Woods, 2007). A graphical illustration of the equilibrium line and the operating line is shown in Figure 4.6 which also shows L_{min}/G and L/G for the scrubber.

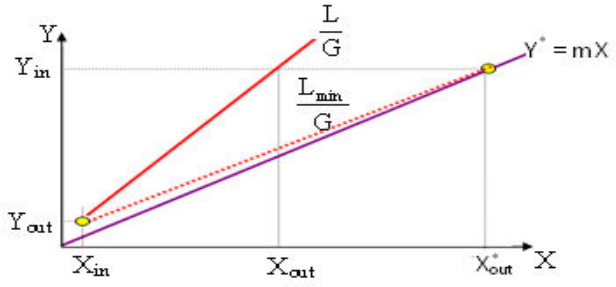

Figure 4.7: A graphical representation of the equilibrium line and operating and their related compositions in a scrubber.

In the present study, Y_{in} can be taken as equivalent to 2.5g tars/Nm^3 gas (Hofbauer, 2002) and Y_{out} as equivalent to 0.6g tars/Nm^3 gas for the scrubber (Babu, 1995). Therefore, the fraction of the tars to be removed is 0.76. Assuming that this is the same fraction to be removed from the liquid phase in the stripper, Equation (4.13) can be rearranged as follows:

$$X_{in} = \frac{0.24 X^*_{out}}{0.76 n_0 + 0.24} \quad (4.14)$$

X^*_{out} can be calculated from the equilibrium coefficient and the inlet gas concentration. Therefore, Equation (4.14) can be used to determine L/G for a selected n_0.

Once the gas to liquid flow rate ratio is determined, the tower height can be determined by either using analytical method or the graphical method. The diameter of the scrubber is estimated by using the actual liquid and gas flow rates and considering the flood limit.

A higher reference tar concentration in the off-gas for the scrubber was chosen as the basis for the scrubber design because of the constraints in the space where the test system was going to be built. Once the test system was built, its performance was investigated and then design parameters were determined so that they could be used to redesign the system as discussed in Chapter 7.

4.4. Diameter of the Scrubber

The diameter of the scrubber was determined using a method proposed by (Benitez, 2002) which involves parameters of liquid and gas flow rates, and density, viscosity and temperature of the fluids in the scrubber. The operating pressure was taken to be the atmospheric pressure because the scrubber is normally operated under atmospheric pressure. A procedure proposed by Benitez (Benitez, 2002) first calculates an intermediate parameter for flood condition, Y_{flood} as follows:

$$\ln Y_{flood} = -\left[3.5021 + 1.028 \ln X_c + 0.11093 (\ln X_c)^2\right] \quad (4.15)$$

In which X_c is defined as follows:

$$X_c = \frac{m_L}{m_G} \sqrt{\frac{\rho_G}{\rho_L}} \quad (4.16)$$

In which m_L and m_G are the mass flows rates (kg/s) of the liquid and gas streams, respectively, and, ρ_L and ρ_G (kg/m^3) are the liquid and gas densities. The actual liquid

to gas flow rate ratio was determined using Equation (4.13) with the safety factor, n_0, being 1.85.

Further, the superficial gas velocity at flooding C_{SF} and the gas velocity at flooding u_{GF} are calculated by the following equations:

$$C_{SF} = \sqrt{\frac{Y_{flood}}{P \cdot F_u \mu_L^{0.1}}} \tag{4.17a}$$

$$u_{GF} = \frac{C_{SF}}{\sqrt{\frac{\rho_G}{\rho_L - \rho_G}}} \tag{4.17b}$$

In which μ_L is the viscosity of the pure biodiesel and P·Fu is the product of the packing factor in m^2/m^3 and its conversion factor of 16. Ultimately, the diameter (D) of the scrubber was estimated by the following equation:

$$D = \sqrt{4\frac{V_G}{f_o(u_{GF})\pi}} \tag{4.18}$$

In which V_G is the volumetric flow rate of the gas stream which can be determined from the gas mass flow rate and the gas density, and f is the ratio of gas velocity to the flooding gas velocity, $0.3 \leq f_o \leq 0.7$ (Woods, 2007). The estimated diameters of the scrubber as a function of the temperature of the CME biodiesel at inlet point to the scrubber are shown in Table 4.3.

Table 4.3: Estimated diameters of the scrubber at 50% flooding gas flow rate

Liquid phase inlet temperature		Actual liquid to gas ratio	Diameter
T(°C)	T(K)	(mole /mole)	(m)
30	303	1.47	0.15
40	313	1.50	0.159

The diameters shown in Table 4.3 are reasonable as they apply for the liquid to gas ratio which is within the recommended range for counter current scrubber columns (Woods, 2007). In this study, the scrubber column is designed to have a

diameter of 0.15m for total gas flow rate of 14.6m^3/h (or 0.01086kmol/min) and liquid to gas flow rate ratio of 1.47.

4.5. Height of packing for the Scrubber

The height of packing for the scrubber is affected by the extent of difficulty and effectiveness of the separation of the tars. The measure of the separation difficulty is usually referred to as the number of transfer units (N_{OL} or N_{OG}) while the effectiveness of separation is the height of the transfer units (H_{OL} or H_{OG}). The two parameters which are based on the driving force of gas phase overall concentrations are represented by N_{OG} and H_{OG}. These two parameters are used to estimate the height of packing (Z) as follows:

$$Z = H_{OG} \times N_{OG} \tag{4.19}$$

The height of packing for the uni-molecular diffusion of tar vapours is determined according to Henley and Seader by the following equation (Henley et Seader et al., 1981):

$$Z = \frac{G}{K_Y a} \int_{Y_{out}}^{Y_{in}} \frac{dY}{\left(Y - Y^*\right)} \tag{4.20a}$$

In Equation (4.20a), the overall height of the transfer unit is $H_{OG} = \frac{G}{K_Y a}$ and overall number of the transfer unit is $N_{OG} = \int_{Y_{out}}^{Y_{in}} \frac{dY}{\left(Y - Y^*\right)}$ with A being the cross sectional area of the scrubber column and, **a** and G being the interfacial area per unit of active equipment volume and molar flow rate of the gas per area, respectively.

The tar concentrations in the gas and liquid reported in Section 4.3 are used to determine the N_{OG}. Those concentrations of the tars in the feed gas for the scrubber are equivalent to 0.0003567 (mole tar/mole gas). On the other hand, the concentration in the exit gas is equivalent to 0.00008561 (mole tar/mole gas). Since the tar concentration in both the liquid and gas phase are less than 10% (Geankoplis, 2003), the N_{OG} was estimated by using the analytical method defined as follows (Henley et Seader et al., 1981):

$$N_{OG} = \frac{Y_{in} - Y_{out}}{\left(Y_{in} - Y_{in}^{*}\right) - \left(Y_{out} - Y_{out}^{*}\right)} \ln \frac{Y_{in} - Y_{in}^{*}}{Y_{out} - Y_{out}^{*}} \tag{4.20b}$$

In which the equilibrium tar concentrations are define as follows:

$$Y_{in}^{*} = m(T) X_{out} \tag{4.21a}$$

$$Y_{out}^{*} = m(T) X_{in} \tag{4.21b}$$

In Equation (4.21a), the concentration of the tars in exit liquid phase, X_{out}, can be determined from material balance as follows:

$$X_{out} = \frac{G}{L}\left(Y_{in} - Y_{out}\right) + X_{in} \tag{4.21c}$$

A combination of Equations (4.14) and (4.20b) to (4.21c) are used to determine the N_{OG} as 3.64 for which the equilibrium coefficient is 0.4140 (mol/mol) and temperature of biodiesel is 303 K. In the end, the overall gas phase height of transfer unit is estimated by using the following equation:

$$H_{OG} = \frac{G}{K_Y a} \tag{4.22}$$

In which the overall gas transfer coefficient (K_Y) is given as follows (Henley et Seader et al., 1981):

$$K_Y = \frac{k_X k_Y}{k_X + m(T) k_Y} \tag{4.23}$$

In which k_X and k_Y are the film mass transfer coefficient which can be estimated as follows (Treybal 1981):

$$k_X = 25.1 \left(\frac{d_S L'}{\mu_L}\right)^{0.45} \left(Sc_L\right)^{0.5} \frac{D_L}{d_S} \tag{4.24a}$$

$$k_Y = 1.195 \left(\frac{d_s G'}{\mu_G \left(1 - \varepsilon_{LoB}\right)}\right)^{-0.36} \left(\frac{G'}{M_G Sc_G^{2/3}}\right) \tag{4.24b}$$

In which $L^{'}$ and $G^{'}$ are the liquid and gas mass flux ($kg/m^2.s$), respectively, Sc_L and Sc_G are Schmidt numbers for the liquid and gas, respectively, μ_L and μ_G are the liquid viscosity and gas viscosity (kg/m.s), M_G is the average molecular weight of the gas, d_s is the diameter of the sphere of the same surface as a single packing particle (m) and ε_{LoB} is the operating void space in the packing. The Schmidt number for the gas phase is calculated by using the properties for the gas (nitrogen) taken from literature, while that of the liquid phase is calculated by using the measured properties of biodiesel.

As the properties of the gas and liquid as well as the equilibrium coefficient vary with temperature, the estimated H_{OG} increases with the temperature of the liquid phase in the scrubber as shown in Figure 4.8. As a result, the height of packing also increases with the temperature of the liquid phase in the scrubber as shown in Table 4.4. This trend can be explained by the significant influence of the tar solubility in biodiesel. The tar solubility decreases as the temperature of the biodiesel increases, therefore, the driving force for the tar transfer from gas to liquid is reduced resulting in a larger contact area between the gas and liquid in a higher column. Therefore, the height of packing required to achieve a desired separation should increase.

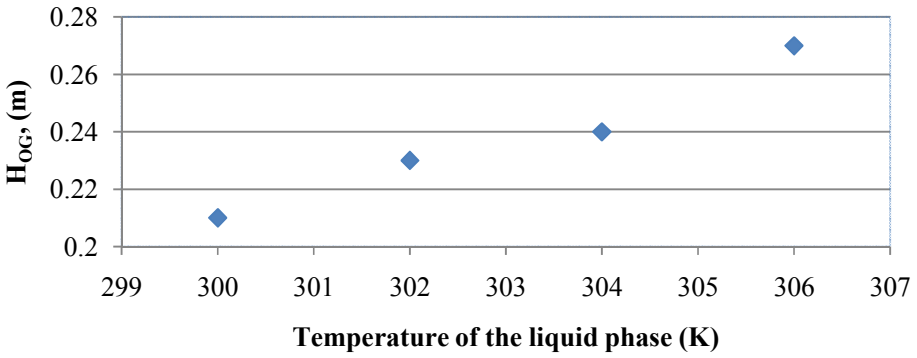

Figure 4.8: Effect of the liquid phase temperature on overall gas height of transfer units.

Table 4.4: Height of packing at inlet temperatures of the liquid phase to the scrubber

Temperature (K)	300	302	304	306
Packing height (m)	0.765	0.8415	0.918	1.071

In this study, the scrubber is designed to have a packing height of 0.85m with liquid temperature of 303 K and gas to liquid flow rate ratio of 1.47.

4.6. The Liquid to Gas Flow Rate Ratio for the Stripper

The L/G for the stripper is estimated by taking the material balances in the same manner as for the scrubber. Therefore, the equation of the operating line is similar to Equation (4.10). However, the operating line is below the equilibrium curve for the stripper. In the stripper where the tars are absorbed by the gas phase from the solvent, the inlet gas concentration and the required liquid concentration are known, thus the maximum liquid to gas flow rate ratio or minimum gas flow rate (G_{min}) at given liquid flow rate can be found when the operating line touches the equilibrium curve. The stripper with higher values of L/G or low gas flow rate at given liquid flow rate requires higher columns to achieve the required recovery target. Therefore, a safety factor is introduced to decrease the liquid to gas flow rate ratio or increase the gas flow rate at given liquid flow rate. In the estimation of the L/G for the stripper, the minimum gas flow rate (G_{min}) is firstly determined as follows:

$$G_{min} = \frac{L(X_{in} - X_{out})}{Y^{*}_{out}} = \frac{L(X_{in} - X_{out})}{k(T)X_{in}} \qquad (4.25)$$

In which L, the molar flux, is used for both scrubber and the stripper, X_{in} and X_{out} are the tar concentrations in the liquid exiting and entering the scrubber respectively and Y^{*}_{out} is the tar concentration in the outlet gas phase in equilibrium with inlet liquid to the stripper. Equation (4.25) can be interpreted graphically as shown in Figure 4.9.

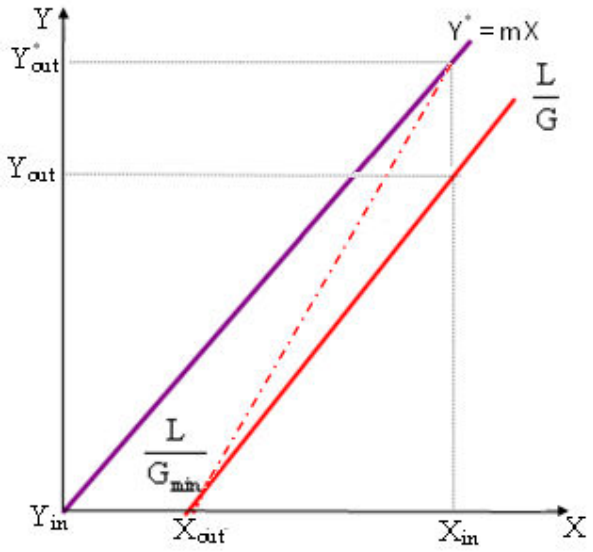

Figure 4.9 : A graphical representation of the equilibrium line and operating and their related compositions in a stripper

In a similar manner as for the scrubber, gas flow rate can be determined by a factor of greater than one (n_o>1). The value of n_o (n_o = 1.85) for the scrubber is used for the stripper in which X_{in} is 0.0005 (mol/mol) and X_{out} is 0.000126 (mol/mol). Therefore, the air required for this regeneration of loaded CME biodiesel of 353 K temperature in the stripper is about 2m^3/h (or 0.0015kmol/min). Following the calculation of gas flow rate, the tar concentration in the outlet gas phase can be determined from the mass balance equation as follows:

$$Y_{out} = \left(\frac{L}{G}\right)\left(X_{in} - X_{out}\right) \tag{4.26}$$

In order to assess whether stripping is possible with this liquid to gas ratio, the stripping factor (S) is determined as follows:

$$S = k(T)\frac{G}{L} \tag{4.27}$$

By Equation (4.27), the value of S for this study, in which equilibrium coefficient is 7.3197 (mol/mol), is 1.4. Since the value of S is greater than 1, the stripping can occur (Roberts et al., 1985; Jenkins et al., 2007). However, the stripping efficiency

would be low. In order to increase the stripping efficiency, G should be increased which will ultimately reduce the number of transfer units, N_{OL}. Therefore, an optimum S should be determined for which G is increased while N_{OL} is reduced. The design equation for the stripper in which N_{OL} is defined as a function of S and solute mole ratios is as follows (Roberts et al., 1985; Wang et al., 2006):

$$N_{OL} = \left(\frac{S}{S-1}\right) \ln\left(\frac{X_{in}(S-1)/X_{out}+1}{S}\right) \qquad (4.28)$$

According to Wang's team, S can be suitably selected in the range 2 – 5 (Roberts et al., 1985; Wang et al., 2006). Therefore, a plot of N_{OL} as a function of S can be used to select a suitable value of S as shown in Figure 4.10.

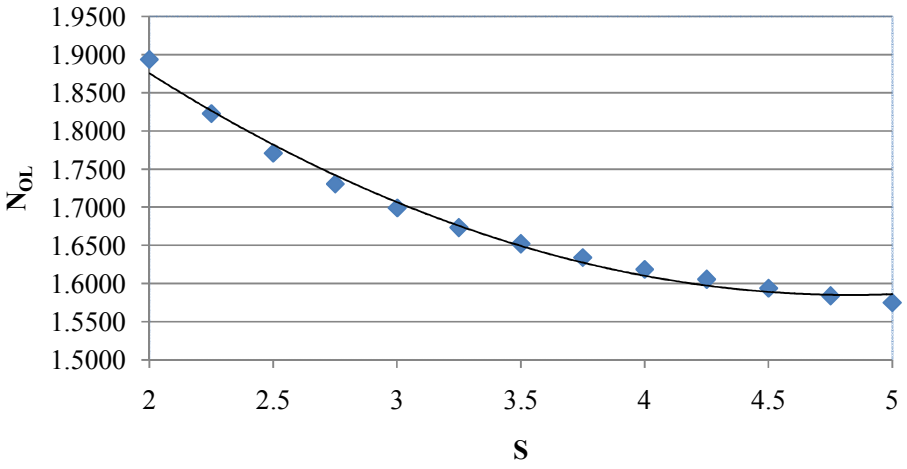

Figure 4.10: A graphical method for the optimization of S

Figure 4.10 shows that N_{OL} reduces as S increases with the curve tending asymptotic between the values of S 4.5 and 5. The S value of 4.75 can be used for the design of the stripper in this study which means 6.5m^3/h (or 0.0048kmol/min) of air is required for this stripping factor.

4.7. Diameter of the Stripper

The diameter of the stripper is estimated at the liquid phase temperature of ranging 343 - 358 K (70 - 85°C). In literature, the temperatures of the gas phase (air)

at inlet and outlet of the stripper are 180 and 160°C (Zwart et al., 2010). In order to ensure that the exit gas temperature is consistent, the liquid phase (thermal oil) is heated prior to stripping, in their system. Since the thermal capacity of biodiesel is much higher than that of the air, the biodiesel temperature would not change much throughout the stripper.

In the estimation of the diameter of the stripper, Equations (4.15) to (4.18) are used in which L/G is about 1.5 and the air flow rate is 6.5m^3/h (or 0.0048kmol/min). Some aspects of mechanical design have been considered so that the pressure drop over the stripper is minimised. As a result, the diameter of the stripper is nearly the same as that of the scrubber, which is 0.15m.

4.8. Height of Packing for the Stripper

In order to determine the height of packing for the stripper, the values of N_{OL} and H_{OL} were estimated. The N_{OL} was estimated by the analytical method. The analytical method for N_{OL} in the stripper is defined as follows (Henley et Seader et al., 1981):

$$N_{OL} = \frac{X_{in} - X_{out}}{\left(X_{in} - X_{in}^{*}\right) - X_{out}} \ln \frac{X_{in} - X_{in}^{*}}{X_{out}} \tag{4.29a}$$

The equilibrium tar composition in the liquid phase is defined as follows:

$$X_{out}^{*} = \frac{Y_{out}}{k(T)} \tag{4.29b}$$

As a result of this procedure, the N_{OL} is estimated as a function of the temperature of the liquid phase in the stripper. The effect of the temperature of the liquid phase in the stripper is shown in Figure 4.11.

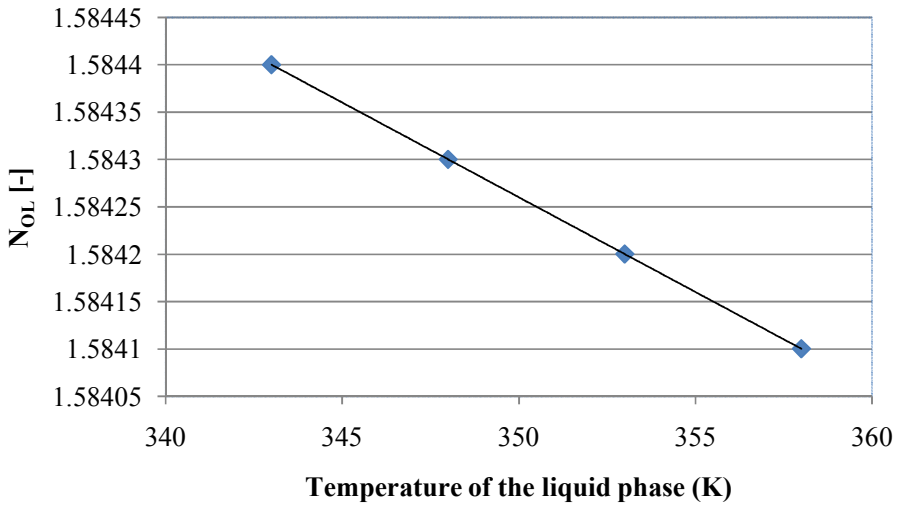

Figure 4.11: Effect of temperature on the N_{OL} in the stripper

Figure 4.11 shows that the N_{OL} decreases slightly with increase in temperature. This is what is expected as at high temperatures the solubility of the tars in the biodiesel is reduced thus the tars easily escape from the biodiesel to the gas. This can also be explained by the increased equilibrium coefficient which will increase the driving force for the transfer of the tars from the CME biodiesel to the gas. As more tars are transferred into the gas phase, the N_{OL} is reduced and so is the height of the packing. The height of packing for the stripper is defined as follows:

$$Z = N_{OL} \times H_{OL} \tag{4.30a}$$

In which H_{OL} can be determined as follows:

$$H_{OL} = \frac{L}{K_X a} \tag{4.30b}$$

In which K_X is given as follows:

$$K_X = \frac{k_X k(T) k_Y}{k_X + k(T) k_Y} \tag{4.30c}$$

The heights of packing for the stripper as a function of the temperature of the tar laden biodiesel are shown in Table 4.5.

Table 4.5: Height of packing at inlet temperatures of the liquid phase to the stripper

Temperature (^{o}C)	70	75	80	85
Temperature (K)	343	348	353	358
Height of packing, H_{OL} (m)	0.86	0.85	0.845	0.844

Since the temperatures of the liquid phase in the stripper and H_{OL} values are close as shown in Table 4.5, the value of 0.85m was used for the height of stripper packing.

4.9. Holdup, Loading and Flooding in the Scrubber and Stripper

Prior to the formal experiments for investigation on holdup, loading and flooding both in the scrubber and in the stripper, a series of tests about effective loading were conducted. In these tests, the liquid mass flow rate was varied at a constant gas flow rate. The result was, at liquid flow rates below a certain level, the liquid did not flow evenly downwards through the packing and channelling occurred. This was confirmed by the fact that some packing was not wetted. The channelling condition should be avoided because it would substantially reduce the contact surface area between the liquid and the gas (interfacial area) and hence the mass transfer rate. When the flow rates of the liquid phase were gradually increased, its flow through the packing was becoming even and the whole packing was wetted. The combination of minimum liquid flow rate with a given gas flow rate is defined as effective loading. In order to obtain the effective loading for different gas flow rates, the tests were repeated at different gas flow rates.

4.9.1. Quantification of Holdup, Loading and Flooding in the Scrubber

The results for the determination of the holdup, effective loading and flooding in the scrubber are given in Table 4.6. In obtaining these results, the pressure drops across the scrubber ($\Delta p/Z$) were measured at gas volumetric flow rates ranging from 12 to 18 *l*/min while the liquid phase flow rate was set at 4.2

l/min. The temperature of the liquid phase over the scrubber was also controlled so that it was consistent at 300 K.

Table 4.6: Measured pressure drop at various gas flow rates in the scrubber with uncertainty at 95% confidence interval for the determination of the loading region

Pressure drop (kPa/m)	Nitrogen volume flow rate (*l*/min)	N_2, G' (kg/m^2.s)
1.90±0.02	12.0±0.6	0.0136±0.001
1.90±0.02	14.0±0.6	0.0159±0.001
1.94±0.02	16.0±0.6	0.0181±0.001
2.10±0.02	18.0±0.6	0.0204±0.001

In the analysis of the results as given in Table 4.6, the pressure drop per unit height of the packing of the scrubber is used which is plotted against the gas mass flux as shown in Figure 4.12.

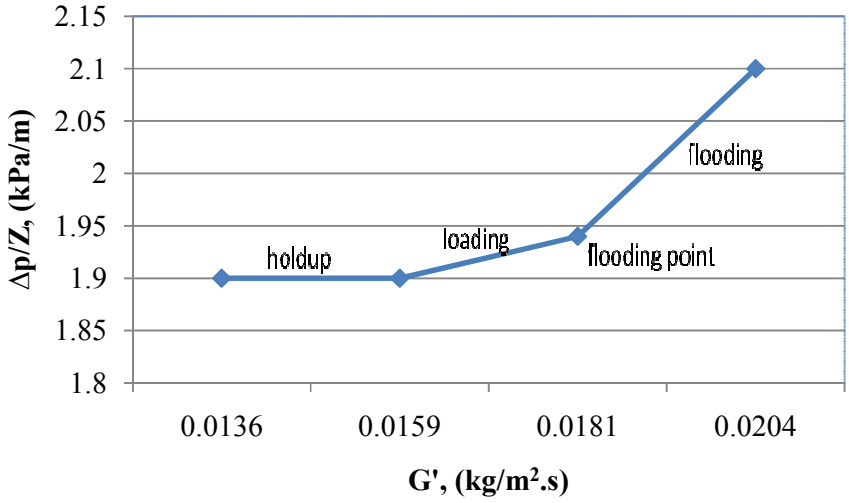

Figure 4.12: Plot of pressure drop per unit packing height against gas mass flux.

For the scrubber to operate normally, it is necessary for the gas flow rates to be high enough to avoid channelling and to achieve effective loading with corresponding pressure drop of at least 1.9kPa/m. However, too high gas flow rates

create flooding thus the gas flow rate should be lower than the flooding limit with corresponding pressure drop of about 1.94kPa/m. At the same time, the liquid flow rates should be high enough for the required purity of the treated gas. Therefore, optimisation was sought to find the most effective flow rates of both gas and liquid. The ratio of the liquid phase flow rate to gas phase flow rate was optimised experimentally in the tar removal system. After this was achieved, mass transfer experiments in the scrubber were done in that region to obtain experimental data to determine the mast transfer coefficient as discussed in Chapter 5. It should be noted here that the field of operation is narrow (i.e. the loading region) because it reflects the experimentally determined region. The narrow field of operation could have resulted because of the wrong size of packing (12 mm) which was used. As a result, it offered poor gas and liquid distribution in longer regions and good distribution in narrow regions. The correct size of packing would have been equivalent one tenth of the column diameter, which would be 15mm. This was the case for the stripper as well.

4.9.2. Quantification of Hydrodynamics in the Stripper

The results for the determination of holdup, effective loading and flooding in the stripper are given in Table 4.7. In obtaining these results, the pressure drops across the stripper ($\Delta p/Z$) were measured at air volumetric flow rates ranging from 35 to 65 *l*/min while the liquid phase flow rate was set at 4.2 *l*/min. The temperature of the liquid phase in the stripper was also controlled so that it was consistent at 353 K.

Table 4.7: Measured pressure drop at various gas flow rates in the stripper with uncertainty at 95% confidence

Pressure drop (kPa/m)	Air volumetric flow rates (*l*/min)	Air, G' (kg/m^2.s)
0.035±0.002	35.0±0.6	0.0411±0.001
0.036±0.002	40.0±0.6	0.0470±0.001
0.04±0.002	50±0.6	0.0587±0.001
0.069±0.002	65±0.6	0.0763±0.001

Using the values in Table 4.7, the pressure drop per unit height of the stripper packing is plotted against the air mass flux as shown in Figure 4.13.

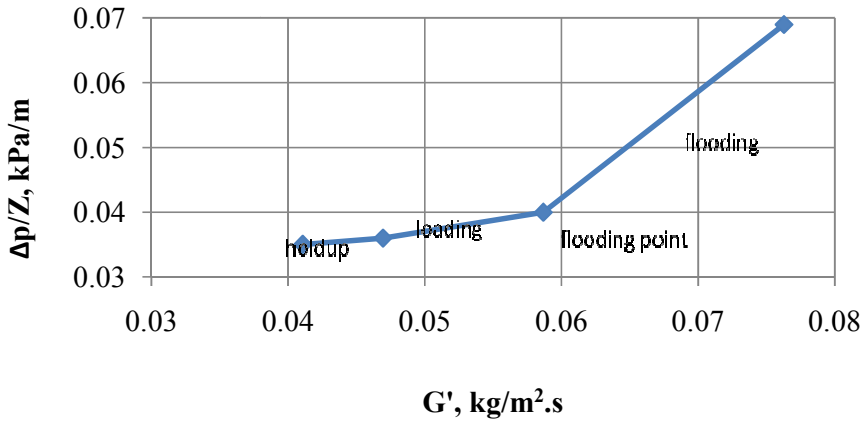

Figure 4.13 : Plot of pressure drop per unit stripper packing height against gas mass flux

Figure 4.13 shows that the holdup occurs at pressure drop of about 0.035kPa/m and the pressure drop for the loading zone is between 0.035 and 0.04kPa/m. With further increase in the gas flow rate, excess flooding zone is reached as evidenced by the steep flooding pressure drop line. This phenomenon is seen where the flooding line increases towards high pressure drop for a small increase in the flow rate of the air.

In the end, the holdup, effective loading and flooding in both the scrubber and stripper had to be monitored so that they were operated in a suitable region. The liquid flow rates in the present study were conducted at the loading zone. At the same time, there was a need to use gas and air flow rates which were large enough for the required purity and regeneration of the gas and CME biodiesel respectively. This precaution was carried out in the preliminary experiments for the scrubbing and stripping of the tars.

4.10. Preliminary Experiments for Scrubbing and Stripping Naphthalene

4.10.1. Experimental System for the Scrubbing of the Naphthalene

An experimental system to study the scrubbing of naphthalene from simulated producer gas (nitrogen) was designed as shown in Figure 4.14.

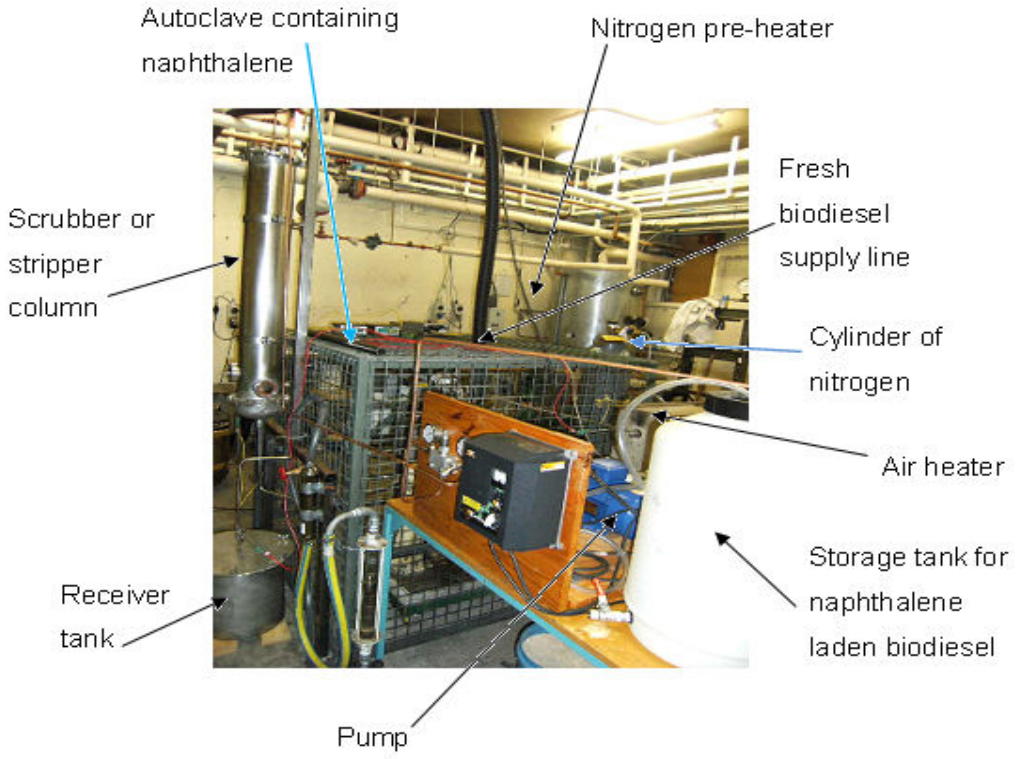

Figure 4.14: Photograph of the schematic diagram of the rig for the naphthalene removal system

The tars in the producer gas were simulated by vaporising solid samples of commercial naphthalene into a stream of nitrogen gas. Naphthalene is the most abundant tar component in the producer of biomass gasification (Bull, 2008).

The gas phase containing nitrogen and vapours of naphthalene was fed into the packed scrubber at temperatures ranging 373 - 473 K, for various runs. This temperature range was achieved by setting the temperature autoclave in the range

623 – 673 K. In this way, the nitrogen stream carried naphthalene vapours whose temperature was in the range 623 – 673 K.

The CME biodiesel was used as the solvent and was purchased from a local biodiesel plant (Bernard, 2007). In the scrubber, the gas phase contacted the liquid phase (CME biodiesel) counter-currently. At the start of the experiment, fresh biodiesel was continuously fed into the column from the top of the scrubber, as shown in Figure 4.15. A sample of 100g naphthalene was placed into the autoclave and heated to temperatures of ranging 623 – 673 K. Once the autoclave reached the near the set point of 673 K, preheated nitrogen gas at set temperatures of 493 – 513 K was passed through the autoclave to carry vapours of the naphthalene to the scrubber. As nitrogen and vapour of naphthalene were flowing through the scrubber, the pump was turned on to deliver the CME through the scrubber.

Note that although the line from 150mm above the flang of the autoclave is insulated and heat traced the line in that distance and also 50mm of flang thickness is not insulated and heat traced. This exposed area is responsible for the heat loss by the gas stream and hence the drop in temperature of the gas phase at inlet to the scrubber from 493 – 513 K to 373 - 473 K.

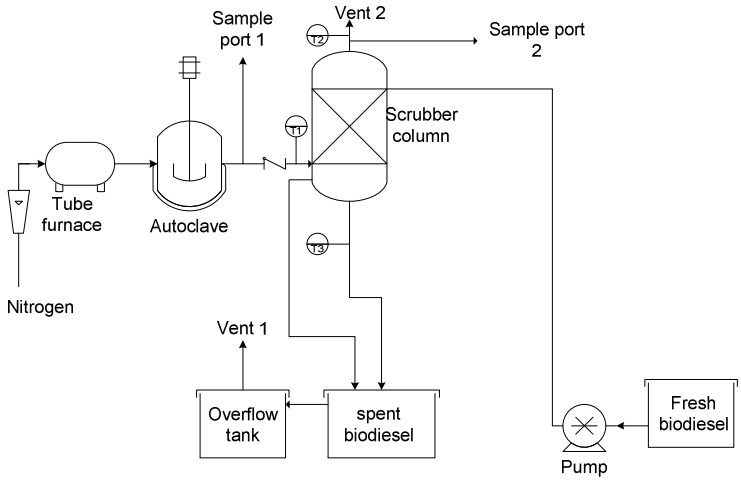

Figure 4.15: Schematic flow diagram of the naphthalene scrubbing system

During the operation, the flow rate of liquid phase was determined by a stopwatch and a measuring cylinder. On the other hand, the flow rates of nitrogen were measured by a flow-meter, as shown in Figure 4.15. Temperatures at the gas

exit point, gas inlet point and liquid exit point of the scrubber were measured as T1, T2 and T3. Once the flow rate of the gas and temperatures T1, T2 and T3 were stable for 5 – 10 minutes, a steady state was assumed to be reached and samples of naphthalene in the gas phases were collected from Sample ports 1 (before scrubbing) and 2 (after scrubbing), measured and analysed. During the experiments, the flow rate of the gas phase was controlled at around 15 *l*/min. On the other hand the flow rate of the biodiesel was controlled at around 4.2 *l*/min.

In order to analyse the concentration of naphthalene in the gas phase, the gas was passed through a series of impinging bottles containing the solvent, isopropyl alcohol (IPA) (Hasler et Nussbaumer et al., 2000; Phuphuakrat et al., 2010). The time taken for the gas in passing through the bottles and its flow rate were recorded and used to analyse the concentration of the naphthalene absorbed by IPA. The concentration in IPA was determined after measuring the absorbance of the solution that resulted from the absorption of the naphthalene in IPA. The Ultra-violet (UV) visible spectrophotometer (Hitachi/101model) was used to measure the absorbance. The measurements were conducted at 270nm, the maximum wavelength of absorption of the UV visible light by naphthalene as shown in Figure 4.16.

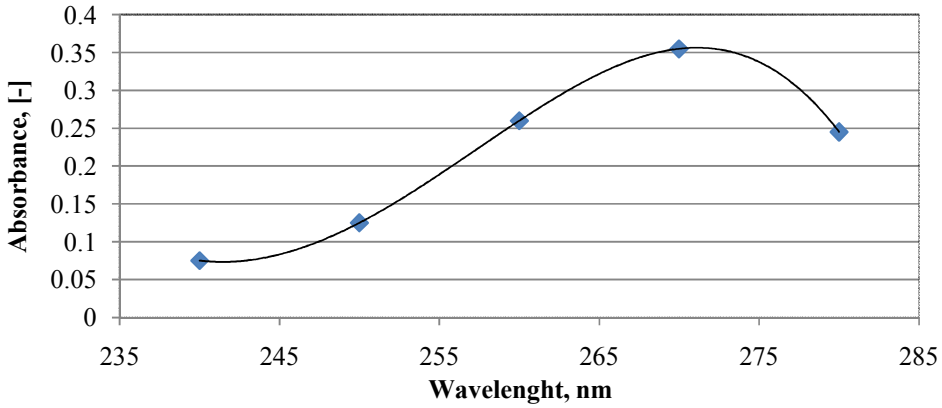

Figure 4.16: Plot to determine wavelength of maximum absorption for naphthalene

Further, standard samples containing naphthalene were prepared and their absorbencies were measured at 270 nm to draw the calibration curve shown in Figure

4.17. The calibration curve was then used to determine the concentrations of the naphthalene in the gas phase.

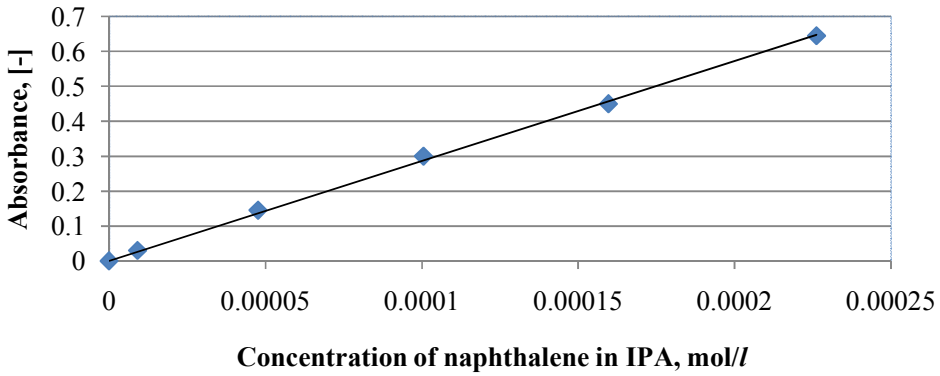

Figure 4.17: A plot for the determine naphthalene concentration in nitrogen

Using Figure 4.17, the concentration (c) of naphthalene in the gas, expressed as g/Nm^3, was determined by the following procedure:

(i) The number of moles of naphthalene (n_n) absorbed by IPA was calculated as follows:

$$n_n = \text{naphthalene concentration in IPA(figure4.17)} \times \text{IPA volume}$$

(ii) The volume of the gas bubbled (v_g) was calculated as follows:

$$v_g = \text{flow rate of slip stream gas} \times \text{bubbling time}$$

(iii) Therefore, the concentration of naphthalene in the gas was determined as

$$c = \frac{n_n \times \text{naphthalen e molar mass}}{v_g}$$

In order to determine the concentration of naphthalene absorbed by the liquid phase (CME biodiesel), standard solutions of naphthalene in biodiesel were diluted with IPA with biodiesel to IPA ratio of 1:5000. The solution of the naphthalene in IPA was diluted to make it colourless so that the spectrophotometer could be used to measure the concentration of naphthalene in the liquid phase. In case of the measurement of the tars concentration in the gas phase, the solution was not diluted because it was already colourless. The absorbencies of the diluted solutions were measured at 270nm to draw the calibration curve shown in Figure 4.18.

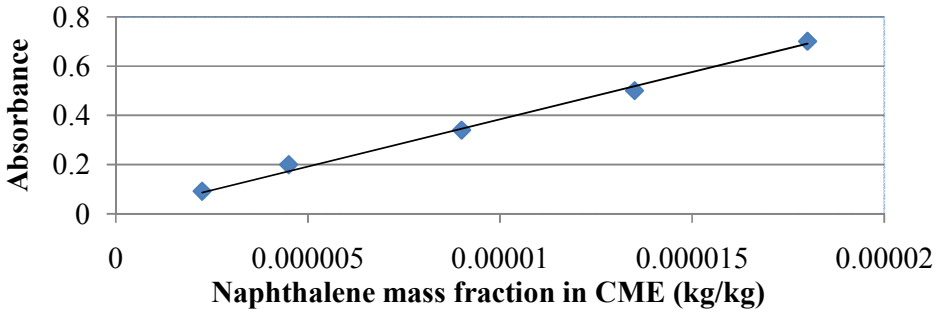

Figure 4.18: Calibration curve for naphthalene absorbance against its mass fraction in CME.

4.10.1.1. Results and Discussion for Tar Scrubbing

In order to analyse the performance of the scrubbing column, the operating temperature of the scrubber was taken as the inlet temperature of the gas (nitrogen). In addition, the percent of removal of naphthalene was defined as the ratio of its concentration change (from the inlet point to the outlet point) to its concentration at the inlet point of the scrubber in the gas phase. The results for the effect of temperature on the removal of naphthalene are shown in the Figure 4.19.

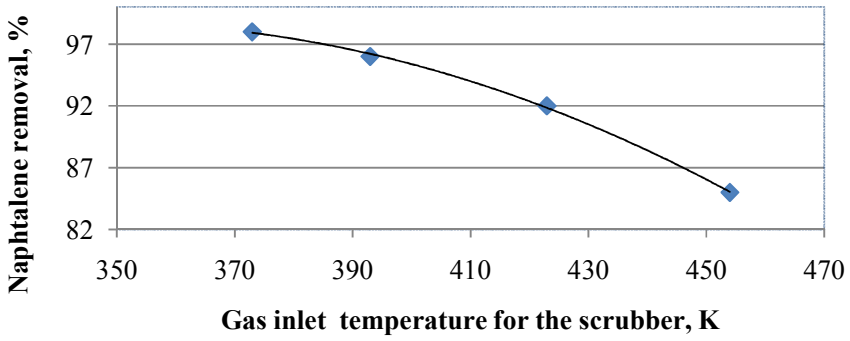

Figure 4.19: Effect of gas inlet temperature on the removal of naphthalene in the scrubber

Figure 4.19 shows that the removal of the naphthalene from nitrogen decreases with increasing in the temperature of the scrubber. This result agrees with theory of solubility of gases in the liquid solvents. In addition, it also agrees with the

concept developed in Chapter 3, in which the concentration of the tars in biodiesel increases as the temperature reduces.

4.10.2. Experimental Systems for Stripping of the Tars

In the preliminary experiments for the stripping of the tars, the loaded CME biodiesel from the scrubbing column was used. The schematic diagram illustrating the stripping process is shown in Figure 4.20 in which the scrubbing part was not shown. In addition, the compressed air was used as the stripping gas.

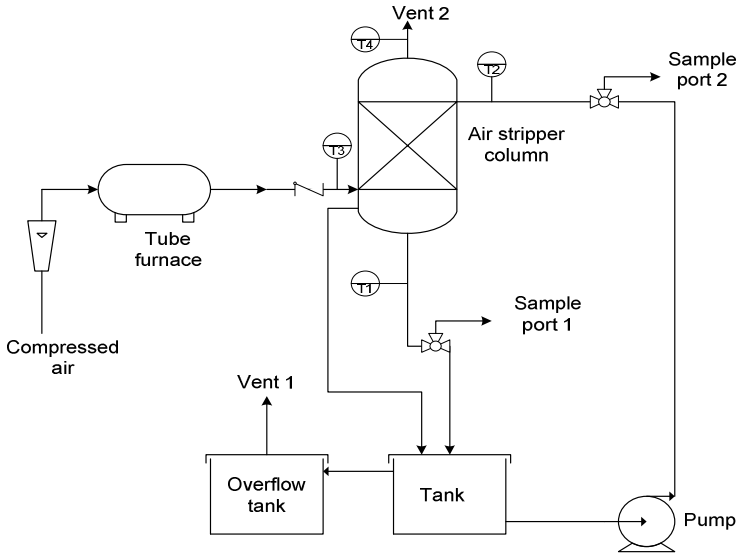

Figure 4.20: Schematic drawing of the air stripping process of the loaded CME

In the operation, the naphthalene loaded CME was heated in the Tank with a hot plate (not shown) placed under the Tank. The loaded CME was heated from 293 to 333 K in the 20 K increments over 8 hours. During this time, the flow rate of the loaded CME was set at 4.2 *l*/min. At the same time, the compressed air was heated by a tube furnace, as shown in Figure 4.18, from 293 to 523 K and its flow rate was varied from 35 to 80 *l*/min. All stream temperatures were recorded by a data logging computer (not shown) at 2 second intervals. When these temperatures and flow rates remained stable at the set value, steady state was attained then liquid samples were collected from Sample ports 1 (after stripping) and 2 (before stripping). The collected

CME samples were then analysed by using Figure 4.18 to determine the concentration of naphthalene in the biodiesel. The stripping percent efficiency was expressed as the ratio of its concentration change after stripping to its concentration in biodiesel at the inlet point of the stripper before stripping. The results are presented and discussed in the next section.

4.10.2.1. Results and Discussion for Tar Stripping

In analysing the performance of the stripper, the operating temperature of the stripper was the average temperature of the air. This average temperature was calculated by using the inlet and outlet temperatures of the air. The average temperature in the stripper was plotted with the percent of naphthalene removed as shown in Figure 4.21.

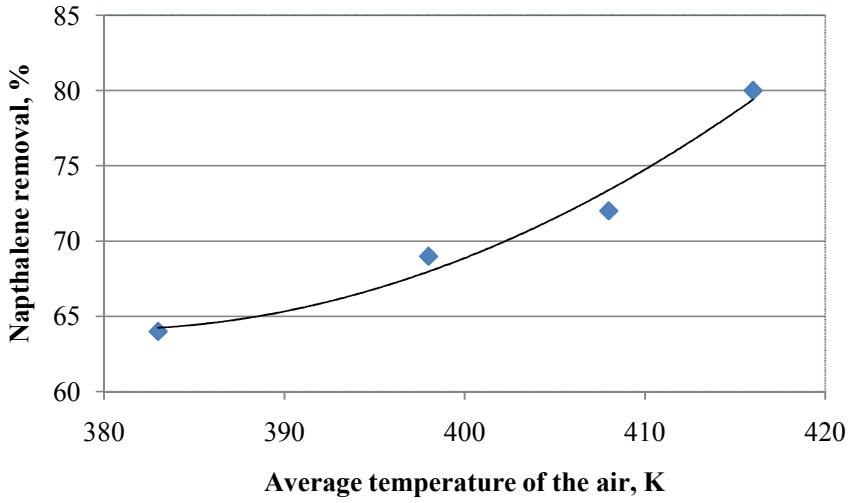

Figure 4.21: Effect of temperature on the removal of naphthalene in the stripper

The difference between the temperature of the inlet air and that of the outlet air was not so large that the average temperature was used in plotting Figure 4.21.

Figure 4.21 shows that the removal of naphthalene increases with temperature. This trend in the stripping of naphthalene can be explained from a point of view of the tar solubility in CME. According to the theory in Chapter 3, the solubility of the tars decreases with increase in temperature. Thus, when the

temperature of the stripper increases, the tar solubility decreases which makes the tars more easily transferrable into air.

4.11. Conclusions

Using CME as solvent is different from using RME, therefore; the equilibrium coefficient is useful for the system design. In this part of study, the effect of operating temperature on the scrubbing and stripping of the tars was also investigated. In the investigation, it was found that low temperatures favour the removal of the tars from nitrogen in the scrubber. On the other hand, high temperatures favour the removal of the tars from biodiesel in the stripper. In both situations, the tar solubility in CME is the major contributing factor. As the temperature increases, the solubility decreases and thus the naphthalene can be removed by air and be carried away. Conversely, lowering the temperature implies enhancing the attraction of the molecules of the tars into CME and thus increasing their solubility.

The results for the above conclusions were drawn from the systems where the flow rates of the CME were controlled at 4.2 *l*/min for the scrubber and stripper respectively. In addition, the temperature of the loaded CME over the stripper was controlled around 353 K. In view of this, a reasonable conclusion should be drawn after more experiments have been conducted in which these parameters will be varied. Such experiments will be presented in Chapters 5 and 6.

Chapter 5 Scrubbing of Tars into CME from Biomass Gasification Producer Gas

5.1. Introduction

The presence of tars in the producer gas of biomass gasification has for a long time been a technical barrier for the commercialisation of thermo-chemical conversion systems. The tars are conventionally defined as poly-aromatic hydrocarbons (PAHs) of molecular weight larger than that of benzene, which are formed together with producer gas during the gasification of the biomass. The tars cause operational problems in the downstream of a gasifier, such as fouling and clogging in process equipment as well as poisoning catalysts in synthesis of liquid fuels. As a result, a great deal of effort has been devoted to the development of technologies for removing the tars from the producer gas.

The tar removal technology employed in the Güssing gasification plant cited in Chapter 2 is successful at removing tars into a solvent of RME, although the RME is continuously consumed in the process. As the RME has similar properties to CME, the results from the current investigation can be applied to the system where RME is used. The knowledge of the mechanism of tar transfer can then be used to devise a technology for the regeneration and recycling of the CME. In addition, the tars which will have been removed from the CME can be recycled to the combustor for heat required in the gasification. The idea of recycling CME and recovery of tars would enhance the existing technology in which this kind of recycling does not exist commercially.

In this chapter, the mechanism of the tar transfer (tar flux) from the simulated producer gas (nitrogen) to CME biodiesel by absorption is investigated. In order to quantify the tar transfer process between the gas phase and liquid phase, the two-film theory and mass balance as well as theoretically determined equilibrium coefficient are used.

The tar transfer processes in the scrubber can be illustrated by a schematic diagram of the vertical column shown in Figure 5.1.

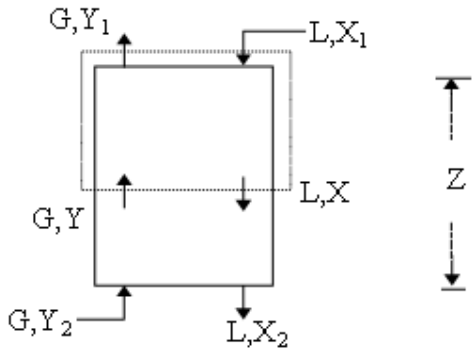

Figure 5.1: Schematic diagram of a tar scrubber column.

In Figure 5.1, the notations 1 and 2 are defined with respect to the liquid phase and gas phase conditions at the top and bottom of the column, respectively. For analysis, a small column height, ΔZ, is taken and the mass transfer of the tars occurs (N) from the gas phase to the liquid phase as shown in Figure 5.2.

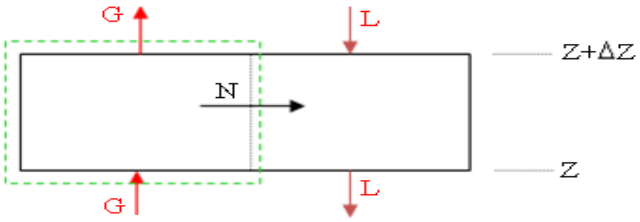

Figure 5.2: Schematic illustration of mass transfer between liquid and gas phase in a small column height.

During the mass transfer process, a small change in the concentration of the tars in both the liquid and gas phases over the small column height, ΔZ, can be defined as follows (Henley et Seader et al., 1981; Geankoplis, 2003):

$$L dX = K_X a\left(X^* - X\right) dZ \tag{5.1a}$$

$$-G dY = K_Y a\left(Y - Y^*\right) dZ \tag{5.1b}$$

Under steady state conditions, the mass transfer rate of the tars across the liquid-gas interface can also be determined from mass-transfer theory as the product

of molar transfer coefficient and the concentration difference, as follows (Henley et Seader et al., 1981; Geankoplis, 2003):

$$N = K_X\left(X^* - X\right) = K_Y\left(Y - Y^*\right) \tag{5.2}$$

The tar concentrations in both liquid phase and gas phase appearing in Equations (5.1) and (5.2) can be illustrated in an X-Y coordinate which presents the operation line and the equilibrium curve for dilute system as shown in Figure 5.3.

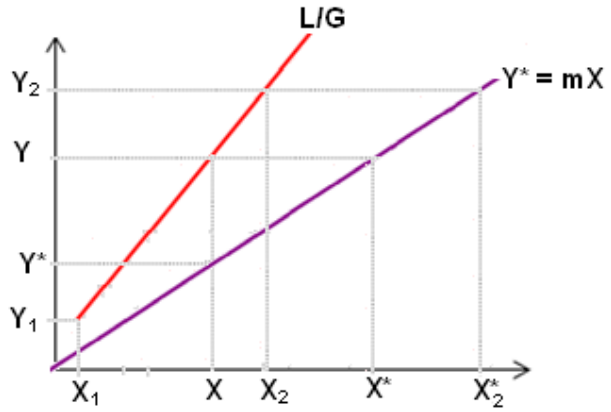

Figure 5.3: Illustration of the operating line and the equilibrium curve in a scrubber.

Since the equilibrium tar concentrations in both the liquid and gas phases, (X^* and Y^*), can be inter-related using the equilibrium coefficient, the overall molar transfer coefficients can be related to each other based on Equation (5.2) and Figure 5.3 as follows:

$$\frac{K_Y}{K_X} = \frac{X^* - X}{Y - Y^*} = \frac{Y/m - X}{Y - mX} = \frac{1}{m}\left(\frac{Y - mX}{Y - mX}\right) = \frac{1}{m} \tag{5.3}$$

From Equation (5.3), once the overall molar transfer coefficient in one phase is known, the overall molar transfer coefficient in the other phase can be determined by using the equilibrium coefficient. The equation for overall molar transfer coefficient based on the liquid phase concentration difference can be derived by rearranging Equation (5.1a) as follows:

$$\frac{dX}{X^* - X} = \frac{K_X a}{L} dZ \qquad (5.4)$$

In order to integrate Equation (5.4), the term (X^*-X) is defined by using the equations of the equilibrium relation (X^*=Y/m) and operating line [Y = (L/G) (X-X_1)+Y_1] as follows:

$$X^* - X = \frac{L}{mG}(X - X_1) + \frac{Y_1}{m} - X \qquad (5.5)$$

Substitution of Equation (5.5) into Equation (5.4) and integrating from X_1 to X_2 over the column with packing height of Z yields the overall volumetric molar transfer coefficient (product of the molar transfer coefficient and the exposing area per unit volume of the column) as follows:

$$K_X a = \frac{L}{\left(\frac{L}{mG} - 1\right)Z} \ln\left[\frac{X_2\left(\frac{L}{mG} - 1\right) - \frac{L}{mG}X_1 + \frac{Y_1}{m}}{X_1\left(\frac{L}{mG} - 1\right) - \frac{L}{mG}X_1 + \frac{Y_1}{m}}\right] \qquad (5.6)$$

The K_Xa is a design parameter for determination of the height of packing for the scrubber and is often correlated with the liquid and gas flow rates as follows (Cypes et Engstrom et al., 2004):

$$K_X a = \varphi L^{\alpha} G^{\beta} \qquad (5.7)$$

In which the parameters φ, α and β are determined from experimental data by a regression method after transforming Equation (5.7) as follows:

$$\ln(K_X a) = \alpha \ln L + \beta \ln G + \ln\varphi \qquad (5.8)$$

The theory discussed above will be used to analyse the performance and efficiency of scrubbing the tars from the gas phase in the system developed in this study. Experiments were performed in which the nitrogen gas was used to simulate the biomass gasification producer gas and where CME was used as the solvent. The objectives of these experiments conducted in this part of study are three-fold, namely:

- Determine the correlation of liquid phase overall volumetric molar transfer coefficient as a function of liquid and gas flow rates;
- Determine the optimum liquid to gas ratio (L/G);
- Determine the tar removal efficiency.

The whole tar removal system developed in this study consists of a scrubber and a stripper. This chapter is devoted to the scrubber section only and the next chapter is for the stripper section.

5.2. Experimental Details

The experiments for the scrubbing of the tars into CME were conducted in a vertically packed column, which is filled with Raschig ceramic rings of 12 mm. The height of the column is 1000 mm and has an inner diameter of 153 mm which is 3mm larger than the design diameter because a prefabricated cylindrical tube was used, and a randomly packed height of 850 mm. In operation, a gas mixture of nitrogen and vapours of the tars is fed from the bottom of the column and flow upwards, contacting the CME which flows downwards from the top to bottom of the scrubber. As the gas mixture contacts with the CME, some tars are preferably dissolved into the CME, which is called the liquid phase. On the other hand, the gas mixture is called the gas phase.

The purpose of this part of study is to analyse the performance of the scrubber for the dissolution of the tars in CME and to determine the optimum liquid to gas ratio for a given tar removal efficiency. The tars which have been used in this study were collected online from the producer gas which was produced by the gasification of woody biomass using the UC gasifier.

5.2.1. Preparation of the Tars

Tar samples collected from the gasifier were placed into an autoclave and heated to vaporise. The tars were collected in two methods and then mixed before placing them in the autoclave. In the first methods, a Bakerbond with 3 ml amino normal solid phase extraction (SPE) column was inserted into a sampling port and, in

turn, a syringe was inserted at the end of the SPE column, then 100 ml of the producer gas was pulled through the assembly. The SPE column retained the tars which were then washed with dichloromethane to extract the tars into liquid state. The extracted tars were transferred into a stainless steel beaker. The tars extracted in this way were insufficient for the experiments and thus a second method was employed to collect more tars. In the second method, the tars were collected from the blended tar-dust mixture that deposited on the inner wall of a pipe beneath the producer gas cyclone of the biomass gasifier. The mixture was dissolved into the dichloromethane and then the tars were separated by filtering under vacuum. The filtrate (tars) was then mixed in the beaker with the tar solution collected by the extraction method with SPE column. The beaker containing the tars was placed into an autoclave before each run of the experiments. In each run, about 62.51g of tars was used which lasted for about 16 hours. After this, the autoclave was heated to a preset temperature ranging 553 – 593 K in which range the most abundant component of tars (naphthalene) are in vapour state. Once the autoclave reached the set point, a continuous hot stream of nitrogen at a temperature of about 623 K was fed into the autoclave and mixed with the vapours of the tars. The gas phase of nitrogen and vapours of the tars was then piped through the scrubber.

5.2.2. Experimental Setup and Procedures

The experimental system is designed as a simulation model in which nitrogen containing tar vapours is simulated as the raw producer gas of biomass gasification. The simulation is tailored to meet the conditions obtaining in gas cleaning. As a result, the temperature of the gas phase entering scrubber is controlled in the range of 453 – 473 K. At the same time, the temperature of the liquid phase entering the scrubber is controlled in range 297 – 317 K. The temperature are set and controlled over those ranges in order to conduct runs at various temperatures

Due to high mass flow rates and high specific heat capacity of the liquid phase, the change in the temperature of the liquid phase over the scrubber is minimal. As a result, the dissolution of the tars into CME is assumed to be at constant temperature. However, a significant change occurred in the gas temperature over the scrubber. As a result, the scrubber also acts as a cooler and condenser for the enhancement of the

dissolution of the tars. The dissolution of the tars involves mass transfer of tars from the gas phase to the liquid phase. This mass transfer process is assumed to be a purely physical process, meaning that there is no chemical reaction between the gas phase and the liquid phase. In addition, the nitrogen is assumed to be insoluble in the liquid phase and the liquid phase is assumed to be non-volatile. Therefore, the process of mass transfer of the tars can be experimentally modelled by the theories as discussed in Section 5.1.

The experimental system consisting of a column for the scrubber and another column for the stripper is shown in Figure 5.4. In the system, tars are firstly removed from the gas phase in the scrubber by the CME and the loaded CME then goes through the stripper in which the absorbed tars are released into hot air.

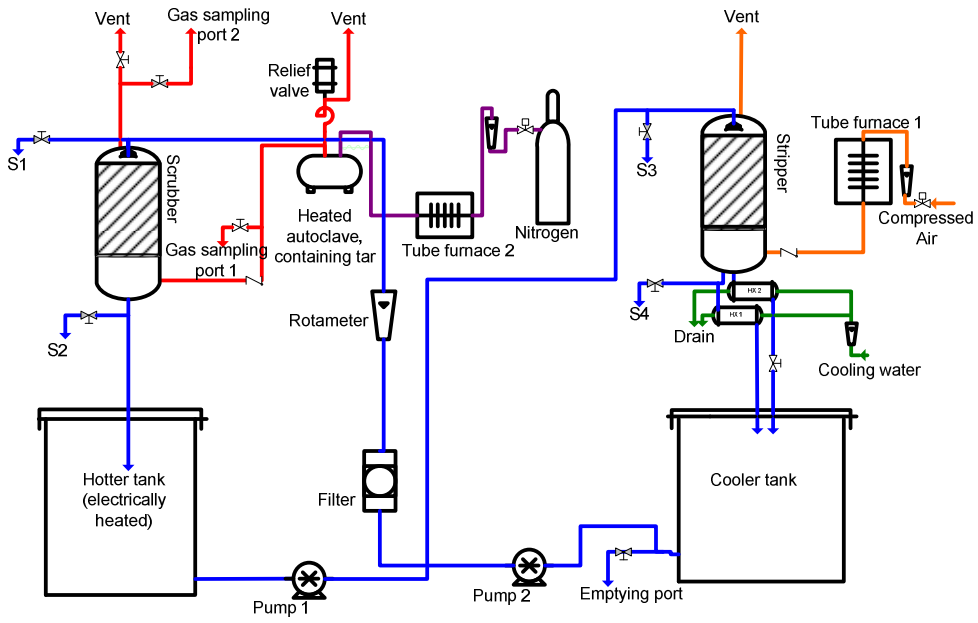

Figure 5.4: Schematic diagram of the tar removal system

As mentioned above, before each run of experiments, tar samples contained in a stainless steel beaker is placed into the autoclave and the autoclave is then sealed air tight. In a complete operation, the autoclave, Tube Furnace 1 and Tube Furnace 2 are set to different temperatures of 623, 493 and 673 K, respectively. Tube Furnace 1 is for heating the nitrogen gas for scrubber and Tube Furnace 2 is for heating the air for

the stripper. When the temperatures of the three units reach the set points, air and nitrogen are introduced into the system. Simultaneously, Pump 1 and Pump 2 for the CME circulation and water supply to the heat exchangers are turned on. As the CME, water, air and nitrogen flow through the system, the temperature data logging computer is turned on (not shown in Figure 5.4). Once it is assured that the data logging is faultless, the electrical heating of the hotter tank is turned on.

During the operation, the flow rate of liquid phase is indicated by the rotameter and determined by a stopwatch and a level indicator. On the other hand, the flow rates of the air and the nitrogen are measured by two separate flow meters which are plumbed in the lines. Once the flow rates and temperatures of the streams at inlet and outlet of the scrubber or stripper remained stable for 5 – 10 minutes, a steady state is reached and samples of liquid and gas are collected and tar concentrations measured. In the scrubbing tests, the liquid samples are drawn at sampling ports S1 and S2 in the scrubber as shown in Figure 5.4 (far left hand side). Simultaneously, the gas phase samples are collected through the gas Sampling Port 2 (over the top of the scrubber).

During the sampling, the sampling train to trap the tars in impinge or wash bottles of isopropyl alcohol (IPA) is used and the flow rate of the liquid phase and the gas phase through the scrubber are measured. The liquid flow rates to the scrubber were controlled in the range 3 – 7 *l*/min and the nitrogen gas phase flow rates were controlled in the range 4 – 12 *l*/min to ensure that the operation was within the determined loading region.

5.2.3. Details of Sampling Method for the Tar Analysis

The selection of a suitable method for the sampling is necessary for reliable analysis of the tars in the system. Conventionally, methods for sampling, measurements and analysis of the tars are based on condensation in a liquid or adsorption on a solid material (Li et Kenzi et al., 2009). The samples are collected and then analysed gravimetrically or by means of a gas chromatography (GC) as illustrated in Figure 5.5.

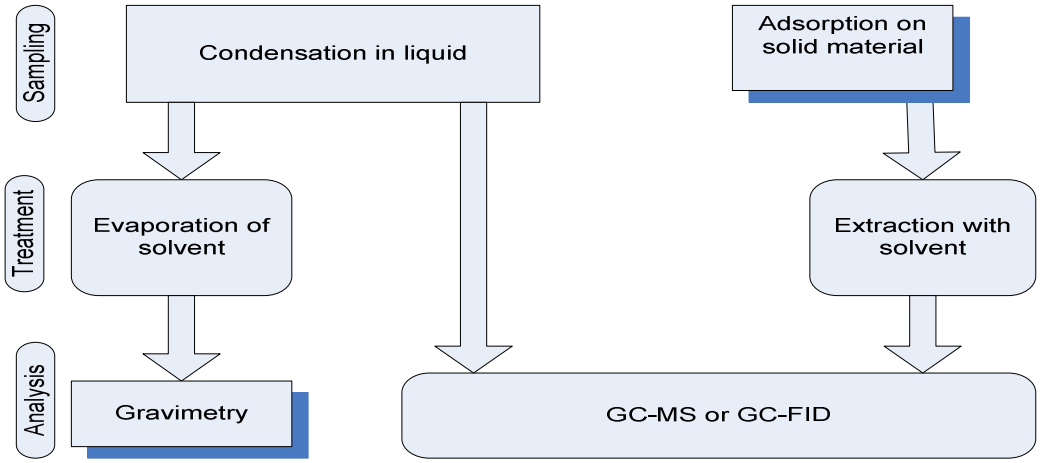

Figure 5.5: Convention methods for the quantitative determination of tars

The methods illustrated in Figure 5.5 have been used successfully to measure the concentration of the tars especially where the gas chromatography is coupled with a mass spectrometer (MS) or flame ionisation detector (FID) (Milne et al., 1998). However, this method is too difficult and complicated to be applied for online analysis of the tars. Therefore a method for the quantitative determination of tars in both the gas and the liquid phases was devised (Giger et Blumer et al., 1974; Milne et al., 1998). In this method, the tars were trapped into IPA contained in four wash bottles, arranged in series, for their quantitative analysis in the gas phase, as shown in Figure 5.6.

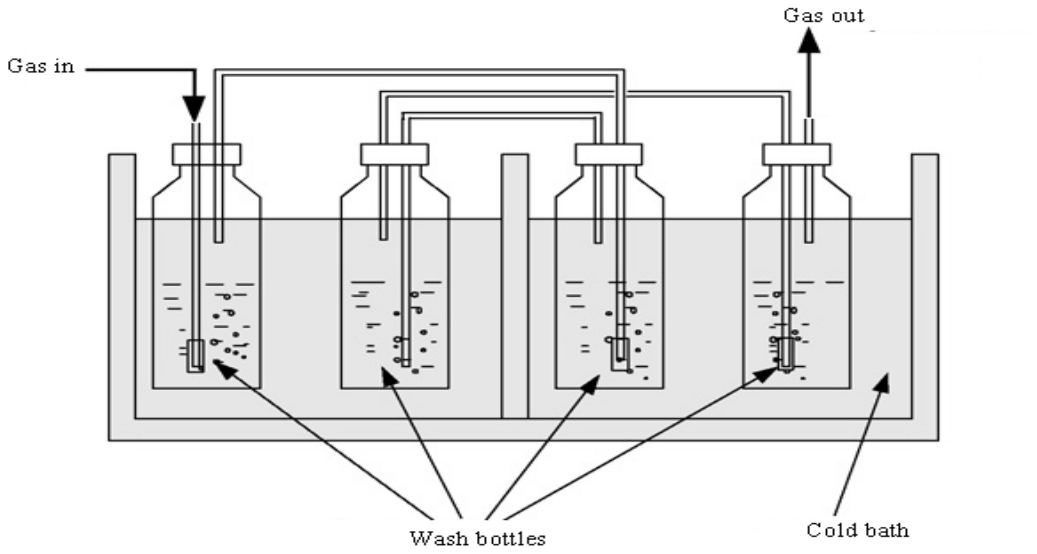

Figure 5.6: Trapping biomass tars in wash bottle of isopropyl alcohol (IPA)

For sampling and analysis of tar concentration in this study, a portion of the gas exiting the scrubber was bubbled through the wash bottles for 10 - 60 seconds at a given flow rate measured by a flow meter. After bubbling, the bottles were swirled to uniformly dissolve the tars, left to settle and then the concentration of tars in the bottles was measured. If the last bottle recorded a zero concentration, then the total concentration in the previous three bottles was used to calculate the concentration of the tars in the gas stream exiting the scrubber. During the experiments, the wash bottles containing IPA were put into a cold bath which was maintained the IPA at the temperature of 0^{o}C to enhance the solubility of the tar. The density of the solution which was formed by trapping the tars in IPA was then measured. The methodology of density measurement is discussed in Section 5.2.4. The concentration of the tars was subsequently calculated by using the measured density and the mixing rule. The concentration of the tars which was absorbed by the liquid phase was determined by the similar procedure, discussed in Section 5.2.4.

5.2.4. Determination of Tar Concentrations

In order to determine the concentration of the tars in CME, the samples were firstly diluted in IPA with a preset dilution ratio. Then absorbance of ultra-violet

(UV) visible light by the diluted sample was measured and then correlated to tar mass fraction in the IPA diluted sample. The correlation was determined by firstly measuring the density of a solution of tars in CME and then measuring the absorbance of this solution. By using the mixing rule, the mass fraction of tars in the solution was determined from the density of the solution and that of fresh CME (Aminabhavi, 1984). The solution was further diluted into 5 successive solutions and their absorbencies were measured to obtain a calibration curve for the correlation.

In the above calibration process, the molecular weights of both the tars and CME biodiesel are firstly determined in order to convert mass fraction to mole ratio. Generally, biodiesel is a liquid substance which belongs to a group of light synthetic organic oils. The common types of biodiesels are methyl esters and are often referred to as methyl ester biodiesels. The CME biodiesel is a complex liquid substance consisting of seven (7) fatty acids which form seven methyl ester constituents in the CME. The CME is manufactured with canola seed oil as one of the feed components.

The methyl ester biodiesels are classified according to their number of carbon atoms and double bonds. The classification can be used to calculate an average molecular weight of a typical biodiesel. The biodiesel CME) which has been used in this study is classified as shown in Table 5.1 (Yuan et al., 2005).

Table 5.1: CME biodiesel constituents and their molecular formulas and compositions (Yuan et al., 2005)

Name	Molecular Formula	Weight, %
Methyl myristate	$C_{15}H_{30}O_2$	0.1
Methyl palmitate	$C_{17}H_{34}O_2$	3.9
Methyl palmitate	$C_{17}H_{34}O_2$	3.9
Methyl oleate	$C_{19}H_{36}O_2$	60.2
Methyl linoleate	$C_{19}H_{34}O_2$	21.1
Methyl linolenate	$C_{19}H_{32}O_2$	11.1
Methyl erucate	$C_{23}H_{44}O_2$	0.5

As result of the classification in Table 5.1, the average molecular weight of the biodiesel (M_b) is calculated as follows:

$$\frac{1}{M_b} = \frac{x_{m1}}{M_1} + \frac{x_{m2}}{M_2} + \cdots = \sum_{all} \frac{x_{mi}}{M_i} \qquad (5.9)$$

In which M_i and x_{mi} are the molecular weight of a particular fatty acid and its mass fraction, respectively.

In a similar manner, the average molecular weight of the tars is calculated from the measured composition of the poly-aromatic hydrocarbons (PAHs) in the tar samples which were collected from the UC gasifier. The result for the analysis of the composition of the tars are shown in Table 5.2

Table 5.2: Composition of tars from CAPE gasifier by Hills Laboratory

PAHs	Molecular formula	Mass, µg per sample	Density, kg/m^3 (Aldrich, 2010)
Acenaphthene	$C_{12}H_{10}$	7.2	1024.2
Acenaphthylene	$C_{12}H_8$	40	898.8
Anthracene	$C_{14}H_{10}$	8.1	1300
Benzo[a]anthracene	$C_{18}H_{12}$	2.7	Unknown
Benzo[b]fluoranthene	$C_{20}H_{12}$	2.4	Unknown
Benzo[a]pyrene (BAP)	$C_{20}H_{12}$	2.1	1400
Benzo[g,h,i]perylene	$C_{22}H_{12}$	0.9	Unknown
Benzo[k]fluoranthene	$C_{22}H_{12}$	0.9	Unknown
Chrysene	$C_{18}H_{12}$	2.5	1274
Dibenzo[a,h]anthracene	$C_{22}H_{14}$	0.5	1284
Fluoranthene	$C_{16}H_{10}$	6	1252
Fluorene	$C_{13}H_{10}$	16.3	1203
Indeno[1,2,3-c,d]pyrene	$C_{22}H_{12}$	1.1	Unknown
Naphthalene	$C_{10}H_8$	44.7	1140
Phenanthrene	$C_{14}H_{10}$	23.8	1065
Pyrene	$C_{16}H_{10}$	7.5	1270

The average molecular weight of tars (M_t) is calculated using Equation (5.10) and the data given in Table 5.2, as follows:

$$\frac{1}{M_t} = \frac{x_{m1}}{M_1} + \frac{x_{m2}}{M_2} + \cdots = \sum_{\text{all PAHs}} \frac{x_{mi}}{M_i} \qquad (5.10)$$

In which M_i and x_{mi} are the molecular weight of a PAH and mass fractions of each component, respectively. The average density of the tars (ρ_{tar}) is also estimated by using the mixing rule (Aminabhavi, 1984) and the data given in Table 5.2 and Equation (5.11):

$$\rho_t = \left(\sum_{\text{all PAHs}} \frac{x_{mi}}{\rho_i} \right)^{-1} \qquad (5.11a)$$

In which ρ_i is the density of a tar component (kg/m^3). In the calculation of tar density, densities of five components are unknown but, fortunately, the concentrations of these five components are very low thus their contribution was ignored. In addition, the average molecular weight which is determined by ignoring the contribution of the above five components is very close to the average molecular weights of four major tar components (i.e. $C_{12}H_8$, $C_{13}H_{10}$, $C_{10}H_8$ and $C_{14}H_{10}$) in the tar sample.

Having determined the average molecular weights and densities of the tars and the CME, the calibration curves for the analysis of the tar concentrations in both liquid and gas phases were drawn. The method adapted from literature was used for the analysis (Giger et Blumer et al., 1974). In this method, a sample of PAHs contained in a liquid mixture of methylene chloride and pentane was separated into eight ring-type concentrates in a chromatography. Each of the eight concentrates was collected as a separate sample, based on its retention time. Reference standards were used to identify the samples by their retention times. Following the identification, the concentration of each sample was measured at its wavelength of maximum absorption by a UV visible spectrophotometer. The reference standards were used to determine the wavelength of maximum absorption. The wavelength for the analysis was in the range 230 to 450 nm. The PAHs which were measured by this method were phenanthrane, anthracene, fluoranthene, pyrene, benzo[a]anthracene, chrysene, peryrene, anthanthrene, benzo[ghi]perylene and coronene, benzo[a]pyrene, benzo[e]pyrene and derivatives of naphthalene.

In the present study, the calibration curves were drawn by dissolving the tars in CME and IPA for the analysis of the tar concentrations in liquid phase and gas phase, respectively. Each of the solutions was then filtered under vacuum. The density and the absorbance of the filtrate were measured by the Anton Paar DMA60 density meter and the UV visible spectrophotometer (Hitachi/101model), respectively.

The spectrophotometer was calibrated for the analysis of tars in both IPA and CME. For the tars in IPA, a blank containing pure IPA was used as a reference. Similarly, a blank containing IPA and CME of 1:5000 dilutions was used for the tar concentration determination in the liquid phase. Thereafter, the spectrophotometer

was calibrated with standard solution of the tars in IPA. A solution of 4.5 mg of tars per kg of IPA was used to obtain the wavelength of maximum absorption. The absorbencies of this solution as a function of wavelengths are shown in Table 5.3.

Table 5.3: Uncertainty in wavelength and absorbance at 95% confidence intervals

Ultra-violet light wavelength (nm)	Absorbance
240.0±20	0.900±0.0006
250.0±20	0.718±0.0006
260.0±20	0.545±0.0006
270.0±20	0.418±0.0006
280.0±20	0.335±0.0006
290.0±20	0.0273±0.0006

The data given in Table 5.3 was used for the graphical analysis to determine the wavelength for which there was the maximum absorption of tars. The wavelength for the maximum absorption was found by optimising the function in Figure 5.7. From Figure 5.7, it can be seen that the absorbance increased with decreasing wavelength. Therefore, the maximum absorbance can be found at the lowest possible wavelength of the instrument that is 240±20 nm which shows the highest absorbance.

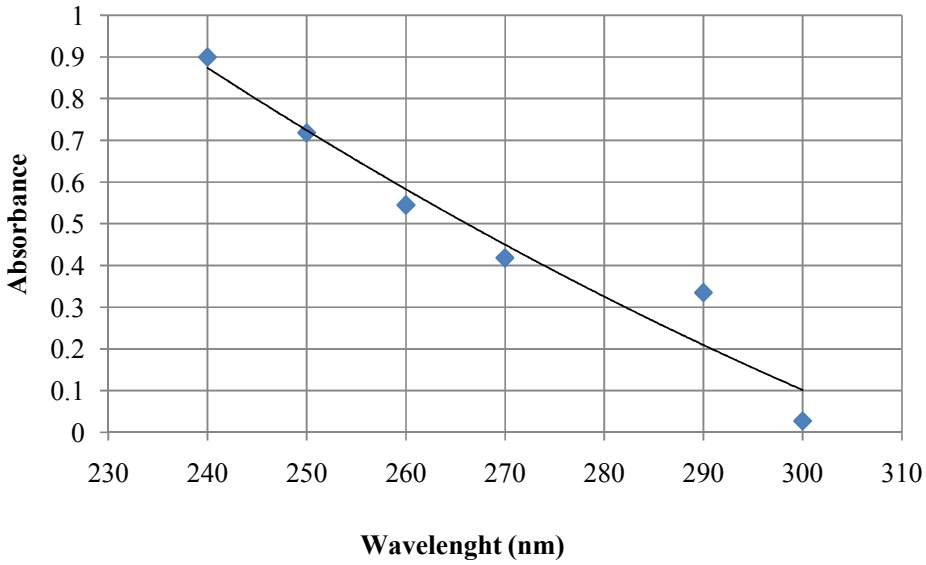

Figure 5.7: Measured absorbance as a function of UV wavelength for tar samples from biomass gasification.

Note that Figure 4.16 and Figure 5.7 are quite different because the later was plotted using data from a sample that contained various real tar components from UC gasifier compared with the former whose data came from a single and commercial tar component of naphthalene. However, they both can be used to determine the wavelength of maximum absorption in two different ways as explained in Chapter 4 and above.

In order to measure the tar concentration at the 240±20 nm wavelength, a 0.5ml tar loaded biodiesel solution was diluted into 50 ml with IPA. Then, a 0.5 ml of this solution was further diluted into 25 ml with IPA and its absorbance measured. The second dilution was necessary to make the IPA solution colourless so that the absorbance of the tars in the solution could be measurable by the UV visible spectrophotometer. By repeating this process for various tar concentrations in the CME, a calibration curve was obtained as shown in Figure 5.8 which was used in the experiments to determine the tar concentrations in the CME.

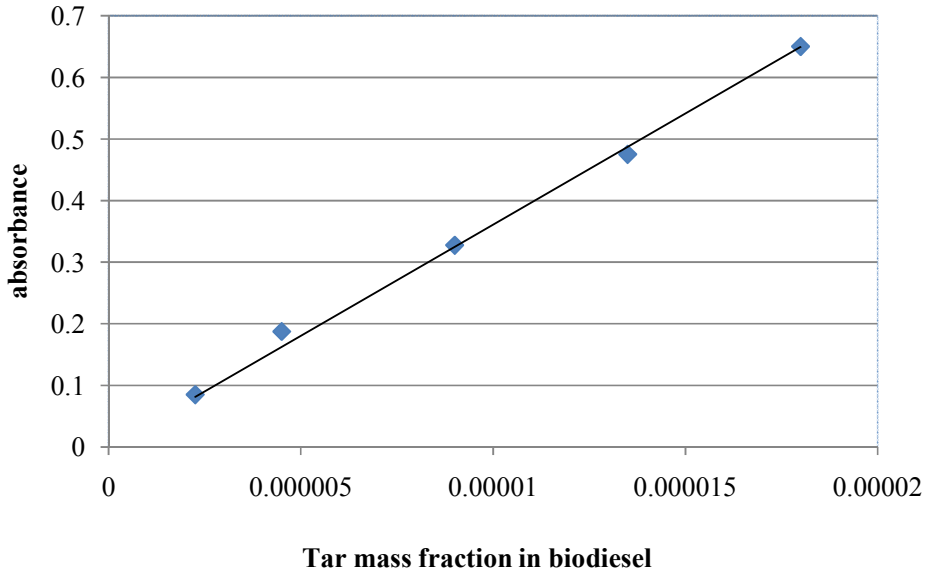

Figure 5.8: Calibration curve for tar absorbance against its fraction in CME

To obtain the calibration curve shown in Figure 5.8, a solution of 0.4g/*l* of tars in CME was prepared by the method described in subsection 5.2.1. Five

solutions were made by diluting the 0.4g/*l* solution with fresh CME in five successive 1:1 dilutions and their densities were measured.

The mixing rule for the densities of the solution of the tars in CME (ρ_{LM}) and fresh CME (ρ_l) was used to determine the tar mass fraction (x_m) as follows:

$$\frac{1}{\rho_{LM}} = \frac{(1 - x_m)}{\rho_l} + \frac{x_m}{\rho_t} \qquad (5.11b)$$

Equation (5.11b) was used to calculate the mass fraction of tars in CME which was used to plot Figure 5.8.

For determination of tar concentration in the gas phase, similar procedure to that discussed above was followed but the IPA was not diluted because it was found that the IPA with the absorbed tars from the gas had been colourless. After the tars had been trapped into the IPA, their absorbance was measured straight away. The calibration curve shown in Figures 5.9 was used to determine the concentrations of the tars in the gas phase.

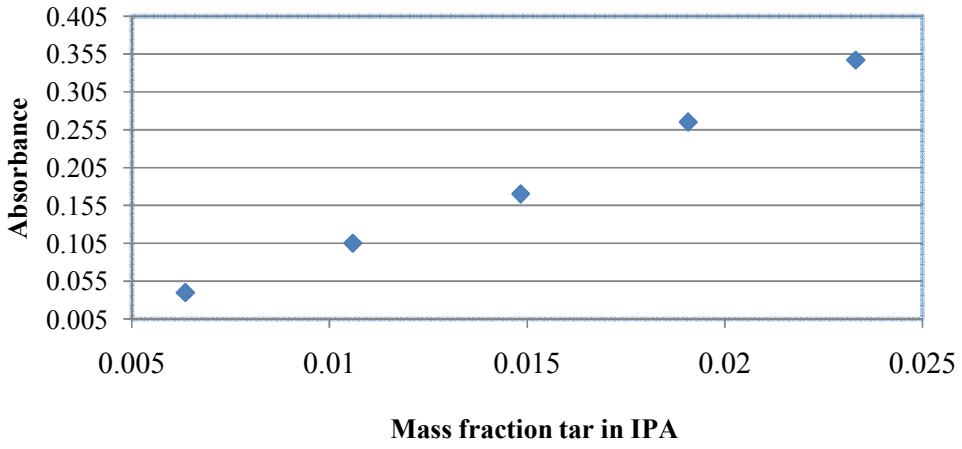

Figure 5.9: Calibration curve for tar absorbance against its mass fraction in IPA

In order to plot Figure 5.9, the densities of the solution of the tars in IPA (ρ_{LM}) and tar free IPA (ρ_l) was used to determine the tar mass fraction (x_m) by using Equation (5.11b).

The concentration of the tars in the exit gas in terms of mole ratio (Y_1) was determined by the following procedure:

(i) A volume of 300ml of tar free IPA was put in each of the 4 bottles in the setup shown in Figure 5.6. A delivery line into the setup was connected from the outlet port of the scrubber and its outlet to a flow meter which measured the volume flow rate v_f (in litre per minute (*l*/min)) of a slip stream of the exit gas.

(ii) In order to sample the gas for tars, the slip stream of the gas exiting the scrubber was directed into the setup in Figure 5.6 which bubbled through the 1200ml IPA solution contained in 4 bottles for a given time t_b, ranging 10 – 60 seconds.

(iii) After time t_b of bubbling the gas, the 4 bottles of IPA were swirled to uniformly distribute the tars absorbed in IPA and immediately taken for absorbance measurements which were always resulting into 1 or 2 last bottles of IPA giving zero absorbance. The absorbance of tars in other bottles was then measured independently and the resulting absorbencies were averaged and recorded against the volume of IPA involved (v_{IPA})

(iv) The measured absorbance was then used in Figure 5.9 to determine the amount of tars absorbed in IPA [as described in (iii)] expressed as mass fraction of tars in IPA and denoted as x_t.

(v) The mass fraction was then expressed as mass ratio, as $x_t/(1-x_t)$

(vi) Using the mass ratio of tars in IPA, the number of moles of tars (n_t) in the gas slip stream were determined using density of IPA ($\rho_{IPA)}$ and tar molecular weight (M_t) as flows:

$$n_t = \frac{x_t}{1-x_t}\left(\frac{\rho_{IPA} V_{IPA}}{M_t}\right) \qquad (5.11c)$$

(vii) The number of moles of the tar free gas n_g which was bubbled at a temperature T was determined as follows

$$n_g = \frac{v_f(\ell/\text{min}) \times 273 \times t_b(\text{min})}{22400 \times T(K)} \qquad (5.11d)$$

(viii) Using Equations (5.11c) and 5.11d), the tar concentration in the exit gas as mole ratio (Y_1) was determined as follows:

$$Y_1 = \frac{n_t}{n_g} \qquad (5.11e)$$

It is worth mentioning that the UV visible spectrophotometer which was used to determine the concentration of the tars in both the liquid and gas phases has an error on the absorbance measurement of ±0.0025. However, the manufacturers of the spectrophotometer recommend that the accuracy of the determination is improved if the measured absorbance is in the range 0.1 – 0.7.

5.3. Results and Discussion

5.3.1. Correlation of $K_X a$ with L and G for the Scrubber

Table 5.4 gives the experimental data and the calculated values of molar transfer coefficient, $K_x a$. In the table, the results shown in columns 1 to 5 were obtained directly from the experiments conducted in the scrubber section of the tar removal system with liquid temperature of 300K. The values of $K_X a$ are determined by Equation (5.6) where the height of packing, Z, is 0.85m, and m, the theoretically predicted equilibrium coefficient, is 0.3818 (mol/mol) for the liquid phase temperature of 300 K. A plot of the results in Table 5.4 to test the viability of correlating $K_X a$ with L is shown in Figure 5.10. Apparently, the correlation proposed by Cypes and Engstrom is appropriate when the data show an increase of $K_X a$ with L (Cypes et Engstrom et al., 2004).

Table 5.4: Tar concentrations and $K_X a$ values for various L/G values in the scrubber at constituent gas molar flow rate per area of 0.0003kmol/m^2.s

L/G, mol/mol	L, kmol/m^2.s	X_1, mol/mol	X_2, mol/mol	Y_1, mol/mol	Y_2, mol/mol	$K_X a$, kmol/m^3.s
32.0	0.01105	0.02829	0.02857	0.01254	0.02150	0.0002837
34.9	0.01188	0.03018	0.03075	0.01365	0.03356	0.0003594
36.0	0.00933	0.03454	0.03511	0.01548	0.03600	0.0002692
38.0	0.01219	0.03355	0.03416	0.01551	0.03869	0.0003277
42.4	0.01462	0.03109	0.03201	0.01545	0.05449	0.0003856
43.0	0.01363	0.02150	0.02250	0.01250	0.05550	0.0003437

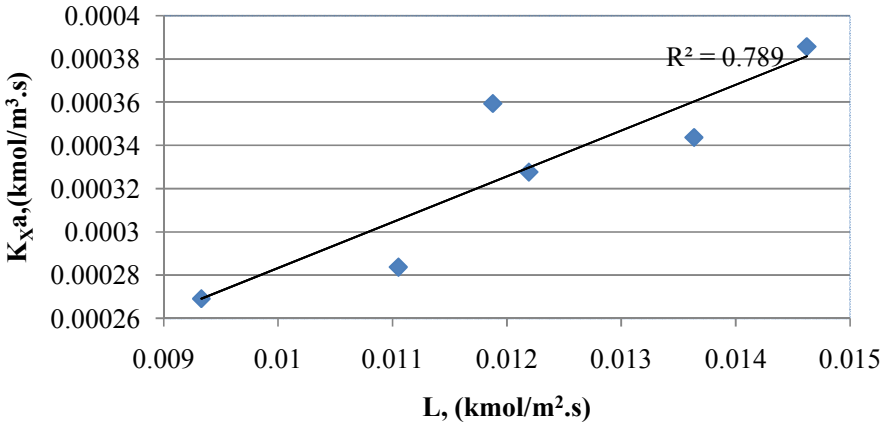

Figure 5.10: Effect of L on $K_X a$ in the scrubber at 300 K

Figure 5.10 show that $K_X a$ increases with L and the square of the correlation coefficient (R^2 = 0.7892) is reasonably satisfactory. The data shown in Table 5.4 were used to correlate $K_X a$ with L and G by a multi-linear regression method in accordance to Equation (5.8), which yields the parameters as shown in Table 5.5.

Table 5.5: The values of parameters in Equation (5.8) for the scrubber at 300 K

Parameter	φ	α	β
Value	0.01234	0.7704	0.02823

The values of the parameters shown in Table 5.5 are in the acceptable range for the correlation in this study. According to empirical correlations for molar transfer coefficient with liquid and gas flow rates, α and β should lie between 0 and 1 (Hsieh et al., 1994).

In order to test the calculated $K_X a$ in a wider range of operation conditions, the values of $K_x a$ determined by the parameters φ, α and β and Equation (5.7) have been compared with the values of $K_x a$ determined by Equation (5.6) for a wider range of L/G values as shown in Table 5.6.

Table 5.6: Comparison of the experimental and correlated values of $K_X a$ at various values of L/G at 300 K

L/G	32	34.9	36	38	42.4	43
$K_X a$, Equation (5.6)	0.000284	0.000359	0.000269	0.000328	0.000386	0.000344
$K_X a$, Equation (5.7)	0.000305	0.000323	0.000268	0.000329	0.000379	0.000359

Table 5.6 shows that the discrepancies between the $K_X a$ determined by Equation (5.6) and (5.7) are larger at lower L/G values and smaller at higher L/G values. This trend can be attributed to the uncertainty in the measurement of the absorbance. As it has been inferred already, the error in the measurement of the absorbance is larger at low concentrations than at higher concentrations of tars in liquid phase. Most low L/G values yielded low concentrations of the tars in the liquid phase, as will be shown later in this study.

5.3.2. Optimum Liquid to Gas Flow rate Ratio (L/G) for the Scrubber

The optimum L/G can be determined, in this study, by a plot of the effect of L/G on the dimensionless separation factor, S_a. Thlbodeaux's team (1977) defined the separation factor as follows (Thlbodeaux et al., 1977):

$$S_a = \frac{Y_2 - mX_2}{Y_2 - mX_1} \qquad (5.12)$$

The results of Thlbodeaux's team show that S_a(L/G) increases with L/G, approaching an asymptotic value with increasing of L/G. Therefore, the results shown in Table 5.4 have been used to determine the optimum L/G at operation temperature of 300K as shown in Figure 5.11 where the function S_a(L/G) tends to be asymptotic. In this study, the Y_2 which is required in Equation (5.12) was not measured because the temperature of the inlet gas stream was too higher to conveniently take a sample. However, values of Y_2 can be determined from a tar material balance about the scrubber.

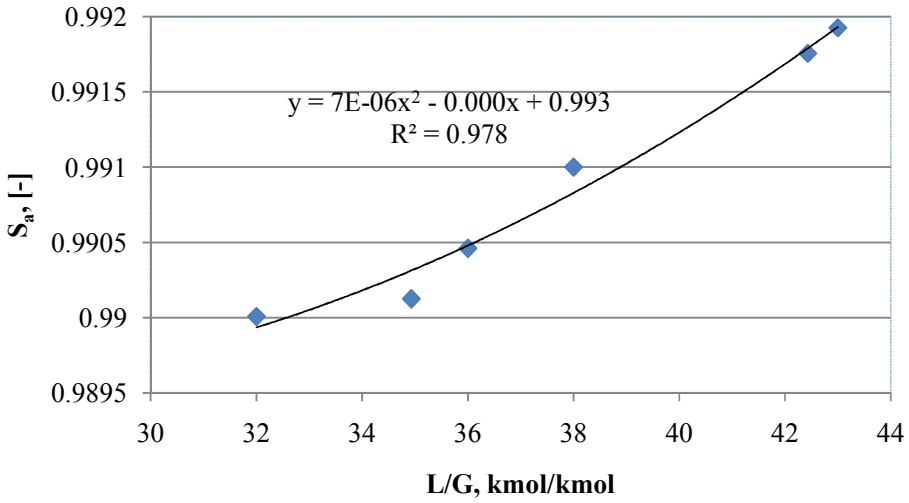

Figure 5.11 : Effect of L/G on the absorption factor in the scrubber at 300 K

From the plot of S_a against L/G (Figure 5.11), the optimum L/G can be determined from a point where the curve tends to be asymptotic. However, the curve in Figure 5.11 does not show a clear asymptotic point. As a result, a mathematical procedure of differentiating the function and equating the resultant to zero was used to determine the optimum L/G. By this procedure, the optimum L/G in this study was determined to be 21.4±0.1. Note that the optimum value of L/G varies with operation temperature. Therefore, the same procedure as given here can be used for other temperatures.

Figure 5.11 shows that the absorption of the tars in CME increases with increase in L/G because the high L/G increases the driving force; therefore, more tars are transferred from the gas phase to the liquids phase. The role of the driving force in the removal of the tars is also illustrated in Figure 5.3 in which the slope of the operating line is equal to L/G.

5.3.3. Determination of Tar Removal Efficiency in the Scrubber

The tar removal efficiency in the scrubber is the key parameter for assessing the performance of the tar removal concept. The tar removal efficiency (η) can be

determined from the drop in the tar concentration in the gas phase divided by its inlet concentration as follows:

$$\eta = \frac{Y_2 - Y_1}{Y_2} \times 100\% \qquad (5.13)$$

The tar removal efficiency was determined for liquid phase temperature of 300 K using data presented in Table 5.4. Similar results of tar removal efficiency were also obtained for liquid phase temperatures of 311 and 317 K at the same L/G value of 43. These results are compared as shown in Figure 5.12.

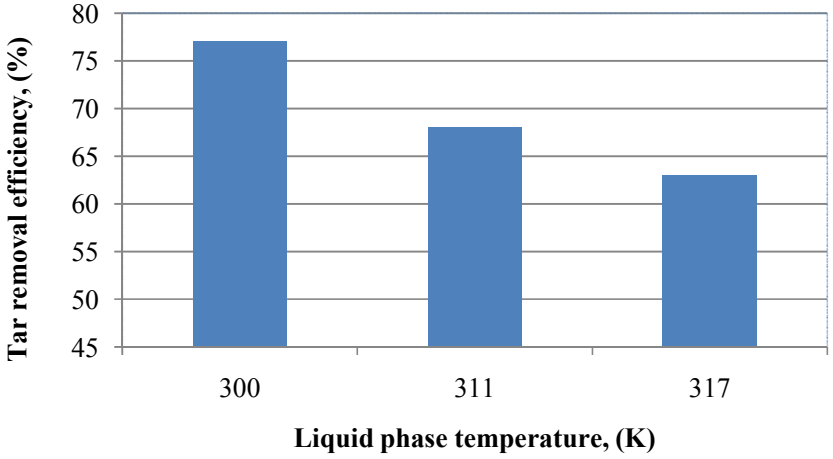

Figure 5.12: Effect of temperature on tar removal efficiency at L/G of 43.

The results in Figure 5.12 confirm the assertion that low temperatures of the CME, or the liquid phase, favour the tar removal in the scrubbing of the tars. Clearly, the tar removal efficiency is the highest at 300 K of the three temperatures examined. The least efficiency is recorded at 317 K which is the highest temperature tested in this study. By considering tar concentration in the inlet gas (369g/Nm^3) which was used in this study, the tar concentration in the gas exiting the scrubber is 85g/Nm^3 at the highest tar removal efficiency of 77%. As this project was to validate the concept of the new gas cleaning technology and to obtain design parameters, the tar concentration in the inlet gas used in this project was much higher than the actual tar concentration in the biomass gasification producer gas which is normally 2.5g/Nm^3 (Hofbauer, 2002). The exit gas tar concentration would be reduced and ultimately the efficiency would increase if

the inlet concentration of the tars in the liquid phase was reduced. Therefore, the test system if applied in practical operation (with lower tar concentrations in the CME) can produce a cleaner gas than which has been found by using the conditions in this study.

5.4. Conclusion

This part of study has investigated and determined design parameters for the scrubber using CME to absorb tars from biomass gasification producer gas, and examined the tar removal efficiency. The design parameters are the liquid phase overall volumetric molar transfer coefficient and the optimum liquid to gas rate ratio.

These parameters have been used to determine the tar removal efficiency which varies with liquid temperature, the liquid to gas flow rate ratio and the inlet tar concentration. At the liquid temperature of 300K and liquid to gas flow rate ratio of 43, the tar removal efficiency of 77% can be achieved when the inlet tar concentration in the gas is 369g/Nm^3. By considering tar concentration in the inlet gas (369g/Nm^3) which was used in this study, the exit tar concentration from the scrubber is 85g/Nm^3 at the highest tar removal efficiency of 77%.

The second part of the test system, the stripper, will be investigated and discussed in the subsequent chapter.

Chapter 6 Air Stripping Loaded CME of Tars

6.1. Introduction

Air stripping is a well known treatment process for removing volatile organic compounds from liquids. Its theoretical basis has been validated in both pilot scale plants (Roberts et al., 1985) and in full scale plants (Wallman et Cummins et al., 1985).

There are numerous studies which have been conducted by using air to remove solutes from water (Rorschach et al., 1989; Nirmalakhandan et al., 1990; Harrison et al., 1993; Nirmalakhandan et al., 1993; Bhowmick et Semmens et al., 1994; Chung et al., 1999). However, only a couple of studies have been found in literature where air has been used to remove solutes from non-aqueous solutions (Sheng et Wang et al., 2004; Zwart et al., 2009). The air stripping of biomass gasification tars from light organic oils of methyl ester types, which are similar to CME, has been conducted at the Energy Centre of the Netherlands (ECN) (Zwart et al., 2009). In this study, the tars in the thermal oil are stripped off by hot air at air temperature more than 180°C (Zwart, Heijden et al. 2010). In essence, the high temperatures of the air enhance the stripping process.

In hot air stripping, the combined effects of the higher air flow rates and high temperatures enhances the solute (tars) to transfer from the liquid phase to the air. The solute material (tars) is then carried out with the air as the liquid phase contacts the gas phase of air and solute. As contacting proceeds within the column, the solute in the liquid phase becomes more depleted while the air becomes more enriched as it travels up the column. The transfer of the solute (tars) between the liquid phase and gas phase can be illustrated by a schematic diagram of the vertical column shown in Figure 6.1.

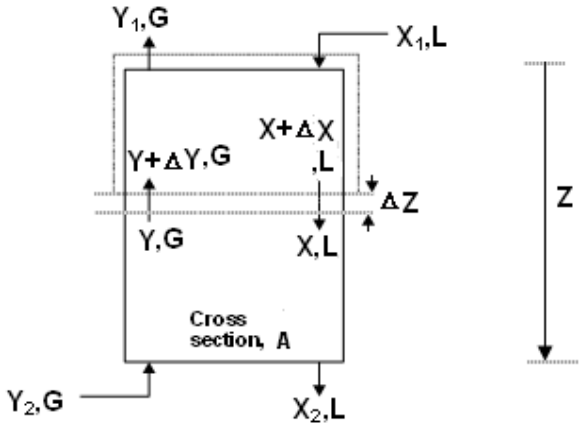

Figure 6.1: Schematic diagram of a tar stripper column with molar flow rates and compositions

In Figure 6.1, the notation 1 and 2 are used to represent the conditions of liquid and gas at the top and bottom of the stripper, respectively.

In this study, the transfer of the tars from the loaded CME occurs at the interface of the liquid film and gas film. As the transfer of the tars takes place between the liquid and gas phases, the tar concentration changes in both the CME and the air. The changes in the tar concentration can be represented in a concentration profile as shown in Figure 6.2.

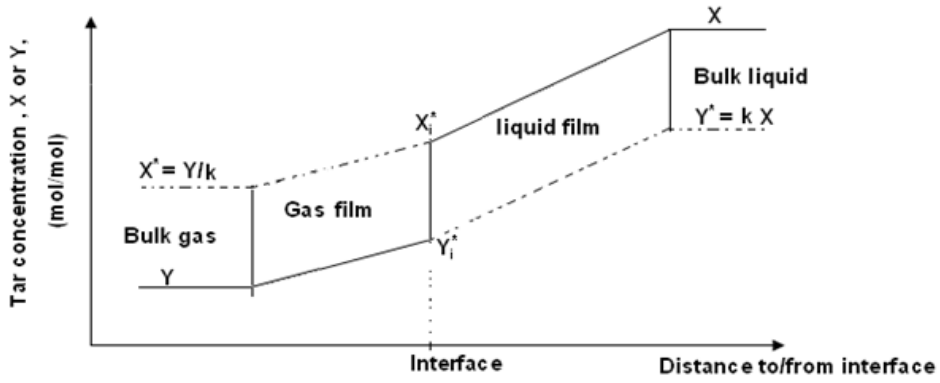

Figure 6.2: The tar concentration profile between CME and gas

The changes in the concentration of the tars over a small column height, ΔZ, as depicted in Figure 6.1 can be determined from tar molar balance and molar transfer theory as follows (Henley et Seader et al., 1981; Geankoplis, 2003):

$$- LdX = K_X a\left(X - X^*\right)dz \tag{6.1a}$$

$$- GdY = K_Y a\left(Y^* - Y\right)dz \tag{6.1b}$$

Under steady state conditions, the tar flux [kmol/(m^{2}s)] across the small column height, ΔZ, can be determined either based on the gas phase concentration difference or the liquid phase concentration difference using corresponding molar transfer coefficient, as follows (Henley et Seader et al., 1981; Geankoplis, 2003):

$$N = K_X\left(X - X^*\right) = K_Y\left(Y^* - Y\right) \tag{6.2}$$

The tar concentrations appearing in Equation (6.2) and Figure 6.1 can be illustrated in an X-Y coordinate in which both operating line and equilibrium curve are presented as shown in Figure 6.3.

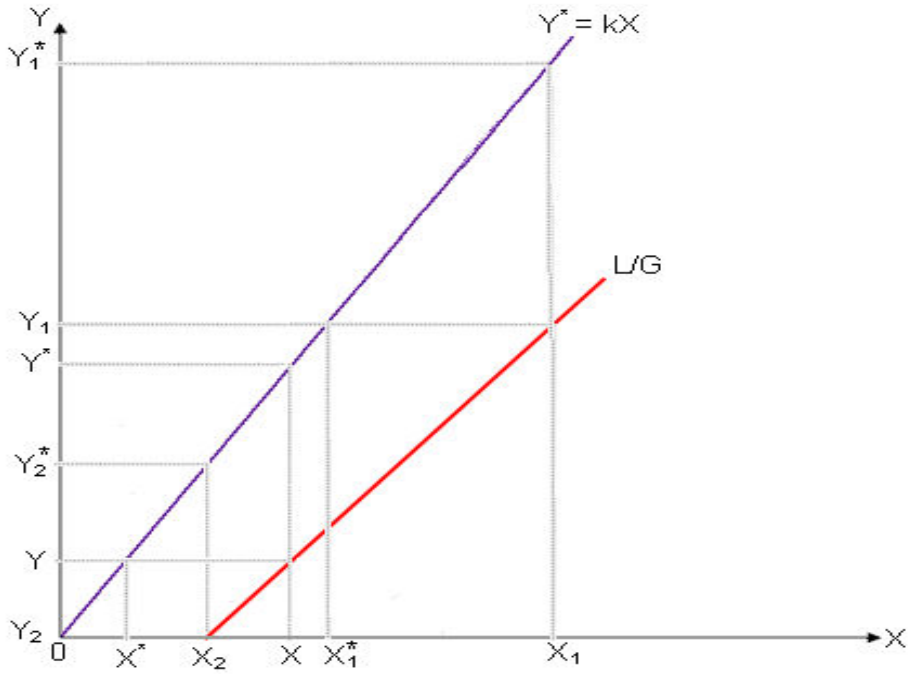

Figure 6.3: Illustration of the operating line and equilibrium curve in the X-Y coordinate in a stripper.

The molar transfer coefficients appearing in Equation (6.2) can be related to each other through the equilibrium coefficient for the stripper, k, as follows:

$$\frac{K_X}{K_Y} = \frac{Y^* - Y}{X - X^*} = \frac{kX - Y}{X - Y/k} = k\left(\frac{X - Y/k}{X - Y/k}\right) = k \tag{6.3}$$

As the equilibrium coefficient, k, can be theoretically determined, experimental data can be used to determined either K_X or K_Y. For instance, K_X can be determined experimentally by firstly rearranging Equation (6.1a) and then integrate it over the column's height of packing, Z.

$$\frac{dX}{X - X^*} = -\frac{K_X a}{L} dZ \tag{6.4}$$

On the basis of the operating line equation and the equilibrium relationship, X-X* can be related to X and X_2 as follows:

$$X - X^* = \left(1 - \frac{L}{kG}\right)X + \frac{L}{kG}X_2 \tag{6.5}$$

Integrating Equation (6.4) over the column's height of packing (Z) for liquid phase concentration from X_1 to X_2 yields:

$$K_X a = \frac{L}{\left(1 - \frac{L}{kG}\right)Z} \ln\left[\frac{X_1 + \frac{L}{kG}(X_2 - X_1)}{X_2}\right] \tag{6.6}$$

$K_X a$ is one of the design parameters for determination of the height of packing for a stripper and can be correlated to liquid and gas flow rates as follows (Cypes et Engstrom et al., 2004):

$$K_X a = \varphi' L^{\alpha'} G^{\beta'} \tag{6.7}$$

The parameters φ', α' and β' can be determined from experimental data by a regression method after transforming Equation (6.7) to the following form:

$$\ln K_X a = \alpha' \ln L + \beta' \ln G + \ln \varphi' \tag{6.8}$$

The theory outlined above was applied in this study in a laboratory scale air stripper which was designed and built to study the operability and performance of

removing tars from CME by using hot air. The objectives of this part of study are as follows:

- Determine the correlation of liquid phase overall molar transfer coefficient as a function of liquid and gas flow rates;
- Determine the optimum liquid to gas flow rate ratio in the stripper;
- Determine the tar removal efficiency of the stripper.

In order to achieve the above objectives, an experimental system was set up and its procedure is outlined in Section 6.2.

6.2. Experimental details

The stripper which was constructed for this study has the same dimensions as the scrubber which is described in Section 5.2. In addition, the experimental procedures and the analysis methods for tar concentration determination in the stripping are also similar to those in the scrubbing studies described in Chapter 5. In the tar stripping, the hot air entered the stripper from its bottom at temperature set points of the range of 473 – 503 K. At the same time, the liquid phase entered the stripper from its top continuously and its temperature was set in the temperature range of 329 – 369 K. The temperature of the liquid phase at the exit of the stripper was measured to be in the range of 330 – 370 K.

In order to analyse the performance of the stripper, liquid samples were collected from sampling ports S3 and S4, shown in Figure 5.4, and analysed for determination of the tar concentrations. Similar procedures as described in Chapter 5 were used for the sampling, analysis and determination of the tar concentrations. The tar concentration in the liquid phase in the stripper decreased when the liquid was flowing downwards from the top of the stripper as the air was continuously contacting the liquid phase. In the experiments, tar concentrations in the CME and operation conditions (flow rate and temperature) were varied in different runs in order to study the performance of the stripper in a wide range of operation conditions. The concentration of the tars in the exit gas phase was not measured. Instead, it was determined by a material balance equation. The concentration of the tars in the inlet air was zero because the tar free air was used. In each run, the flow

rates of the liquid phase and air were measured at steady state. In addition, the temperatures of the air stream and liquid stream were also measured at steady state during each run.

6.3. Results and Discussion

6.3.1. Correlation of $K_X a$ with L and G for the Stripper

Table 6.1 gives the results of tar concentrations in the CME and calculated molar transfer coefficient obtained from the experiments at liquid temperature of 353 K in the stripper and with various liquid to gas ratios.

Table 6.1: Measured liquid and gas flow rates, tar concentrations at the inlet and outlet of the stripper and values of $K_X a$ at 353 K liquid phase temperature

L/G, mol/mol	L, kmol/m^2.s	X_1, mol/mol	X_2, mol/mol	$K_X a$, kmol/m^3.s Equation (6.6)
11.5	0.01800	0.1083	0.04539	0.05815
12.32	0.01800	0.1005	0.04618	0.05046
15.06	0.01800	0.1008	0.05579	0.03842
16.91	0.01797	0.08897	0.05345	0.03301
19.22	0.01802	0.09665	0.06269	0.02775

The values of $K_X a$ in Table 6.1 were determined by Equation (6.6) where the height of packing, Z, is 0.85m, and k, the theoretically predicted equilibrium coefficient, is 7.32 (mol/mol) for the liquid phase temperature of 353 K.

The correlation of $K_X a$ with L and G was fitted by a multi-linear regression method in accordance to Equation (6.8), which yields the square of regression coefficient (R^2) of 0.8011. The determined parameters for Equations (6.7) are as shown in Table 6.2.

Table 6.2: Values of parameters in Equation (6.7) and (6.8) for the stripper at 353 K

Parameter	φ'	α'	β'
Equation (6.7)	3094.49	0.4462	1.411

The parameter β', determined in this study, is generally within the range cited in similar studies (Hsieh et al., 1994; Cypes et Engstrom et al., 2004). Therefore, the correlation is reasonably satisfactory because both the values of α'and β' lie within 0 and 1.5

In order to test the proposed correlation (Equations 6.7) in a wider range of operation conditions, the correlations was used to calculate the molar transfer coefficients and the results are compared with those directly derived from Equation (6.6) for a wider range of L/G values. The results are given in Table 6.3.

Table 6.3: Comparisons of differently determined $K_X a$ values at various L/G values at the stripper at 353 K

L/G	11.5	12.32	15.06	16.91	19.22
$K_X a$, Equation (6.6)	0.05815	0.05046	0.03842	0.03301	0.02775
$K_X a$, Equation (6.7)	0.05671	0.05146	0.03876	0.03291	0.02747

Table 6.3 shows that the values of $K_X a$ obtained by the two equations compare very closely for a wide range of L/G values. Therefore, the correlation was satisfactory.

The effect of the gas flow rates at various loaded CME temperatures of 333, 343, and 353 K was also investigated and the results are shown in Figure 6.4.

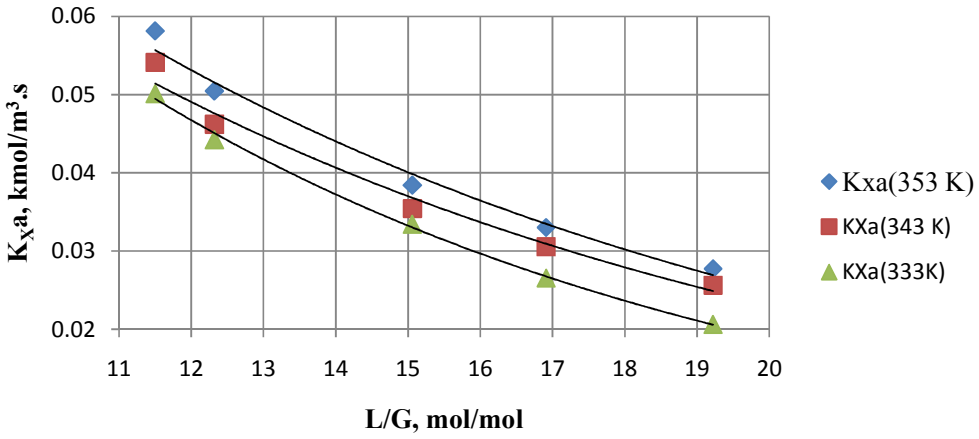

Figure 6.4: Effect of gas flow rate and liquid temperature on K_Xa in the stripper.

Figure 6.4 shows that K_Xa increases with temperature as well as with the flow rate of the gas phase. This trend agrees with Equation (6.3), in the theory, in which the ratio of overall molar transfer coefficient based on liquid phase concentration difference to that based on gas phase concentration difference increases with the equilibrium coefficient in the stripper. Since the equilibrium coefficient increases with temperature of the loaded CME in the stripper, the molar transfer coefficient based on the liquid phase concentration difference will increase with the CME temperature.

6.3.2. Optimum Liquid to Gas ratio (L/G) for the Stripper

The optimum liquid to gas flow rate ratio (L/G) for the stripper can be determined in a similar manner as in the case for the scrubber described in Section 5.3.2 of Chapter 5. However, the separation factor for the stripper can be plotted against the gas phase flow rate. In analogy to Equation (5.12), the separation factor (S_s) for the stripper can be defined as follows (Thlbodeaux et al., 1977):

$$S_s = \frac{X_1 - Y_1/k}{X_1} \qquad (6.9)$$

In which Y_1 can be determined from an equation for the material balance about the stripper and experimental results shown in Table 6.1. The plot for the effect of the gas phase flow rate on the separation factor in the stripper is shown in Figure 6.5.

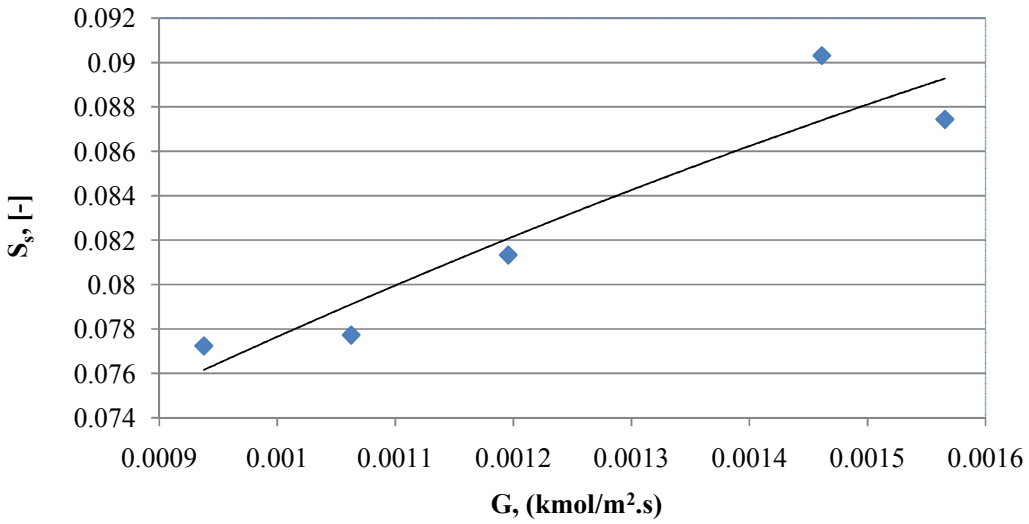

Figure 6.5: Effect of gas phase flow rate on the separation factor in the stripper.

Figure 6.5 shows that the stripping of the tars from the tar loaded biodiesel into air increases with the gas phase flow rate which can be explained by the fact that with low value for L/G (high value for G with constant value for L), the driving force in the gas phase is increased as shown in Figure 6.3. Therefore, as the driving force increases more tars are transferred from the tar loaded CME to the air.

Similarly, as in the case of the scrubber, the curve in Figure 6.5 does not show a clear asymptotic point. As a result, a mathematical procedure of differentiating the function, $S_s(G)$, and equating the result to zero was used to determine the optimum gas phase flow rate, which in this study is 0.003153 (kmol/m^2.s), Since the flow of the tar loaded biodiesel was virtually constant at 0.01800 (kmol/m^2.s), the optimum L/G was determined to be 5.7±0.1. This L/G translates into the air flow rate of 78*l*/min.

6.3.3. Determination of Tar Removal Efficiency in the Stripper

The determination of the tar removal efficiency in the stripper is one of the criteria for assessing the performance of the tar removal system. The tar removal efficiency was determined as the ratio of the difference between the inlet and outlet tar concentrations to the inlet tar concentration in the CME, as follows:

$$\eta = \frac{X_1 - X_2}{X_1} \times 100\% \qquad (6.10)$$

By using the data in Table 6.1 for the CME temperature of 353K, the tar removal efficiency was calculated to be from 35% at L/G value of 19.22 and 58% at L/G value of 11.5. In order to examine the effect of CME temperature on the tar removal efficiency, Equation (6.10) was employed for experimental data with L/G value of 11.5 and loaded CME temperatures of 333, 343 and 353 K in the stripper, and the results are shown in Figure 6.6.

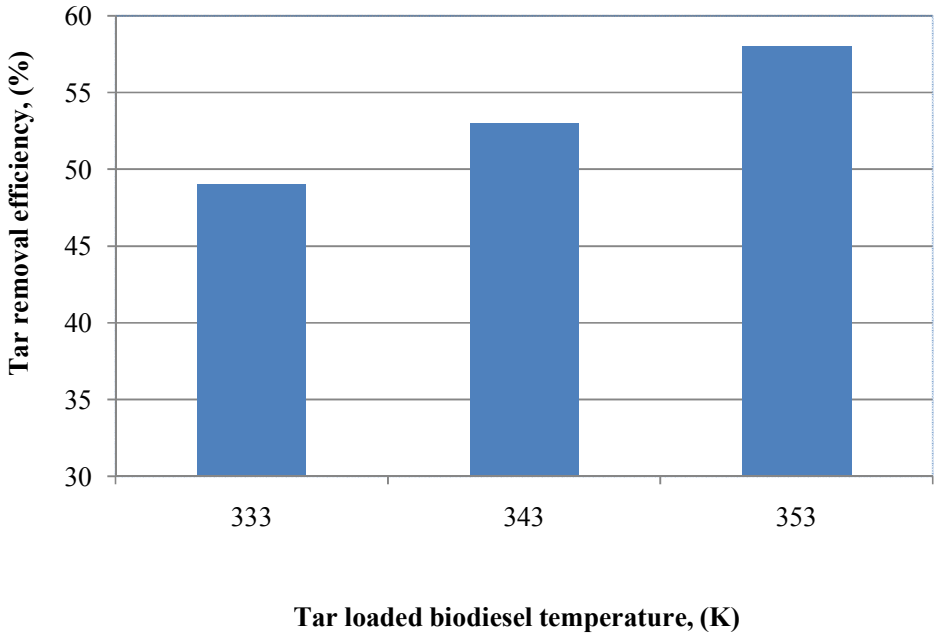

Figure 6.6: Effect of temperature on tar removal efficiency in the stripper

From Figure 6.6, it is clearly seen that the tar removal efficiency increases with the CME temperature and the value of approximately 58% is the highest at CME temperature of 353 K which is the highest temperature tested in the study.

This trend is in agreement with theory of the solubility of the tars in CME. As the temperature of the tar loaded CME increases, the solubility of the tars in CME decreases. As a result, the tars can easily transfer from the liquid phase (CME) to the gas phase (air).

6.4. CME Stream for Dilution

A dilution stream of tar free CME is required in the system to ensure that tar concentration in the liquid phase at inlet point to scrubber is negligible. The dilution CME stream can be incorporated in the system as shown in Figure 6.7

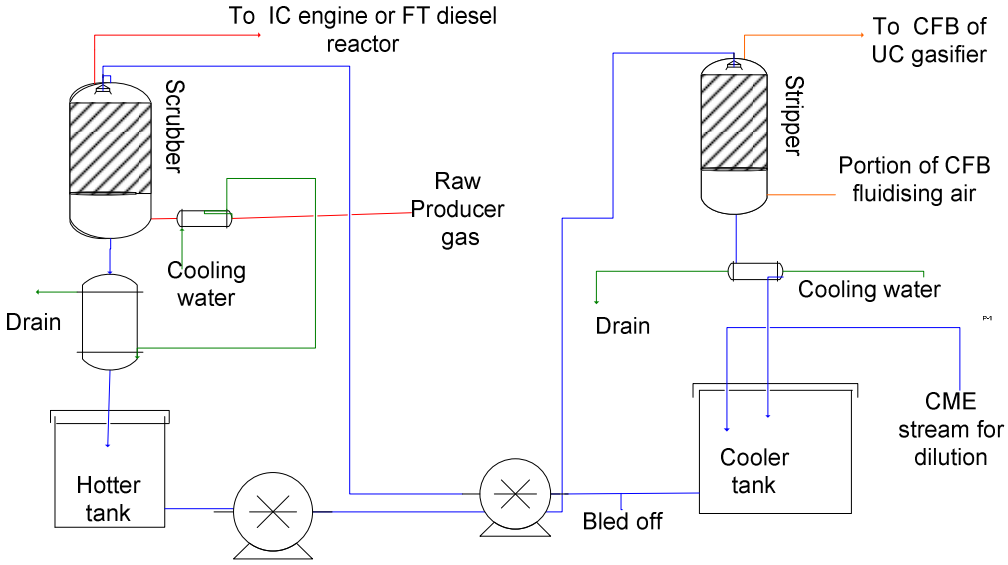

Figure 6.7: Schematic diagram of the UG gasifier's tar removal system

In order to determine the flow rate of the CME stream for dilution, energy and material balances around the system of Figure 5.4 have been undertaken. As a result, it has been determined that the producer gas cooler and the CME cooler would remove 3.25 and 5.4kW of heat respectively. However, the CME heater and air heater would require 5 and 0.19kW respectively. Since the heat requirement for the CME heater can be supplied by cooling the producer gas (as shown in Figure 6.7), the heat requirement for the system would be supplied internally at steady state. Therefore, the flow rate of the CME stream for dilution would only be 3 litres per hour for an 8 MW gasifier (as the Gussing plant). However, if there was not a

stripper, the makeup tar free CME would be 15 litres per hour. In the case of the 100 kW UC gasifier, the makeup tar free CME would be 0.0375 litres per hour.

In the system shown in Figure 6.7, the accumulation of the CME would be eradicated by bleeding off 0.0375 litres per hour of diluted CME biodiesel. During the same operation, the tar loaded CME is stripped of tars which would be carried away by air to the gasifier to recover their energy. In this way, the UC system would be more beneficial than the Guessing one because the energy in tars would be recovered in addition to saving the CME. In case of the Guessing system, a portion of tar loaded RME is combusted to recovery energy in the tars. Therefore, that portion of the RME is wasted.

6.5. Redesign of the Tar Removal System

The redesign of the gas cleaning system which has been discussed in Chapter 4 of this thesis is undertaken here so that it can be modified and then used downstream the UC gasifier to achieve the target state of the art off-gas quality. The redesign has been necessitated by the fact that the state of the art tar concentration for off-gas quality is more than 20 times lower than that on which the first design was based. The scrubber and stripper columns in the test system were designed based on tar concentration in the scrubber's off-gas of 0.6g/Nm^3 which is much higher than the ones obtaining in some state of the art gas cleaning systems (Hofbauer, 2002; Zwart et al., 2009). However, the first design was made mainly with the view of investigating the capability of canola methyl ester (CME) biodiesel at removing tars and the system's performance. In the process of these investigations, the overall molar transfer coefficients for the scrubber and the stripper were determined as design parameters for the designing of the actual system.

In the redesign of the system, particular attention has been paid on the total concentration and tar dew point of the off-gas. If the off-gas is applied in an IC engine to generate electricity, the tar dew point is important because it can be used to tell if the tars can condense and clog the engine. In this case, a gas of lower tar dew point than the operating temperature of the engine could be used regardless of the total tar concentration. On the other hand, either only negligible or none at all

concentration of total tar is permitted in chemical, SNG and FT synthesis. Some of the successful gas cleaning systems have reported their off-gas quality for all round gas application as shown in Table 6.4.

Table 6.4: Off-gas quality and end use for various successful gas cleaning systems

Gas cleaning system	Off-gas quality		Gas application or end use	Reference
	Tar, mg/Nm^3	Dew point, ^{o}C		
Guessing	10 - 40	< 40	Heat, power and FT diesel	**(a)**
OLGA	10	5	Heat, power, liquid fuels and chemicals	**(b)**
VTT	5	-10	Heat and power	**(c)**
References: **(a)** (Hofbauer, 2002; Proll et al., 2005; Zwart et al., 2009) **(b)** (Zwart et al., 2009) and **(c)** (Kurkela, 1989)				

The information in last row of Table 6.4 is for gas quality of many downdraft and updraft gasifiers developed at VTT and installed in many parts of Finland and Sweden. Since the source is quite old, the gas applications might have now advanced into liquid fuels and chemical synthesis.

The design of the actual system for tar removal downstream UC gasifier can now be based on the off-gas quality similar to those in Table 6.4 and the design parameters obtained in Chapter 5 and Chapter 6. In this case, the sizes of the scrubber and stripper columns are the ones to be designed. Since the overall volumetric molar transfer coefficients as design parameters were obtained by using specific liquid to gas flow rate ratios which are also used to determine the column diameter, the diameters of the scrubber and stripper will remain the same as in the test system. However, the height of packing for both the scrubber and stripper will change because the target off-gas concentration has changed.

6.5.1. Design of the Actual scrubber

In this design, the height of the packing for the scrubber will be determined based on an average value of 10 – 40mg/Nm^3 for Guessing's off-gas quality. Since the tar concentration in the gas inlet to RME scrubber at Guessing is about

2500mg/Nm^3(Hofbauer, 2002), the scrubber would be designed at 99% which is typical of conventional scrubber efficiency (Woods, 2007). In addition, the concentration of the tars in the liquid phase at inlet point of the scrubber will be assumed to be negligible because the CME stream for diluting the recycle stream from the stripper is 0.0375 litres per hour which is negligibly small, implying that the tar concentration in the liquid phase entering the scrubber also is negligibly small.

In the practice of designing a scrubber, the solute (tars) composition in gas and gas flow rate are known and used with the equilibrium coefficient to determine actual liquid flow rate and then the height of packing. However, the experimentally determined overall volumetric molar transfer coefficient (K_Xa) and its liquid to gas flow rate ratio (L/G) only can also be used to determine the height of packing. In this study, the K_Xa for the scrubber was experimentally determined as a function of the liquid and gas molar flow rates per unit time per unit area as follows:

$$K_Xa = 0.01234\mathbf{L}^{0.7704}\mathbf{G}^{0.02823} \qquad (6.11)$$

Equation (6.11) was determined at optimum L/G of 21.4 for the scrubber operating at a temperature of almost 300 K. Therefore, such a scrubber with 10% producer gas output flow rate (Bull, 2008) or 0.0009913kmol/m^2.s would have K_Xa of 0.0005216kmol/m^{3}s for the CME flow rate of 7.8 litres per minute which is equivalent to 0.02121kmol/m^2.s. Since the height of packing is a product of number of transfer units (N_{OL}) and height of transfer units (H_{OL}), the later can be determined as follows:

$$H_{OL} = \frac{L}{K_Xa} \qquad \text{(Equation 4.30b)}$$

On the other hand, the former can be determined as follows (Henley et Seader et al., 1981):

$$N_{OL} = \frac{X_2 - X_1}{\Delta X_{LM}} \qquad (6.12)$$

In Equation (6.12), the term ΔX_{LM} is log mean mole ratio difference and defined as follows:

$$\Delta X_{LM} = \frac{\Delta X_2 - \Delta X_1}{\ln(\Delta X_2 / \Delta X_1)} \tag{6.13}$$

The terms in the right side of Equation (6.13) are defined as follows:

$$\Delta X_1 = X_1^* - X_1 = \frac{Y_1}{m(T)} - X_1 \tag{6.14a}$$

$$\Delta X_2 = X_2^* - X_2 = \frac{Y_2}{m(T)} - X_2 \tag{6.14b}$$

The m(T) of 0.3846mol/mol and tar concentration at inlet (2500mg/Nm^3 or 0.0003562mol/mol) and outlet (25mg/Nm^3 or 0.000003562mol/mol) of the scrubber operating at temperature of almost 300 K can then be used to determined the N_{OL} as shown in Table 6.5:

Table 6.5: Calculation for the determination of N_{OL} for the scrubber

X_1^*	X_2^*	ΔX_1	ΔX_2	ΔX_{LM}	N_{OL}
0.000009261	0.0009261	0.000009261	0.0009097	0.0001963	0.08395

The calculation of the N_{OL} is done analytically because the tar concentration in the liquid phase is very dilute as evidenced by the tar mole ratios in Table 6.5 (Sinnott, 2005). The product of the N_{OL} and H_{OL} (of 40.67m) results into the scrubber's height of packing of 3.4m.

6.5.2. Design of the Actual Stripper

The height of the packing for the stripper will be designed based on 99% tar removal efficiency, typical of conventional stripper efficiency (Woods, 2007) and the exit tar concentration from the scrubber. Therefore, the exit tar concentration from the stripper would be one hundredth of the tar concentration at inlet point to the stripper.

In designing a stripper, the solute (tars) composition in liquid phase and flow rate of the liquid phase are known and used with the equilibrium coefficient to determine actual gas flow rate and then the height of packing. However, the experimentally determined overall volumetric molar transfer coefficient (K_Xa) and its liquid to gas flow rate ratio (L/G) only can also be used to determine the height of packing. In this study, the K_Xa for the stripper was experimentally determined as a function of the liquid and gas molar flow rates per unit time per unit area as follows:

$$K_Xa = 3098.49\mathbf{L}^{0.4462}\mathbf{G}^{1.411} \tag{6.15}$$

Equation (6.15) was determined at optimum L/G of 5.7 for the stripper operating at a temperature of almost 353 K. On this basis, the exit gaseous tar concentration is 0.000093mol/mol and the K_Xa for the stripper is 0.2071kmol/m^{3}s for the air flow rate of 92 litres per minute which is equivalent to 0.0032kmol/m^2.s. As in the case of the scrubber, the stripper's height of packing is a product of number of transfer units (N_{OL}) and height of transfer units (H_{OL}) and Equations 4.30 is used to determine $H_{OL.}$ Conversely, the N_{OL} is determined as follows (Henley et Seader 1981 et al.,):

$$N_{OL} = \frac{X_1 - X_2}{\Delta X_{LM}} \tag{6.16}$$

In Equation (6.16), $X_1 = X_2$ (i.e. for scrubber) = 0.00001648 and the term ΔX_{LM} is log mean mole ratio difference and defined as follows:

$$\Delta X_{LM} = \frac{\Delta X_1 - \Delta X_2}{\ln(\Delta X_1/\Delta X_2)} \tag{6.17}$$

The terms in the right side of Equation (6.17) are defined as follows:

$$\Delta X_1 = X_1 - X_1^* = X_1 - \frac{Y_1}{k(T)} \tag{6.18a}$$

$$\Delta X_2 = X_2 - X_2^* = X_2 - \frac{Y_2}{k(T)} \tag{6.18b}$$

The k(T) of 7.32mol/mol for the stripper operating at temperature of almost 353 K can then be used to determined the N_{OL} as shown in Table 6.6:

Table 6.6: Calculation for the determination of N_{OL} for the stripper

X_1^*	X_2^*	ΔX_1	ΔX_2	ΔX_{LM}	N_{OL}
0.0000127	0	0.000003776	0.0000001648	0.000001153	14.15

The calculation of the N_{OL} is done analytically because the tar concentrations in the liquid phase are very dilute as evidenced by the tar mole ratios in Table 6.6 (Sinnott, 2005). The product of the N_{OL} and H_{OL} (of 0.1024m) results into a stripper's height of packing of 1.4m.

6.6. Conclusion and Recommendation

The theoretically determined equilibrium coefficients at the temperatures of 333, 343 and 353 K and tar concentrations in the solvent (CME) in the stripper have been used in this part of the study to obtain design parameters for the stripper and to analyse the stripper performance. A series of experiments were conducted at various operation conditions from which the tar concentrations in both the CME and in the hot air were determined using the same methods described in Chapter 5. The design parameters are the liquid phase overall volumetric molar transfer coefficient and the optimum liquid to gas rate ratio. The performance of the stripper has been analysed in terms of the tar removal efficiency and the tar concentration in the recycle CME.

The correlation of the liquid phase overall volumetric molar transfer coefficient has been found to satisfy the power law function regression. The exponents of the liquid phase and gas phase flow rates have been found to be 0.4462 and 1.411 for the correlation in stripper in this study. In terms of the performance of the stripper, the tar removal efficiency of 74% for the optimum liquid to gas flow rate ratio of 5.7 has been found which can achieve the cleanness for the biomass gasification producer gas to meet the requirement for a gas engine. This translates into the stripping air flow rate of 78*l*/min.

The experimentally determined design parameters of overall liquid phase molar transfer coefficients and liquid to gas flow rate ratios for both the scrubber and stripper have been used to determine the height of packing for the scrubber and stripper as 3.4 and 1.4m respectively. The flow rate of the CME and that of the air have also been determined to be 7.8 and 92 litres per minute respectively. These flow rates require 0.0375 litres per hour of tar free CME stream to be added to the recycle stream so that the tar concentration in the system does not accumulate. At the same time, 0.0375 litres per hour of CME is bled off the system to avoid accumulation of the liquid phase. This design ensures that the tar removal efficiency in both the scrubber and the stripper is 99%. However, it can be recommended that the packing be replaced by large ones of the same type to conform to the conventional design relation between size of the packing and diameter of the column to enhance the efficiency. The test system is currently packed with 12mm Raschig ceramic rings and the diameter for both columns is 153mm. Since the conventional design relation between size of the packing and diameter of the column is that the size of packing should be one tenth of the column diameter (Woods, 2007), 15mm Raschig ceramic rings should be used.

Chapter 7 General Discussion, Conclusion and Recommendations

The aims of this thesis were to select a tar removal system from successful exiting ones, modify it, test its performance and obtain design parameters for the actual practical system to be integrated with UC gasifier. Various methods for reducing tar concentration in the producer gas were explored in the open literature. Considering the operation conditions of the UC gasifier, costs and sustainability, wet scrubbing using CME as a solvent was selected and further developed in this project as the suitable method. The choice of CME was based on an extensive review of literature on tar removal by wet scrubbing. In addition, CME was chosen with the view that it could be regenerated and reused. For recovery of the tar energy, the tar loaded CME from the scrubber was regenerated in a stripper by using heated air and recycled to the scrubber. In the mean time, the tars carried away by the hot air can be combusted in a burner. In this case, the tars can be burnt in the combustion column of the UC gasifier system.

In order to effectively remove the tars from the gas in the scrubber and from the CME in the stripper, the size of the scrubber and stripper had to be determined and the operation conditions (temperature, liquid to gas flow rate ratio) had to be optimised. In the determination of the size of the scrubber and stripper, the equilibrium coefficients for the transfer of the tars between the gas and CME, and between the CME and air had to be researched from literature. However, these coefficients are not directly available in the open literature. Therefore, these coefficients were theoretically predicted based on well known thermodynamic theories and available data for the compositions of tars and CME as well as properties of each component. The unavailable properties which are required, such as density and viscosity of the tars and CME biodiesel, were measured in this project. Furthermore, the experimental data and the equilibrium coefficients were used to obtain molar transfer coefficients and optimum liquid to gas flow rate ratios both in the scrubber and the stripper which were used to analyse the performance of the gas cleaning test system as well as determining the design parameter for the actual practical system.

7.1. General Discussion

Wet scrubbing separation process for gas cleaning involves the transfer of a solute from the gas to scrubbing liquid (solvent) where the solute is dissolved in the solvent. In most operations, the separation takes place in a packed column where the gas contacts the liquid counter currently through the filled packings. The size of the packed column depends on many factors which include the solubility of the solutes in the solvent, the mass transfer coefficients, and the liquid to gas flow rate ratio (L/G). The solubility data of most common gases in common solvents have been experimentally determined and published in open literature. However, the solubility data of the tars in CME is not found in literature. Therefore, the solubility data for the dissolution of the tars in CME was theoretically predicted in Chapter 3. In the prediction of the solubility of the tars, naphthalene was taken as the representative tar component. Naphthalene is the most abundant poly-aromatic hydrocarbon (tar component) in the producer gas of biomass gasification generated by most types of gasifiers including the UC gasifier. Naphthalene has been used in experiments for determination of heat and mass transfer fundamental properties such as diffusivity and mass transfer coefficient (Goldstein et Cho et al., 1995). Hence, the properties of naphthalene such as solubility parameter, molar volume and vapour pressure which can be used to predict its solubility are readily available in the literature. However, properties of CME are not available in literature because it is a liquid mixture of methyl esters made from various fatty acid constituents. Therefore, a thermodynamic approach based on the regular solution theory was used to define the solubility of the gaseous naphthalene in CME. Since the regular solution theory is applied to the estimation of the solubility of non-polar gases (or vapours) in non-polar solvents, a characteristic constant to correct the solubility of non-polar naphthalene in the polar CME was used. In this regards, a correlation for the characteristic constant with the solubility parameters of 10 polar solvents was used to determine the characteristic constant for CME. Further, the solubility parameters, molar volumes and vapour pressures of the constituents of CME were used. The correlated characteristic constant for CME was then used to predict the naphthalene solubility which was found to decrease with increase in the temperature of the CME. This trend was later validated in the preliminary experiments for the gas cleaning system

A tar removal test system has been designed where the liquid to gas flow rate ratio, L/G, in the scrubber was determined from the predicted equilibrium coefficients and tar solubility in the CME at various temperatures. In addition, the densities of nitrogen and air were taken from literature and used for the calculation of the L/G. The measured densities of CME at various temperatures and tar concentrations were reasonably correlated with temperature and tar concentrations as evidenced by small deviations and the value of the square of the correlation coefficient (R^2).

On the other hand, the L/G for the stripper was determined from the optimum stripping factor. A plot of number of transfer units (N_{OL}) in the stripper as a function of the stripping factor (S) was used to determine the optimum S. After the optimum S had been determined, the L/G for the stripper was estimated as the ratio of the equilibrium coefficient to the optimum S. This method to determine the L/G for the stripper was adopted from literature which is different from the classical method. It was found that the classic method resulted into the S value of 1.4 which yields low stripping efficiencies. The estimated L/G for the stripper was used to calculate the diameter and height of the stripper which turned out to be about the same as those of the scrubber. As a result, the design of the scrubber and stripper was reasonably reliable.

After the design and construction of the lab-scale scrubber and stripper columns, hydrodynamic experiments were conducted to find out the regions of effective loading in both columns. The investigation determined distinctly defined effective loading at 1.9 to 1.93kPa/m for the scrubber and 0.035 to 0.04kPa/m for the stripper, respectively. These pressure drops are reasonably small and desirable for smooth and effective operations.

After the hydrodynamic experiments, the preliminary experimentations on tar removal test system were performed with the scrubber and the stripper as stand-alone units. The experimental results confirmed the hypothesis that the tar removal efficiency increases with decrease in temperature in the scrubber. In the stripper, the efficiency increased with the temperature. The results of these experiments also proved the theory for the solubility of naphthalene in CME. In this regard, its solubility was promoted by lower temperatures in the scrubber and inhibited by

higher temperature in the stripper. In addition, the results agreed with the prediction of the equilibrium coefficients for both the scrubber and stripper. In the scrubber, the equilibrium coefficient is lower at low temperatures of CME which means that more naphthalene transfers from the gas phase to the liquid phase. As a result, the naphthalene removal efficiency in the scrubber is increased with decrease in temperature of the CME. On the other hand, the equilibrium coefficient is large in the stripper at higher temperatures for the CME which means more tars transfer from the biodiesel to the air.

The results of the preliminary experiments were further consolidated by integrating the scrubber with the stripper in the system where the CME circulated between the two units in a closed loop. In the loop, the CME was cooled down before the scrubber and heated before the stripper. In the preliminary experiments, the sampling and analysis method of the tar concentration in the CME and in the gas (nitrogen) was developed. The concentrations of CME and gas samples which were taken from the test system were determined by an innovative method which has not been published, to the knowledge of this thesis' author. The method is based on the concept that UV absorbance of a liquid mixture is related to the mixture density, and the mixture density is, in turn, related to the mass fraction of the tar in the solvent. Therefore, the mass fraction can be calculated based on the mixture density and the densities of the tar and the solvent as given in Equation (5.11b) (Aminabhavi, 1984):

$$\frac{1}{\rho_{LM}} = \frac{(1 - x_m)}{\rho_l} + \frac{x_m}{\rho_{tar}} \qquad (5.11b)$$

Since the new method is based on the density of liquid mixtures, it should be applied mostly for liquid mixtures formed by dissolving a liquid solute in liquid solvent. Nevertheless it was applied in this study where tars were dissolved in a liquid solvent because the solutions so formed were dilute, less than 10% (mol/mol). The new method was used in the determination of tar concentration in the CME which was firstly diluted in a solvent called isopropyl alcohol (IPA) and then the UV absorbance of this liquid mixture was measured.

The method was also used for determination of tar concentration in the gas phase in which the gas was bubbled through the IPA. It was found that the

measurement of the absorbencies is inherent with errors when the absorbencies are less than 0.1 and more than 0.7 because the accuracy of the UV visible spectrophotometer is poor outside the range of 0.1 - 0.7. Therefore, the absorbance data which were less than 0.1 could have been so inaccurately measured that the analysis of the performance of system could have been affected.

7.2. General Conclusion

A gas cleaning test system has been designed and constructed to investigate its performance at removing tars from the gas and liquid phases. Using the test system, design parameters for an actual tar removal system have been determined. The system consists of two units, a scrubber for tar absorption by CME as solvent and a stripper for CME regeneration and tar recovery. The design of the test system was based on the concept that the tar solubility in CME increases with decrease in operation temperature and decreases at high temperature, therefore the scrubber should be designed and operated at low temperatures whereas the stripper should be designed and operated at high temperatures in the actual tar removal system. The tar solubility in the CME and equilibrium coefficients have been predicted using reported data of CME and tar compositions as well as measured densities and viscosities of the CME-tar mixture. Most importantly, the predicted equilibrium coefficients and experimental data have been used to determine the design parameters such as molar transfer coefficients and optimum liquid to gas flow rate ratios both for the scrubber and for the stripper.

Experiments have been conducted on the constructed gas cleaning system to analyse its performance. In the analysis, the percent of the tars removed from nitrogen has been found to increase with the decrease in the temperature of the CME. On the other hand, the percent of the tars removed from the tar loaded biodiesel has been found to increase with the increase in the temperature of the loaded CME. The results for the scrubber and the stripper have validated the theories which have been used in this study to predict the tar solubility and equilibrium coefficients in the scrubber and stripper. The determined design parameters and the new innovative method for the determination of the tar concentration underscore major contributions to the literature for the removal of tars from producer gas in biomass gasification. In

this regards, the molar transfer coefficients have been correlated as a function of liquid and gas flow rates in both the scrubber and the stripper which are consistent with literature.

Using the optimum liquid to gas flow rate ratios, the optimum tar removal efficiency of 77% can be achieved for the scrubber at operation temperature of 300K and the efficiency of 74% for the stripper at operation temperature of 353 K. The tar removal efficiency in the scrubber would be increased; if the temperature of CME in the scrubber were further reduced by cooling it in a larger cooler before feeding the scrubber. Similarly, the tar removal efficiency in the stripper would be increased; if the temperature of the tar loaded CME were further increased by heating the CME to higher temperatures.

As regards the performance of the actual tar removal system, the tar removal efficiencies are likely to improve because the heights of packing have increased. In both the scrubber and stripper, the practical tar removal efficient is likely to be close to the redesign value of 99%. In any case, there would still be amount of the tars remaining in the liquid recycle stream from the stripper which would be negligible judging by the typical tar concentrations (10 – 40mg/Nm^3) used in the redesign of the system. The tar concentration remaining in the recycle stream would be those contributed by naphthalene and acenaphthylene because these are the most abundant tar components generated by the UC gasifier, as shown in Table 2.7. However, the amounts of these components in the recycle were not quantified because the experiments which were done in Chapters 4, 5, and 6 measured total tar concentrations as opposed to individual tar component concentrations.

7.3. Recommendations

7.3.1. Consistent Tar Concentration in the Feed Gas

A reliable analysis of the system performance would need a consistent tar concentration in the feed gas. The simulation of tar concentration into nitrogen does not yield a reliable analysis of the scrubber performance as the tar in the autoclave deplete over some time and cannot easily be replenished during the runs. In addition, the simulation concentrations are always going be higher than the actual tar

concentration in producer gas. Therefore, the gas cleaning system should be tested with the raw producer gas of the UC gasifier.

7.3.2. Tar Sampling and Analysis

The new method developed in this study for tar concentration determination is reasonably reliable for both the liquid phase and the gas phase. However, it requires a reliable UV visible spectrophotometer, preferably a digital one that has very high accuracy and sensitivity even at very low and high concentrations. Therefore, this method and a modern UV visible spectrophotometer can be employed in an actual system where a real producer gas is used.

7.4. References

Aldrich, (2010). Reagent Data Book, Sigma-Aldrich. New York, Alderich

Aminabhavi, T (1984). "Use of Mixing Rules in the Analysis of Data of Binary Liquid Mixtures." Journal of Chemical Engineering Data. **29**: 54 - 55.

Anonymous (1995). Cleaning of Hot Producer Gas in a Catalytic, Reverse Flow Reactor, BTG Biomass Technology Group BV; Novem Report no. 9605

Argonne-National-Laboratory (2005). Basic Research needs for Solar Energy Utilization. the report on the US DOE basic energy sciences workshop on solar energy utilization.

Babu, S. P. (1995). "Thermal Gasification of Biomass Technology Developments: End of Task Report for 1992 To 1994 " Biomass and Bioenergy **9**: 271 - 285.

Babu, S. P. (2006) "IEA Bioenergy Agreement workshop No.1: Perspective on biomass gasification." Task 33: Thermal Gasification of Biomass.

Barton, A. F. (1983). CRC Handbook of Solubility Parameters and Other Cohesion Parameters. Florida, CRC Press, Inc.

Beenackers, A. A. C. M. and W. P. M. van Swaaiji (1984). Gasification of Biomass, a State of the Art Review. Thermochem. Process. Biomass. A. V. Bridgwater. London, Butterworths**:** 91 - 136.

Begley, S. (2009). We can't get there from here. Newsweek Magazine, Newsweek.

Belgiorno, V., G. De Feo, et al. (2003). "Energy from gasification of solid wastes." Waste Management **23**: 1 - 15.

Benitez, J. (2002). Principles of Modern Appliactions of Mass Transfer Operations. New York, John Wiley & Sons, Inc.

Bernard, W. (2007). Bio diesel. Rangiora, New Zealand, Biodiesel Manufacturing Ltd.

Bhattacharya, S. and A. Dutta (1999). "Two-stage Gasification of Wood with Preheated Air Supply: A Promising Technique for Producing Gas of Low Tar Content." ISES 99 Solar World Congress, Israel.

Bhowmick, M. and M. J. Semmens (1994). "Batch Studies on a Closed Loop Air Stripping Process." Water Research **28**: 2011 - 2019.

Bilbao, R., L. Garcia, et al. (1998). Steam Gasification of Biomass in a fluidised bed. Effect of a Ni-Al catalyst. Proceedings of the Tenth European Conference and Technology Exhibition on Biomass for Energy and Industry. H. Kopetz, T. Weber, W. Palz, P. Chartier and G. L. Ferrero. Wurzburg, Germany**:** 1708 - 1711.

Boerrigter, H. (2002). Gas Cleaning at ECN, Leasons learned... and Results achieved. J. Beesteheerde and H. J. Veringa, GasNet & IEA Bioenergy Agreement Meeting 2 October 2002.

Boerrigter, H., S. vaan Paasen, et al. (2005). "OLGA" Tar Removal Technology. Proof-of-Concept (PoC) for application in integrated biomass gasification combined heat and power (CHP) systems. H. J. Veringa. Petten, Netherland, Energy Research Centre of the Netherlands (ECN).

Bolhar-Nordenkkampf, M. and H. Hofbauer (2004). Gasification Demonstration Plants in Austria. IV. International Slovak Forum. Bratislava, Slovenia, Slovak Biomass Forum, 227 - 230**:** 227 - 230.

Bradbury, A. G. W., Y. Sakai, et al. (1979). " A kinetic model for pyrolysis of cellulose. ." Journal of Applied Polymer Science **23**: 3271 - 3280.

Brage, C., Q. Yu, et al. (1997). "Use of Amino Phase Adsorbent for Biomass Tar Sampling and Separation." Fuel **76**: 137 - 142.

Bridgwater, A. (2001). Progress in Thermochemical Biomass Conversion. New York, Wiley - Blackwell.

Brouwers, J. J. H. (1997). "Particle Collection Efficiency of the Rotational Particle Separator." Powder Technology **92**: 89 - 99.

Brown, R. C. (2003). Biorenewable Resources, Engineering New Products from Agriculture. New York, USA, Academic press.

Brown, R. C. (2003). Biorenewable Resources: Engineering New Products from Agriculture, Iowa State Press.

Buhler, R., U. Energie, et al. (1997). IC Engines for LCV Gas from biomass Gasifiers. Proceedings of the IEA Thermal Gasification Seminar; Zurich, Switzerland, IEA Bioenergy and Swiss Federal Office of Energy.

Bull, D. (2008). Thesis: Performance Improvements to a Fast Internally Circulating Fluidised Bed (FICFB) Biomass Gasifier for Combined Heat and Power Plants. Department of Chemical and processing Engineering Christchurch, New Zealand, University of Canterbury. **Master of Engineering.**

Carlsson, K. (2008). "Removal of particles in flue gas from combustion of biomass – a practical approach." Retrieved,cited:16/05/2009, from http://www.thermalnet.co.uk/docs/Gasification%20WS%20K%20Carlson%20Vicenza.pdf.

Chen, Y., Y. Luo, et al. (2009). "Experimental Investigation on Tar Formation and Destruction in a Lab-Scale Two-Stage Reactor." Energy & Fuels **23**: 4659 - 4667.

Chung, T. W., C. H. Lai, et al. (1999). "Analysis of Mass Transfer Performance in an Air Stripping Tower." Separation Science and Technology **34**: 2837 - 2851.

Corella, J., J. Herguido, et al. (1988). Fuidised bed steam gasification of biomass with dolomite and with commercial FCC catalyst. Research in thermochemical biomass conversion. A. V. Bridgwater and J. L. Kuester. London, Elsevier**:** 754 - 765.

Coulson J M and J. F. Richardson (1996). Chemical Engineering Volume 1 Oxford, England, Butterworth-Heinemann Ltd.

Cypes, S. H. and J. R. Engstrom (2004). "Analysis of a Toluene Stripping Process: A Comparison between a Microfabricated Stripping Column and a Conventional Packed Tower." Chemical Engineering Journal **101**: 49 - 56.

Dasappa, S., P. J. Paul, et al. (2004). "Biomass gasification technology - a route to meet energy demand." Current Science **87**(10): 908 - 916.

Dayton, D. (2002). A Review of the Literature on Catalytic Biomass Tar Destruction. Cole Boulevard, Golden, Colorado, National Renewable Energy Laboratory (NREL); NREL/TP-510-32815.

Delgado, J., M. P. Aznar, et al. (1995). Fresh tar (from biomass steam gasification) cracking over dolomites: Effects of their particle size and porosity.

Proceedings of the 8th European Biomass Conference for Energy and Environment, Agriculture and Industry. P. Chartier, A. A. C. M. Beenackers and G. Grassi, Pergamon**:** 1825 - 1829.

Devi, L., K. J. Ptasinski, et al. (2002). A Review of the Primary Measures for Tar Elimination in Biomass Gasification Process. Eindhoven, Eindhoven University of Technology.

Devi, L., K. J. Ptasinski, et al. (2005). "Catalytic Decomposition of Biomass Tars: Use of Dolomite and unreacted Olivine." Renewable Energy **30**(4): 565 - 587

Dou, B., J. Gao, et al. (2003). "Catalytic Cracking of Tar Component from High-temperature Fuel Gas " Applied Thermal Engineering **23**: 2229 - 2239.

Dutta, B. K. (2007). Principles of Mass Transfer and Separation Processes. New Delhi, Prentice-Hall of India.

El-Rub Abu, Z. (2008). Biomass Char as an In-Situ Catalyst for Tar Removal in Gasification Systems. Twente, University of Twente,. **PhD Thesis**.

Fernandez, J. C. (1997). Revalorzacion de Residuos Solidos Mediante la Gasification en Lecho Fluidizao: Estudio de los Sistemas de Acondicionamiento de Gases y Valoaracion Ambiental del Proceso. PhD Thesis. Barcelona, Catalinga, Spain, UPC.

Franco, C., I. Gulyurlu, et al. (2002). The Study of Reactions Influencing the Biomass Steam Gasification Process.

Garcia, X. A. and K. J. Hiuttinger (1989). "Steam Gasification of Naphthalene as a Model Reaction of Homogeneous Gas/Gas Reactions Reactions during Coal Gasification." Fuel **68**: 1300 - 1310.

Geankoplis, C. (2003). Transport Processes and Separation Process Principles. New Jersey, Pearson Education, Inc.

Giger, W. and M. Blumer (1974). "Polycyclic Aromatic Hydrocarbons in the Environment: Isolation and Characterization by Chromatography, Visible, Ultraviolet and Mass Spectrometry." Analyical Chemistry **46**: 1663 - 1671.

Gmehling et al., (1998). "A Modified UNIFAC (Dortmund) Model. 3. Revision and Extension." Industrial and Engineering Chemistry Research **37**: 4876 - 4882

Goldstein, R. J. and H. H. Cho (1995). "A Review of Mass Transfer Measurements using naphthalene sublimation." Experimental Thermal and Fluid Science **10**(4): 416-434.

Goodrum, J. W. (1996). Review of Biodiesel Research at University of Georgia. Proceedings of Liquid Fuel Conference, 3rd, , St Joseph, Michigan, USA, , American Society of Agricultural Engineering, 128 - 135.

Guanxing, C., K. Sjostrom, et al. (1994). Co-gasification of Biomass and Coal in a Pressurised Fluidised Bed Reactor; Biomass for Energy, Environment, Agriculture and Industry, Proceedings of the 8th European Biomass Conference, Vienna, Austria.

Guascor (2005) "Fuel Gas Specifications-Gas from Thermochemical processes. Biomass and Tires." IC Group. Product IC-G-D-30-004e.

Guzhev, G. P. (1971). "Granular bed gas filters." Chemical and Petrochemical Engineering **7**: 47 - 49.

Hamelinck, C. N., A. P. C. Faaij, et al. (2004). "Production of FT Transportation Fuels from Biomass; Technical Options, Process Analysis and Optimisation, and Development Potential." Energy **29**: 1743 - 1771.

Han, J. and H. Kim (2008). "The Reduction and Control Technology of Tar During Biomass Gasifcation/Pyrolysis: An Overview." Renewable and Sustainable Energy Reviews **12**: 397 - 416.

Harrison, D. P., K. T. Valsaraj, et al. (1993). "Air Stripping Organics from Groundwater." Waste Management **13**: 417 - 429.

Hasler, P. and T. Nussbaumer (1999). "Gas cleaning for engine applications from fixed bed biomass gasification." Biomass & Bioenergy **16**(6): 385 ~ 395.

Hasler, P. and T. Nussbaumer (1999). "Gas Cleaning for IC Engine Applications from Fixed Bed Biomass Gasification." Biomass & Bioenergy **16**(16): 385 - 395.

Hasler, P. and T. Nussbaumer (2000). "Sampling and Analysis of Particles and Tars from Biomass Gasifiers." Biomass & Bioenergy **18**: 61 - 66.

Hasler, P., T. Nussbaumer, et al. (1997). Evaluation of Gas Cleaning Technologies for Small Scale Biomass Gasifier. Berne, Switzerland, Report for Swiss Federal Office of Energy.

Hedden, K., T. Heike, et al. (1986). Testing and Optimization of Commercial Biomass Gasifiers. DVGW-Forschungsstelle, Karlsuhe Univ. (T.H).

Henderick, P. and R. H. Williams (2000). "Trigeneration in a northern Chinese village using crop residues." Energy for sustainable development **4**: 26 - 42.

Henley, E. J. and J. D. Seader (1981). Equilibrium-Stage Separation Operations in Chemical Engineering. New York, John Wiley & Sons.

Herguido, J., J. Corella, et al. (1992). "Steam Gasification of Lignocellulosic Residues in a Fluidized Bed at a Small Pilot Scale. Effect of the Type of Feedstock." Industrial and Engineering Chemistry Research **31** (5): 1274 - 1282.

Higman, C. and M. Burgt (2003). Gasification, Gulf Professional Publishing.

Hofbauer, H. (2002). Biomass CHP - Plant Güssing: A Success Story. Pyrolysis and Gasification of Biomass and Waste, Expert Meeting. Strasbourg.

Hofmann, P., A. Schweiger, et al. (2007). "High temperature electrolyte supported Ni GDC/YSZ/LSM SOFC operation on two-stage Viking gasifier product gas." Journal of power source **173**: 357 - 366.

Holdings, C. Z. (2006). Retrieved 15th December, 2006,, from http://www.climatezone.co.nz/hot_water_heat_pumps.html.

Hosoya, T., H. Kawamoto, et al. (2007). "Cellulose–hemicellulose and cellulose–lignin interactions in wood pyrolysis at gasification temperature " Journal of Analytical and Applied Pyrolysis **80**: 118 - 125.

Houben, M. P. (2004). Analysis of tar removal in a partial oxidation burner. Eindhoven, Technische Universiteit Eindhoven, Dissertation, **PhD:** 108.

Houben, M. P., H. C. de Lange, et al. (2005). "Tar Reduction through Partial Combustion of Fuel Gas." Fuel **84**: 815 - 824.

Hsieh, C., R. W. Babcock, et al. (1994). "Estimating Semivolatile Organic Compound Emission Rates and Oxygen Transfer Coefficients in Diffused Aeration." Water Environment Research **66**: 206 - 210.

Incropera, F. P. and D. P. Dewitt (2002). Fundamentals of Heat and Mass Transfer. New York, John Wiley & Sons.

Ising, M., C. Unger, et al. (2002). Cogenerationm from Biomass Gasification by Producer gas-Driven Block Heat and Power Plant. 12th European Biomass Conference and Exhibition, 17 - 21 June 2002. Amsterdan, The Netherlands.

Iveson, S. M. (2000). "Calculated Minimum Liquid Flowrates-A New Method for Rich Phase Absorption Columns." Chemical Engineering Education **Fall 2000**: 338 - 343.

Japas, M. L., C. P. C. Kao, et al. (1992). "Experimental Determination of Molecular Hydrogen Solubilities in Liquid Fluorocarbons." Journal of Chemical and Engineering Data **37**: 423 - 426.

Jenbach. (2009). "Jenbacher Documentation: Fuel gas quality, special gases." 15/10/2011, from http://www.brbcontractors.com/projectdocs/Jennbacher/Beschreibung/1000-0302_EN.pdf.

Jenkins, D. H., D. A. McCallum, et al. (2007). "Air Stripping of Ammonia and Methanol in a Bubble-Cap Column." Environmental Progress **26**: 365 - 374.

Jensen, P. A., E. Larsen, et al. (1996). Tar Reduction by Partial Oxidation. Biomass for Energy and Environment: Proceeding of the 9th European Biomass Conference, Copenhagen, Denmark, Pergamon.

Jess, A. (1996). "Catalytic upgrading of tarry fuel gases: A kinetic study with model components " Chemical Engineering and Processing **35**: 487 - 494.

Jess, A. (1996). "Mechanisms and Kinetics of Thermal Reactions of Aromatic Hydrocarbons from Pyrolysis of Solid Fuels." Fuel **75**: 1441 - 1448.

Kalisz, S., R. Abeyweera, et al. (2004). Energy balance of high temperature air/steam gasification of biomass in updraft, fixed bed type gasifier. IT3' 04 Confrence. Phoenix, Arizona, USA**:** 1 - 15.

Kaupp, A., K. Creamer, et al. (1983). "The Characteristics of Rice Hulls for the Generation of Electricity and Shaft Power on a Small (5 - 30 Hp) Scale." Energy Res (Alternative Energy Sources) **3**: 103 - 117.

Kiel, J. H. A., S. V. B. van Paasen, et al. (1999). Primary Measures to reduce tar formation in Fluidise-bed biomass gasifiers. J. Beesteheerde and H. J. Veringa. Petten, The Netherland, ECN.

Kimura, T., T. Miyazawa, et al. (2006). "Development of Ni catalysts for tar removal by steam gasification of biomass " Applied Catalysis B: Environmental **68** (3 - 4): 160 - 170.

Kinoshita, C. M., Y. Wang, et al. (1994). "Tar Tormation Under Different Bimoass Gasification Conditions." Journal of Analytical and Applied Pyrolysis **29**: 168 - 181.

Kurkela, E. (1989). "Updraft gasification of peat and biomass." Biomass **19**: 37 - 46.

Leva, M. (1954). "Flow Through Irrigated Dumped Packing-Pressure drop, Loading and Flooding." Chem. Eng. Progr. Symp. Ser **50**: 51 - 59.

Leva, M. (1954). "Flow through Irrigated Dumped Packing - Pressure drop, Loading and Flooding." Chem Eng Progr Symp Ser **50**: 51 - 59.

Li, C. and S. Kenzi (2009). "Tar property, analysis, reforming mechanism and model for biomass gasification-An overview." Renewable and Sustainable Energy Reviews **3**(3): 594 - 604.

Lobo, W. E., L. Friend, et al. (1945). "Limiting Capacity of Dumped tower Packings." Trans Am Inst Chem Eng **41**: 693 - 710.

McKinnon, H. (2010). Thesis: Improved Hydrogen Production from Biomass Gasification in a Dual Fluidised Bed Reactor. Chemical and Process Engineering. Christchurch, New Zealand, University of Canterbury. **Master of Engineering**.

Milne, T. A., N. Abatzoglou, et al. (1998). "Biomass gasifier Tars": Their Nature, Formation and Conversion; NREL/TP-570-25357.

Morf, P., P. Hasler, et al. (2002). " Mechanisms and kinetics of homogeneous secondary reactions of tar from continuous pyrolysis of wood chips " Fuel **81**: 843 - 853.

Nair, S. A., K. Yan, et al. (2004). "Tar Removal from Biomass Derived Fuel Gas by Pulsed Corona Discharges: A Chemical Kinetic Study." Industrial and Engineering Chemistry Research **43**: 1649 - 1658.

Narva'ez, I., A. Orio, et al. (1996). "Biomass gasification with air in an atmospheric bubbling fluidized bed. Effect of six operational variables on the quality of produced raw gas." Industrial and Engineering Chemistry Research **35**: 2110 - 2120.

Nirmalakhandan, N., W. Jang, et al. (1990). "Counter-current Air Stripping for the Removal of Volatile Oraganic Containments." Water Research **24**: 615 - 623.

Nirmalakhandan, N., R. E. Speece, et al. (1993). "Operation od Counter-current Air Stripping Towers at Higher Loading Rates." Water Research **27**: 807 - 813.

Orio, A., J. Corella, et al. (1997). "Performance of different dolomites on hot raw gas cleaning from biomass gasification with air." Industrial and Engineering Chemistry Research **36**: 3800 - 3808.

Parikh, P. P., A. Paul, et al. (1987). Why and How Much? Energy Biomass Wastes. D. H. Klass. Chicago, Institute of Gas Technology**:** 1633 - 1637.

Parr, G. (2008). Heat Exchanger. Christchurch, Savage Manufacturing Limited.

Perez, P., P. M. Aznar, et al. (1997). "Hot gas cleaning and upgrading with a calcined dolomite located downstream from a biomass fluidised bed gasifier operating with steam-oxygen mixture." Energy & fuels **11**: 1194 - 1203.

Perez, P., P. M. Aznar, et al. (1997). "Hot Gas Cleaning and Upgrading with a Calcined Dolomite Located Downstream from a Biomass Fluidised Bed Gasifier Operating with Steam-Oxygen Mixtures." Energy & Fuels **11**: 1194 - 1203.

Pfeifer, C. and H. Hofbauer (2008). "Development of Catalytic Tar Decomposition Downstream from a Dual Fluidized Bed Biomass Steam Gasifier " Powder Technology **180**: 9 - 16.

Pfeifer, C., R. Rauch, et al. (2004). "In-bed catalytic tar reduction in a dual fluidised bed biomass steam gasifier " Industrial and Engineering Chemistry Research **43**: 1634 - 1640.

Phuphuakrat, T., T. Namioka, et al. (2010). "Tar Removal from Biomass Pyrolysis Gas in Two-Step Function of Decomposition and Adsorption." Applied Engineering **87**: 2203 - 2211.

Pierobon, L. (2010). Analysis of a gasification plant fed by woodchips integrated with SOFC and Steam cycle. Department of Mechanical Engineering. Kongens Lyngby, Technical University of Denmark. **M. SC Thesis**.

Pino, G., M. Paolucci, et al. (2006). Syngas production by a modified biomass gasifier and utilisation in a moten fuel cell (MCFC). Advances in energy studies, 'perspective into energy future'. Porto venere, The 5th International Biennial Workshop.

Pipatmanomai, S. (2011). "Overview and experience of biomass fluidized bed gasification in Thailand." Journal of sustainable energy and environmental **special issues**: 29 - 33.

Prausnitz, J. M., R. N. Lichtenthaler, et al. (1999). Molecular Thermodynamics of Fluid-Phase Equilibria. New Jersey, Prentice Hall PTR.

Probstein, R. H. and E. R. Hicks (2006). Synthetic Fuels. Cambridge, Dover Publications Inc.

Proll, T., G. Siefert, I , et al. (2005). "Removal of NH3 from Biomass Gasification Producer Gas by Water Condensing in an Organic Solvent Scrubber." Industrial and Engineering Chemistry Research **44**: 1576 - 1584.

Rabou, L. P. L. M. (2005). "Biomass Tar Recycling and Destruction in a CFB Gasifier." Fuel **84**(5): 577 - 581.

Rabou, L. P. L. M., R. W. R. Zwart, et al. (2009) "Tar in Biomass Producer Gas, The Energy Centre of The Netherlands (ECN) Experience: An Enduring Challenge." Energy & Fuels DOI: 10.1021/ef9007032.

Rabou, L. P. L. M., R. W. R. Zwart, et al. (2009). "Tar in Biomass Producer Gas, the Energy research Centre of The Netherlands (ECN) Experience: An Enduring Challenge." Energy & Fuels **23**: 6189 - 6198.

Rapagna, S., N. Jand, et al. (1998). Utilisation of a suitable catalyst for the gasification of biomass. 10 th European Conference and Technology Exhibition on Biomass for Energy and Industry, Wurzburg, Germany.

Rapagna, S., N. Jand, et al. (2000). "Steam gasification of biomass in a fluidised-bed of olivine particles." Biomass and Bioenergy **19**: 187 - 197.

Rashid, U. and F. Anwar (2008). "Production of biodiesel through optimized alkaline-catalyzed transesterification of rapeseed oil." Fuel **87**: 265 - 273.

Rauch, R. (2004). Steam Gasification of Biomass at CHP Plant Guessing-Status of the Demonstration Plant. Getreidemarkt, Institute of Chemical Engineering, Vienna.

Rauch, R., H. Hofbauer, et al. (n.d.). Six Years Experience with the FICFB-Gasification Process, Institute of Chemical Engineering, Vienna.

Rensfelt, E. (1996). Atmospheric Pressure Gasification Process for Power Generation. Analysis and Coordination of the Activities Concerning a Gasification of Biomass, ESpoo, Finiland, (AIR3-CT94-2284), Second Workshop.

Rensfelt, E. and C. Ekstrom (1988). Fuel Gas from Municipal Waste in an Integrated circulating Fluid-bed Gasification/Gas-Cleaning Process. Energy from Biomass and Wastes. D. H. Klass. Chicago, Institute of Gas Technology.

Roberts, P. V., G. D. Hopkins, et al. (1985). "Evaluating Two-Resistance Models for Air stripping of Volatile Oragnic Contaminants in a Countercurrent, Packed Column." Environmental and Science Technology **19**: 164 - 173.

Roberts, P. V., G. D. Hopkins, et al. (1985). "Evaluating Two Resitance Models for Air Stripping of Volatile Organic Contaminants in a Counter Currrent Packed Column." Environmental and Science Technology **19**: 164 - 173.

Rorschach, R. C., R. L. Autenrieth, et al. (1989). "Air Stripping of Hexachlorobiphenyl from Aqueous Phase." Journal of Hazardous Materials **22**: 256.

Schweiger, A. (2007). Small scale hot gas cleaning device for SOFC utilisation of woody biomass product gas. Graz, Institute of Thermal Engineering**:** Report no.502759.

Shafizadeh, F. J. (1982). " Introduction to pyrolysis of biomass. ." Journal of Analytical and Applied Pyrolysis **3**: 283 - 305.

Shafizadeh, F. J. and Y. Z. Lai (1972). " Thermal Degradation of 1,6-Anhydro-p-β-glucopyranose." Journal of Organic Chemistry **37**: 278 - 284.

Sharan, H. N., H. S. Mikunda, et al., Eds. (1997). IISc-DASAG Biomass Gasifiers: Development, Technology, Experience and Economics. Development in Thermochemical Biomass Conversion. London, Blackie Academic and Professional.

Sheng, H. L. and C. S. Wang (2004). "Recovery of Isopropyl alcohol from Waste Solvent of a Semiconductor Plant." Journal of Hazardous Materials 106B **106**(161 - 168).

Sherwood, T. K., G. H. Shipley, et al. (1938). "Flooding Velocities in Packed Columns." Industrial and Engineering Chemistry **30**: 765 -769.

Shibata, Y., H. Koseki, et al. (2008). "Spontaneous Ignition of Biodiesel: A Potential Fire Risk." Thermal Science **2**: 149 - 158.

Simell, P., E. Kurkela, et al. (1996). "Catalytic Hot Gas Cleaning of Gasification Gas." Catalysis Today **27**: 55 - 62.

Sinnott, R. K. (2005). Chemical Engineering Design. Massachusetts, Elsevier Butterworth-Heinemann.

Skoulou, V., A. Swiderski, et al. (2009). "Process characteristic and products olivine kernel high temperature gasification." Bioresource technology **100**: 2444 - 2451.

Smith, J. M., H. C. Van Ness, et al. (1996). Introduction to Chemical Engineering Thermodynamics. New York, The McGraw-Hill Companies.

Sutton, D., B. Kelleher, et al. (2001). Review of Literature on Catalysts for Biomass Gasification, Centre for Environmental Research, University of Limerick.

Thlbodeaux, L. J., D. R. Daner, et al. (1977). "Mass Transfer Units in Single and Multiple Stage Packed Bed, Cross-Flow Devices." Industrial and Engineering Chemistry Process Design and Development **16**: 325 - 330.

Toosen, R., N. Woudstran, et al. (2008). "Exergy analysis of Hydrogen production plants based on biomass gasification." International journal of hydrogen energy **33**: 4074 - 4082.

Treybal, E. R. (1981). Mass-Transfer Operations. Singapore, McGraw-Hill Book Co.

Umsicht, F. (2009). Syngas cleaning with Catalytic tar reforming. Presentation at Gasification 2009, Stockholm, UMSICHT.

van der Drift, A., M. C. Carbo, et al. (2005). The TREC-module: integration of tar reduction and high-temperature filtration. 14th European Biomass Conference & Exhibition. Paris, France.

van Heesch, E. J. M., A. J. M. Pemen, et al. (1999). Experimental Program of the Pulsed Corona Tar Cracker. 12th IEE International Pulsed power Conference, Monterey, Canada, Eindhoven University of Technology (CUT).

Wallman, H. and M. D. Cummins (1985). Design Scale-up Suitability for Air Stripping Columns, EPA Report Under Agreement No. CR-810247-01.

Wang, C., T. Wang, et al. (2010). "Steam Reforming of Biomass Raw Fuel Gas over NiO-MgO Solid Solution Cordierite Monolith Catalyst." Energy Conversion and Mangement **51**: 446 - 451.

Wang, C., T. Wang, et al. (2008). "Partial Oxidation Reforming of Biomass Fuel Gas over Nickel-Based Monolithic Catalyst with Naphthalene as Model Compound." Korea Journal of Chemical Engineering **25**: 738 - 743.

Wang, L. K., Y. T. Hung, et al., Eds. (2006). Handbook of Environmental Engineering. Advanced Pysicochemical Treatment Processes, Humana Press Inc.

Watanabe, T. and S. Hirata. (2004). "Development of a gasifier that produces less tar." Retrieved 12/10/2007, from http://www.khi.co.jp/earth/english/pdf/04_houkokusyo_e17.pdf.

Watson, K. M. (1943). "Thermodynamics of Liquid State." Industrial and Engineering Chemistry **35**: 398 - 406.

Woods, D. R. (2007). Rule of Thumb in Engineering Practice. Germany, Wiley-VCH Verlag GmbH & Co.

Yen, L. C. and J. McKetta, J Jr (1962). "A Thermodynamic Correlation of Nonpolar Gas Solubilities in Polar Nonassociated Liquids." AIChE **8**(4): 501 - 507.

Yuan, W., A. C. Hansen, et al. (2005). "Vapor pressure and normal boiling point predictions of pure methyl esters and biodiesel fuels." Fuel **84**: 943 - 950.

Zevenhoven, R. and P. Kilipinen (2001). Particulates. A. Lyngfelt and A. B. Mukherjee. Helsinki, Helsinki University of Technology.

Zhou, L. and Y. Zhou (2001). "Determination of compressibility factor and fugacity coefficient of hydrogen in the studies of adsorptive storage." International Journal of Hydrogen Energy **26**: 597 - 601.

Zwart, R. W. R., S. Heijden, et al. (2010). Tar Removal from Low-temperature Gasifier, Report: ECN-E-10-008, ERA-NEJ Bioenergy.

Zwart, R. W. R., A. Van der Drift, et al. (2009). "Oil-based Gas Washing-Flexible Tar Removal for High-Efficient Production of Clean Heat and Power as well as Sustainable Fuel and Chemicals." Environmental Progress and Sustainable Energy **28**: 324 - 335.